LAPPEENRANTA UNIVERSITY OF TECHNOLOGY
LUT School of Engineering Science
Degree Program of Chemical Engineering

Minna Laitinen

KRAFT RECOVERY BOILER DISSOLVING TANK MASS AND ENERGY BALANCE

Examiners: Ass. Professor, D.Sc. (Tech.) Eeva Jernström
Professor, D.Sc. (Tech.) Esa Vakkilainen

Instructor: M.Sc. (Tech.) Lauri Pakarinen

FOREWORDS

This Master's thesis was written in the Technology department of Andritz Oy, Finland in Varkaus between June and December 2016.

My deepest gratitude for enabling this work belongs to my instructor M.Sc. Lauri Pakarinen, and examiners professors Eeva Jernström and Esa Vakkilainen, who despite of their tight time schedule provide me valuable support and guidance throughout the whole work.

I would like to also express my thanks to M.Sc. Esa Vihavainen for advices and sharing material concerning the topic. Thanks also to Tomi Vaaljoki, Ilkka Mänttäri, and other colleagues for helping me collect process feedback data from different pulp mills. I would like also to thank "4th floor"-colleagues for pricelessly bad and still good jokes and keeping up good spirit during the work.

Finally, thanks to all my friends and chemical engineering fellow students in Lappeenranta for unforgettable time there and good memories. I am grateful that I have had a privilege to know you all.

"Asialliset hommat suoritetaan, muuten ollaan kuin Ellun kanat."

– Vilho Koskela, in *Tuntematon sotilas* by Väinö Linna, 1954

Varkaus, December 2nd, 2016

Minna Laitinen

ABSTRACT

Lappeenranta University of Technology
LUT School of Engineering Science
Degree Program of Chemical Engineering

Minna Laitinen

Kraft Recovery Boiler Dissolving Tank Mass and Energy Balance

2016

98 pages, 36 figures, 12 tables

Examiners: Ass. Professor, D.Sc. (Tech.) Eeva Jernström
Professor, D.Sc. (Tech.) Esa Vakkilainen
Instructor: M.Sc. (Tech.) Lauri Pakarinen

Keywords: dissolving tank, smelt, mass and energy balance, vent gas formation

Due to the tightened emission regulations and the urge of decreasing investment and operational costs of recovery boiler, the understanding of dissolving tank operation and vent gas handling system have become important topics. However, complete knowledge of vent gas formation and reactions occurred during smelt dissolution are lacking.

The objectives of master's thesis were to understand phenomena behind dissolving tank vent gas formation and create a workable numerical model for describing that. Another objective was to validate modelled results based on the process feedback data collected from pulp mill data systems.

Process feedback data was collected from four pulp mills and used for the tuning of the dissolving tank balance model. The results of the simulation were compared to the results of feedback data. The effects of boiler load, weak white liquor temperature, green liquor density and temperature on the evaporation of green liquor and vent gas formation were determined.

Created model provided good reference data for analyzed feedback data. The increasing of boiler load was observed to increase the enthalpy of vent gas. The effect of green liquor temperature was similar to boiler load, even though the trend was more valid in individual boiler cases. Contrary to initial expectations the effect of weak white liquor temperature on the evaporation of green liquor was not unambiguous as observed from the model. The increasing of weak white liquor temperature increased the heat output of vent gases. The increasing of green liquor density was also observed to increase the enthalpy of vent gas in case of individual boilers. In order to enhance reliability of the study, more feedback data with higher boiler loads and capacities is recommended to collect. Leak air test, determination of green liquor composition and smelt temperature will be essential questions in future research.

TIIVISTELMÄ

Lappeenrannan teknillinen yliopisto
LUT School of Engineering Science
Kemiantekniikan koulutusohjelma

Minna Laitinen

Soodakattilan liuotussäiliön massa- ja energiatase

2016

98 sivua, 36 kuvaa, 12 taulukkoa

Tarkastajat: Tutkijaopettaja, TkT Eeva Jernström
Professori, TkT Esa Vakkilainen
Ohjaaja: Diplomi-insinööri Lauri Pakarinen

Hakusanat: liuotussäiliö, sula, massa- ja energiatase, höngän muodostuminen
Keywords: dissolving tank, smelt, mass and energy balance, vent gas formation

Tiukentuvat päästörajoitukset ja halu pienentää soodakattilan investointi- sekä käyttökustannuksia ovat kasvattaneet mielenkiintoa liuotussäiliön ja hönkien käsittelyjärjestelmän toimintaa kohtaan. Huolimatta siitä, että liuottajalla on keskeinen rooli soodakattilan toiminnassa, ilmiötä liuottajan reaktioiden ja höngän muodostumisen taustalla ei ymmärretä.

Diplomityön tarkoituksena oli selvittää liuottajan hönkien muodostumiseen vaikuttavat tekijät ja luoda säiliön toimintaa kuvaava laskennallinen massa- ja energiatasemalli. Työn toisena tarkoituksena oli myös validoida mallinnuksen tuloksia sellutehtaiden tietokannoista kerättyjen prosessiarvojen avulla.

Prosessiarvoja kerättiin neljästä eri sellutehtaasta, jotta tasemalli saatiin vastaamaan todellisia prosesseja. Lisäksi simuloinnin tuloksia verrattiin todellisiin prosessiarvoihin. Soodakattilan lipeäkuorman, heikkovalkolipeän lämpötilan, viherlipeän tiheyden ja lämpötilan vaikutus liuottajassa tapahtuvaan viherlipeän höyrystymiseen tutkittiin.

Havaittiin, että luodun mallin tulokset antoivat hyvän vertailupohjan todellisille prosessiarvoille. Kun kattilan kuormaa nostettiin, höngän tuntuvan lämmön havaittiin kasvavan**.** Viherlipeän lämpötilan vaikutus höngän lämpömäärään oli samanlainen, vaikka ilmiö oli havaittavissa vain yksittäisten kattiloiden kohdalla. Vastoin ennakko-olettamuksia heikkovalkoisen lämpötila vaikutti liuottajan höngän muodostumiseen suhteellisen vähän. Yksittäisten kattiloiden kohdalla heikkovalkolipeän lämpötilan nousu lisäsi höyrystymistä. Höyrystymisen havaittiin myös lisääntyvän, kun viherlipeän tiheys kasvoi. Tulevaisuudessa on suositeltavaa, että prosessiarvoja kerätään korkeammilla kattilakuormilla ja kapasiteeteilla eri tehtailta tulosten luotettavuuden parantamiseksi. Vuoto-ilmatesti, viherlipeän koostumuksen ja sulan lämpötilan määrittäminen ovat myös olennaisia tutkimuskohteita tulevaisuudessa.

SYMBOLS

A	area	m^2
B	an empirical constant	$kmol/m^3$
b_i	molality of smelt compound	mol/kgDS
$b_{Na_2CO_3}$	molality of Na_2CO_3 in smelt	mol/kg
b_{Na_2S}	molality of Na_2S in smelt	mol/kg
[C]	carbon concentration of the smelt	$kmol/m^3$
$C_{GL,s}$	vapor concentration at the surface of green liquor	$kmol/m^3$
$C_{GL,int.}$	vapor concentration at the interface	$kmol/m^3$
C_m	mass transfer constant	ms
C_{is}	coefficient of isentropic exponent	–
c_p	specific heat capacity	kJ/kgK
E_a	activation energy	kJ/kmol
f_D	pressure loss factor	–
$\dot{H}$	enthalpy flow of fluid	kW
h_c	specific enthalpy of the compound	kJ/kgDS
$\bar{h}_m$	convection mass transfer coefficient	m/s
h_m	melting enthalpy of the compound	kJ/mol
$h''(T_{GL})$	enthalpy of saturated vapor at green liquor temperature	kJ/kg
i	van't Hoff constant	–
k	isentropic exponent	–
K_2	the amount of potassium, in molar equivalents	mol
K_b	ebullioscopic constant	Kkg/mol
K_{dr}	the coefficient of discharge	–
K_{red}	pre-exponential factor for sulfate reduction	1/s
$\dot{m}$	mass flow	kg/s
$N_{GL,evap}$	molar flux of vapor evaporated from green liquor	kmol/s

Na_2	the amount of sodium, in molar equivalents	mol
NaOH	the amount of sodium hydroxide in molar equivalents	g/l
Na_2S	the amount of sodium sulfide	mol
Na_2SO_4	the amount of sodium sulfate	mol
$[Na_2CO_3]$	sodium carbonate concentration	g NaOH/L g Na_2O/L
[NaOH]	sodium hydroxide concentration	g NaOH/L g Na_2O/L
$[Na_2S]$	sodium sulfide concentration	g NaOH/L g Na_2O/L
P_{mix}	power of mixing	kW
R	gas constant	J/molK
S_{tot}	the total amount of sulfur determined as sodium sulfide in molar equivalents	mol
[SO]	sulfate concentration of the smelt	kmol/m^3
$[SO_4]$	concentration of sulfate in the smelt	kmol/m^3
$[S_{tot}]$	total concentration of sulfur	kmol/m^3
T_b	the boiling point of solution	K
T_b^*	the boiling point of pure water	K
TTA_{NaOH}	total titratable alkali	g NaOH/l
v	specific volume of steam	m^3/kg
$\dot{V}$	volume flow	m^3/s or l/s
x_i	mass fraction	kg/kDS or –
$\Delta H_{vap}(T_b^*)$	enthalpy of vaporization of pure water	J/mol
$\Delta h_{V\circ}$	latent heat of water	kJ/kg
Δp_{tank}	under pressure in the dissolving tank	Pa
$\eta_{reduction}$	fractional sulfur reduction efficiency	–
ρ_{air}	density of air	kg/m^3
ρ_{GL}	density of green liquor	kg/l
ϑ	temperature of saturated gas	K

φ	relative humidity	–

SUBCRIPTS

b	boiling
BL WO ASH	black liquor without ash
D	water vapor
DS	saturated water vapor
GL	green liquor
GL as NaOH	green liquor property expressed in terms of NaOH mass equivalents
GL, evap	evaporated green liquor
H_2O	water
i	a component
int.	interface
m	melting
mix	mixing
NaOH	in terms of NaOH equivalents
oc	other condensates
red	reduction
Ref	reference
s	surface
sat	saturated
sc	scrubber condensate
tot	total
VG dried	dried vent gas
VG wet	wet vent gas
WWL	weak white liquor
0	initial

ABREVIATIONS

ACD	Andritz remote data collection system
BP	Boiling Point
DIT	Dissolving Tank
DS	Dry Solids
ESP	Electrostatic precipitator
GL	Green Liquor
TRS	Total Reduced Sulphur
TTA	Total Titratable Alkali
VG	Vent Gas
WWL	Weak White Liquor

CHEMICAL COMPOUNDS

C	organic carbon
$CaCO_3$	calcium carbonate
CaO	calcium oxide
CaS	calcium sulfide
$(CH_3)_2S$	dimethyl sulfide
$(CH_3)_2S_2$	dimethyl disulfide
CH_3SH	methyl mercaptan
CO	carbon monoxide
CO_2	carbon dioxide
H^+	proton
HS^-	hydrogen sulfide anion
H_2	hydrogen
H_2O	water
H_2S	hydrogen sulfide
N_2	nitrogen
$NaCN$	sodium cyanide

Na_2CO_3	sodium carbonate
$Na_2CO_3 \cdot H_2O$	sodium carbonate monohydrate
$Na_2CO_3 \cdot CaCO_3 \cdot 2H_2O$	pirssonite
$NaHS$	sodium hydrogen sulfide
$NaOCN$	sodium cyanate
$NaOH$	sodium hydroxide
Na_2S	sodium sulfide
Na_2SO_4	sodium sulfate
$Na_6(SO_4)_2(CO_3)$	burkeite
$Na_2S_2O_3$	sodium thiosulfate
NH_3	ammonia
$(NH_4)_2SO_4$	ammonium sulfate
NO_x	nitrogen oxides
O_2	oxygen
SO_2	sulfur dioxide
S^{2-}	sulfide anion

Table of Contents

1 INTRODUCTION

Black liquor, a by-product of kraft pulping, was traditionally considered as a discharge without any further application. The demand for increasing mill size and process intensification, for instance achieving positive cost effects of recycling chemicals, lead to the invention of recovery boiler. (Vakkilainen, 2008a; Vakkilainen, 2005)

Recovery boiler has three main functions in the recovery cycle:

- to recover valuable inorganic chemicals from black liquor, mainly Na_2S reduced from sulfur compounds of combusted black liquor
- to exploit chemical energy combined to black liquor via combustion and steam generation
- to reduce mill environmental impacts by combusting flue gases and other discharges from waste streams.

(Adams, 1997; Hupa & Hyöty, 2002; Vakkilainen, 2005; Vakkilainen, 2008b)

In addition to previous functions, one important function of recovery boiler is to produce green liquor by dissolution of molten smelt in the dissolving tank (Vakkilainen, 2005). Produced green liquor is then led to recausticising plant for further processing and production of white liquor (Engdahl, et al., 2008). Due to being linked to each other, boiler and dissolving tank operation have significant effect on the operation of white liquor plant. However, despite of its importance relatively small number of research concerning smelt dissolution and green liquor have been made, when compared to number of research made concerning black liquor and other variables affecting steam and electricity generation.

Recently, the interest in the understanding of dissolving tank operation and vent gas system has been increased due to continuously tightened emission regulations and increased boiler capacities. Additionally, the urge of reducing investment costs, increasing boiler efficiency and power production have also influenced on the optimization of recovery boiler technology and discovering new state of the art solutions. The aim of increasing power-to-heat ratio and boiler availability

have increased the importance of non-process elements (NPEs) reduction, such as black liquor chloride (Cl) and potassium (K) concentrations, in the pulping processes. Additionally, NPEs may cause corrosion and other problems in recausticising and evaporating plant (Engdahl, et al., 2008; Salmenoja, 2015).

1.1 Objectives

This master's thesis work is done as a part of development project concerning the dissolving tank and vent gas handling system of kraft recovery boiler. The main objectives of the work are:

- to understand phenomena behind dissolving tank vent gas formation and create a workable numerical model for describing that
- to validate modelled results based on the process feedback data collected from pulp mill data system, Andritz remote data collection system (ACD), and field data measurements.

In the literature part of this thesis it is concentrated on the processes of recovery boiler furnace, namely reactions of char bed, and the principle and practice of dissolving tank. Theory of smelt and vent gas formation are in the main focus of the literature section. Vent gas handling system including scrubber technology is also introduced briefly.

The calculation procedure and results of created dissolving tank mass and energy balance model are presented in the experimental part. The mass and enthalpy flows of evaporated vapor and total vent gases produced are determined. The effect of green liquor density, weak white liquor temperature, green liquor temperature and boiler operation load on dissolving tank operation are studied. Finally, the results got from the model are compared to process feedback data collected from four different pulp mills.

LITERATURE PART

2 THE PRINCIPLE OF KRAFT RECOVERY BOILER

A schematic configuration of a modern recovery boiler is presented in Figure 1. In recent years recovery boilers with single-drum solutions have outstripped the two-drum recovery boilers in popularity. Single-drum boilers are more often selected due to higher dry solids load handling capacity, vertical heat exchangers and higher steam pressure conditions. (Vakkilainen, 2005; Vakkilainen, 2008b)

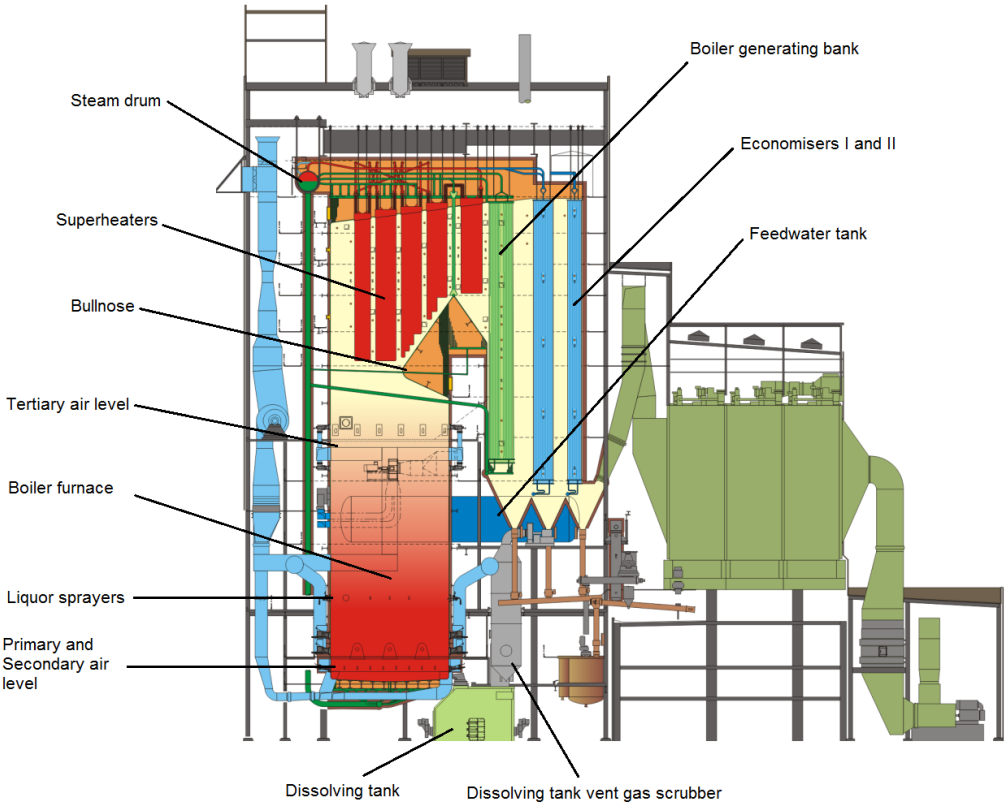

Figure 1. A side view of a modern recovery boiler, courtesy of Andritz Oy

Recovery boiler design is strongly dependent on black liquor dry solids content, which determines the combustion capacity and boiler size, including the most of operating variables such as steam flow, the amount of char formed, and flue gas produced. (Jones & Nagel, 1998; Vakkilainen, 2005) According to Vakkilainen (2008b) 7 % of more steam flow is generated as the dry solids content of black liquor is increased from 65 % to 80 %. Currently, most of the modern recovery

boilers combust black liquor with dry solids content more or equal than 80 %. (Vakkilainen, 2008b)

During boiler operation, as-fired black liquor with air is sprayed into the boiler furnace through liquor guns above primary and secondary air level. The location of liquor guns can vary depending on the boiler size. At old boilers liquor guns have been located in the height of 5 to 6 meters above the furnace floor, but at modern boilers they may be positioned at higher level. (Adams, 1997; Andritz Oy, 2016a)

Combustion gases flow upward through tertiary air level, where final burning of mixed fuel and air occurs, to superheaters. The nose arch or also called bullnose divides the boiler roughly into two sections: a furnace and a heat transfer section, including superheaters, boiler generating bank and economisers. (Adams, 1997; Vakkilainen, 2005) In some boilers a low temperature heat surface – a screen is placed in front of the superheaters in order to prevent unburned black liquor particles enter and protect the surface of the superheaters from direct heat radiation of the furnace and corrosion (Adams, 1997; Vakkilainen, 2005).

The furnace walls are constructed of vertical tubes connected with fins. The material compositions of furnace tubes vary along the furnace conditions (Andritz Oy, 2008). Furnace wall tubes are typically made of either composite or hot resistance carbon steel tubes (Andritz Oy, 2016a). All four walls of furnace are made of vertical tubes, which are connected to the headers in the upper part of the boiler. Water flows inside the tubes and recovers the heat of burned gases and char bed by radiation. Traditionally, water and combustion gases flow in co-current direction in the most part of the boiler. (Adams, 1997)

The role of lower furnace, including char bed and smelt, is significant in the performance of recovery boiler. During liquor spraying, the sizes of black liquor drops are carefully controlled in order to ensure optimum conditions for main reactions of char bed, such as black liquor burning, sulphur reduction, and smelt formation. If sprayed liquor drops are too small, the amount of carry-over dust will increase and induces corrosion of the boiler upper part. Too large drops, however, tend to accumulate on the surface of char bed and induce excessive

growth of the bed. (Costa, et al., 2005; Hupa & Hyöty, 2002) Molten smelt produced in the bed runs off the boiler through smelt spouts into the dissolving tank, where green liquor is produced. (Adams, 1997; Cardoso, et al., 2009; Costa, et al., 2005)

3 BLACK LIQUOR

Despite of its common utility as fuel, the properties and behavior of black liquor are rather poorly known (Hupa & Hyöty, 2002). Kraft black liquor is composed of water, organic and inorganic compounds. Typically as-fired black liquor contains 20 to 40 w-% of water, which will be evaporated during the combustion. Due to its high water and ash content, the utilization and combustion of black liquor requires special attention and technology. As an example the furnaces of kraft recovery boilers are usually wider and have more space than the furnaces of conventional boilers using other fuels. (Hupa & Hyöty, 2002; Vakkilainen, 2008a)

During kraft pulping process, main compounds of wood: lignin and polysaccharides are reacted with sodium sulfide and sodium hydroxide from white liquor to form degradation products, such as alkali lignin and polysaccharinic acids. (Frederick & Söderhjelm, 1997) The specific composition of black liquor is strongly dependent on wood species and cooking method used (Cardoso, et al., 2009; Llamas, et al., 2007). An example of virgin black liquor chemical composition from North American wood is illustrated in Table I. According to Vakkilainen (2008b), organic compounds represent the main part of virgin black liquor as relation to dry solids content, namely 78 w-%. The rest of liquor dry solids, 22 w-%, are inorganic chemicals, such as sodium (Na) and potassium (K) salts and non-process elements (NPEs). Hupa and Hyöty (2002) estimate the amount of organic and inorganic matter in virgin black liquor to be 60 and 40 w-%, respectively.

Table I The chemical composition of virgin kraft black liquor from North American wood, adapted from the table of (Frederick & Söderhjelm, 1997)

Chemical compound	Range [w-%]
Alkali lignin	30–45
Hydroxy acids	25–35
Extractive	3–5
Acetic acid	5
Formic acid	3
Methanol	1
Sulfur	3–5
Sodium	15–20

Similarly as chemical composition, elementary composition of black liquor varies depending on the wood species used and the growth region. The list of black liquor elements in Nordic, North American and tropical woods are presented in Tables II–III. In the case of Nordic and North American woods both hardwood and softwood compositions are presented. One may observe that chlorine (Cl) concentrations are higher in North American woods and eucalyptus than in Nordic woods. Nordic wood, however, contains higher amount of sulphur (S) than woods from the other region. High chlorine concentrations of eucalyptus wood have also been recorded in the experimental studies performed at Brazilian pulp mills (Cardoso, et al., 2009).

Table II Elementary composition of virgin black liquor from Nordic wood and North American wood, adapted from the table of Vakkilainen (2008a)

Nordic wood					
Element		**Softwood**		**Hardwood**	
		Typical [w-%]	**Range [w-%]**	**Typical [w-%]**	**Range [w-%]**
Carbon	**C**	35.0	32–37	32.5	31–35
Hydrogen	**H**	3.6	3.2–3.7	3.3	3.2–3.5
Nitrogen	**N**	0.1	0.06–0.12	0.2	0.14–0.2
Oxygen	**O**	33.9	33–36	35.5	33–37
Sodium	**Na**	19.0	18–22	19.8	18–22
Potassium	**K**	2.2	1.5–2.5	2.0	1.5–2.5
Sulphur	**S**	5.5	4–7	6.0	4–7
Chlorine	**Cl**	0.5	0.1–0.8	0.5	0.1–0.8
Inert.	**–**	0.2	0.1–0.3	0.2	0.1–0.3
TOTAL	**–**	100.0		100.00	
North American wood					
Element		**Softwood**		**Hardwood**	
		Typical [w-%]	**Range [w-%]**	**Typical [w-%]**	**Range [w-%]**
Carbon	**C**	35	32–37.5	34	31–36.5
Hydrogen	**H**	3.5	3.4–4.3	3.4	2.9–3.8
Nitrogen	**N**	0.1	0.06–0.12	0.2	0.14–0.2
Oxygen	**O**	35.4	32–38	35	33–39
Sodium	**Na**	19.4	17.3–22.4	20	18–23
Potassium	**K**	1.6	0.3–3.7	2	1–4.7
Sulphur	**S**	4.2	2.9–5.2	4.3	3.2–5.2
Chlorine	**Cl**	0.6	0.1–3.3	0.6	0.1–3.3
Inert.	**–**	0.2	0.1–2.0	0.5	0.1–2.0
TOTAL	**–**	100		100	

Table III Elementary composition of virgin black liquor from eucalyptus wood, adapted from the table of Vakkilainen (2008a)

Tropical wood			
Element		**Harwood (eucalyptus)**	
		Typical [w-%]	**Range [w-%]**
Carbon	**C**	34.8	33–37
Hydrogen	**H**	3.3	2.7–3.9
Nitrogen	**N**	0.2	0.1–0.6
Oxygen	**O**	35.5	33–39
Sodium	**Na**	19.1	16.2–22.2
Potassium	**K**	1.8	0.4–9.2
Sulphur	**S**	4.1	2.4–7.0
Chlorine	**Cl**	0.7	0.1–3.3
Inert.	**–**	0.5	0.2–3.0
TOTAL	**–**	100	

3.1 Black liquor properties

Black liquor properties have an effect on boiler operation, such as combustion and formation of char bed. Since smelt formed in the bed is further processed in dissolving tank, properties of black liquor will also have an indirect effect on smelt dissolution.

Black liquor physical and chemical properties are mainly affected by chemical and elementary composition of liquor. From boiler operation point of view main properties of black liquor are viscosity, density, surface tension, and specific heating value (Hupa & Hyöty, 2002; Theliander, 2009; Vakkilainen, 2008a).

3.1.1 Viscosity of black liquor

The rheological behavior of black liquor is dependent on the dry solids content and temperature of black liquor. As dry solids content increases, viscosity increases exponentially. The increasing of black liquor viscosity as a function of eucalyptus black liquor dry solids content is presented in Figure 2 (Llamas, et al., 2007). Generally, black liquor can be considered as non-Newtonian fluid, even though it can achieve Newtonian behavior at low shear rates (Frederick & Söderhjelm, 1997; Vakkilainen, 2008a). The increasing of viscosity might be partly explained by large macromolecules of black liquor, namely lignin and polysaccharides, which tend to increase viscosity due to the different molecular alignment. (Cardoso, et al., 2009)

From boiler operation point of view high viscosity affects the ability of liquor pumping and spraying. The plugging of black liquor sprays, for instance, may occur, if viscosity is increased too much. (Frederick & Söderhjelm, 1997) According to Llamas et al. (2007) the pumpability of black liquor decreases, as dry solids content of liquor exceeds 70 w-% and liquor temperature decreases under 100 °C. One explanation for the phenomenon is the change of continuous material in black liquor, since in concentrated black liquors polymeric phase replaces water as a solvent. (Llamas, et al., 2007) Thus black liquor viscosity is typically maintained under 300 mPas for securing good operation conditions of mill and boiler (Frederick & Söderhjelm, 1997). Several methods of viscosity

control are available, even though heat treatment and chemical addition to black liquor are the most common ones (Frederick & Söderhjelm, 1997; Hupa & Hyöty, 2002; Llamas, et al., 2007; Vakkilainen, 2008b).

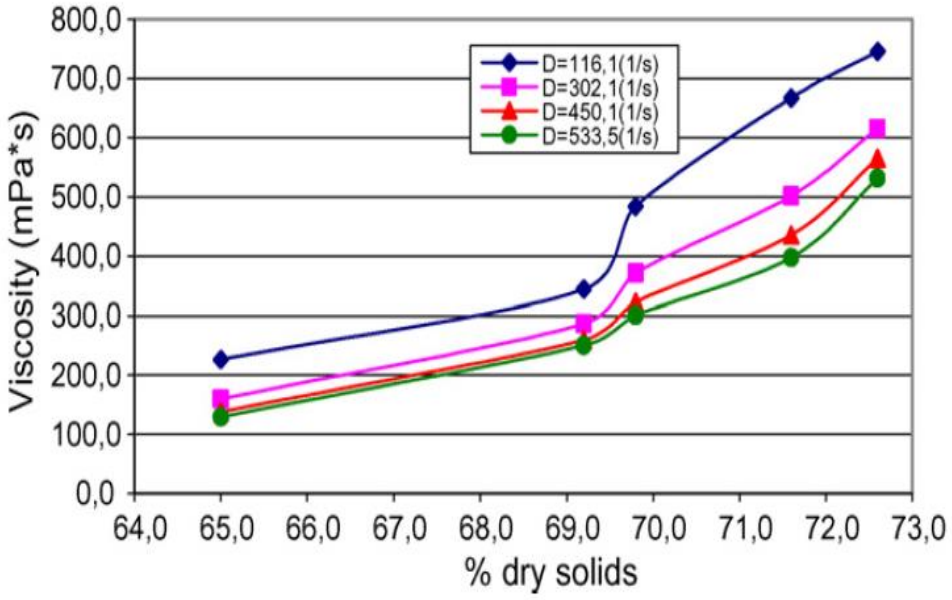

Figure 2. Viscosity of eucalyptus black liquor with different dry solids content of liquor and shear rates. (Llamas, et al., 2007)

3.1.2 Density and surface tension of black liquor

The trend of black liquor density as a function of dry solids content is similar to the trend of viscosity. With low dry solids content, density of black liquor is near of water density ranging approximately between 1000 kg/m^3 and 1100 kg/m^3. (Vakkilainen, 2008a) The increasing of black liquor concentration increases the density of liquor, as one may observe in Figure 3.

Figure 3 illustrates also the effect of temperature on density. The density of low dry solids liquor converges to density of water as temperature of black liquor increases over 100 °C. Typical density of high dry solids black liquor is approximately 1400 kg/m^3. (Vakkilainen, 2008a)

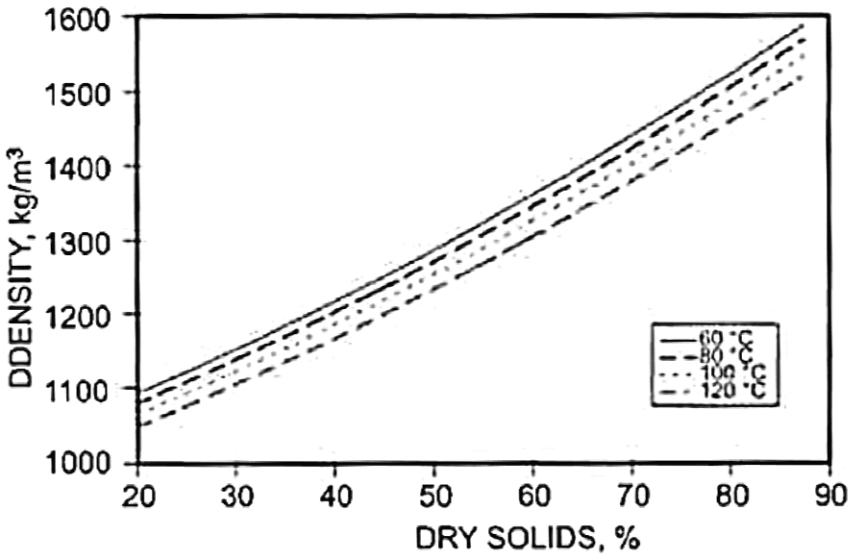

Figure 3. Density of black liquor presented with different black liquor dry solids content. (Vakkilainen, 2008a)

Surface tension is a variable, which affects the formation of black liquor droplet during fuel spraying in the boiler. Typical surface tension value for black liquor with dry solids content of 20 to 60 w-% is 0.025 N/m, being approximately the half of water surface tension. There is no specific data available for black liquors with higher solids content than 60 w-% due to the challenging measurement procedure. (Hupa & Hyöty, 2002; Vakkilainen, 2008a)

3.1.3 Heating value of black liquor

Heating value of black liquor indicates to the heat released during the combustion. Higher heating value (HHV) represents the heat released including the latent heat of evaporated vapor. Typical HHV value of black liquor is in the range between 13.4 and 15.5 kJ/kg of black liquor solids. The organic and inorganic content of black liquor can increase or decrease the HHV value, respectively. (Frederick & Söderhjelm, 1997)

3.2 Black liquor combustion

The combustion process of a black liquor droplet has been divided into three main phases: drying, devolatilization or pyrolysis, and char burning (Figure 4). Char burning ends, when particle structure collapses and smelt bead is formed. Thus smelt coalescence can be considered as the fourth stage of burning. (Frederick, et al., 1997)

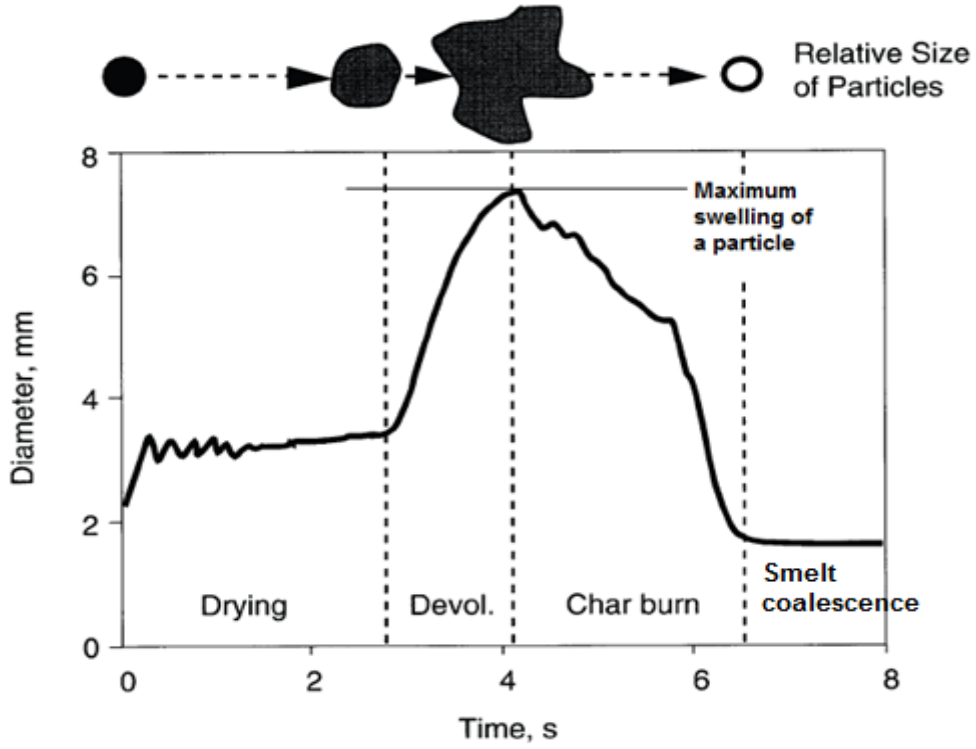

Figure 4. Combustion phases and the swelling of a black liquor particle during combustion, adapted from the figures of Hupa et al. (1987) and Hupa and Hyöty (2002)

In the beginning of the combustion water from black liquor droplet starts to evaporate leading to the drying of a droplet. Particle diameter expands in the beginning of drying due to the heating and boiling. Typical duration of droplet drying ranges between 0.5 and 3 seconds. In the end of drying phase the droplet is ignited and burned with a visible bright yellow flame. From this point the second phase – devolatilization or pyrolysis will start. (Hupa & Hyöty, 2002)

Great number of volatile organic gases, such as hydrogen, carbon monoxide, carbon dioxide, light hydrocarbons, tar, and light sulfur gases, are formed and released from the black liquor droplet during pyrolysis. Approximately 30 w-% of

black liquor dry solids are released as volatile gases. (Hupa & Hyöty, 2002) The amount of organic carbon in combusted black liquor is in the range between 5 and 30 w-% of original carbon in black liquor dry solids (Frederick & Hupa, 1991). Hupa and Hyöty (2002) estimate, however, the amount of carbon or char in combusted black liquor to be 20 w-%.

During pyrolysis the droplet swells extensively, leading three to four times greater growth of diameter than in the beginning of combustion (Hupa & Hyöty, 2002; Järvinen, et al., 2003). Due to the droplet swelling particle surface area and porosity are increased, which in turn will enhance mass and energy transportation, including reactivity and burning characteristics of black liquor. (Frederick, et al., 1997) The stage of pyrolysis will last approximately 0.5 to 2 seconds. (Hupa & Hyöty, 2002)

In the end of pyrolysis unburned carbon and the most of inorganic salts are remained in black liquor. During the next stage unburned carbon in char is burned, causing slow shrinking of black liquor droplet. (Frederick & Hupa, 1991; Hupa & Hyöty, 2002) Char combustion and its duration are dependent on the amount of oxygen around the black liquor particle. At high oxygen levels char burning of a 2-millimeter droplet lasts 2 to 5 seconds. If oxygen level is decreased, burning time will be prolonged for several tens of seconds. (Hupa & Hyöty, 2002) Finally, the structure of remained char particle collapses and it turns to molten smelt, containing mainly sodium sulfide (Na_2S) and sodium carbonate (Na_2CO_3). (Frederick & Hupa, 1991; Hupa & Hyöty, 2002)

4 CHAR BED CHEMISTRY

Char bed chemistry, including smelt reactions, is not completely known, even though the understanding of processes have been increased in recent years. A possible reason for the lack of proven data is the complex nature of smelt and char bed material. For instance the sampling of smelt is challenging, which may hinder the gain of reliable results and hence the determination of accurate composition. Additionally, the number of literature available and experts in the field are few.

A schematic flow diagram of the whole black liquor combustion process in the recovery boiler is presented in Figure 5. Air, make-up chemicals and as-fired black liquor are fed to furnace as inlet streams. As a result of combustion, smelt and flue gases are produced. In addition, produced heat is used for steam generation from feedwater. (Theliander, 2009)

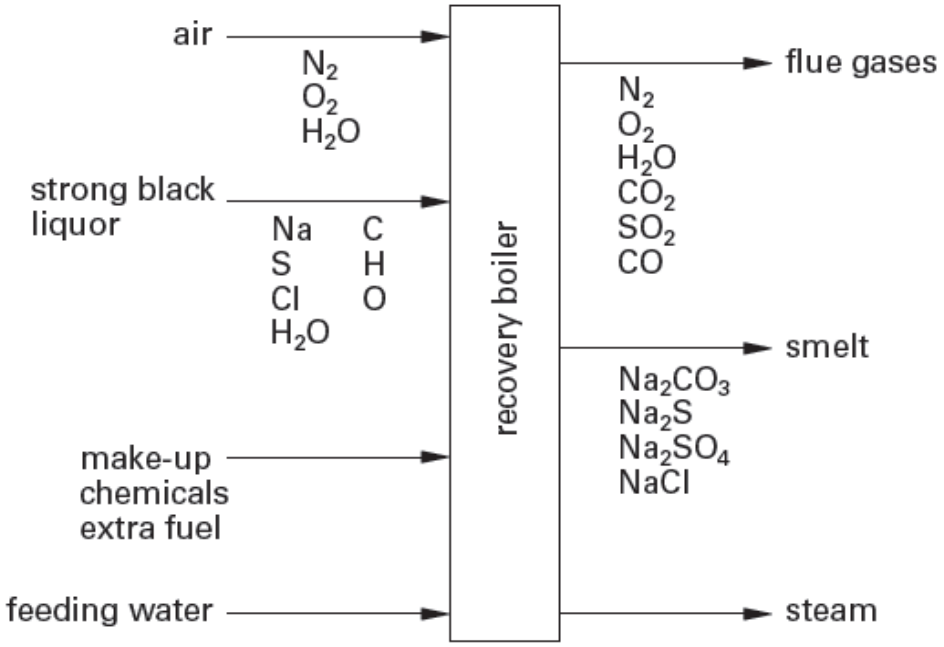

Figure 5. The schematic block diagram of recovery boiler reactants and end-products. (Theliander, 2009)

From chemical engineering point of view recovery boiler can be considered as a large chemical reactor (Hupa, 2004). Generally, the boiler furnace can be divided into three reactive zones: oxidation, drying, and reduction zone, in which main chemical reactions occur. Oxidation occurs above tertiary air level in the upper

part of the boiler furnace. Black liquor is dried in the levels of secondary and primary air. The completion of char combustion, reduction reactions and the recovery of inorganic compounds occur in the char bed. Thus reduction zone has a central role in the recovery boiler operation. (Biermann, 1996; Grace, 2004)

4.1 Oxidation and drying

Oxidation zone reactions are mainly related to flue gas formation and the oxidation of sodium and sulfur containing gases (Equations 1–4) (Biermann, 1996). Carbon monoxide, hydrogen sulfide and sodium sulfide gases are released from the lower part of the boiler and oxidized by oxygen from tertiary air, when reaching the upper part of the boiler. (Hupa & Hyöty, 2002) Sodium sulfide is converted back to sodium sulfate. Additionally, water vapor is formed. (Biermann, 1996)

$$CO + \frac{1}{2}O_2 \rightarrow CO_2 \quad (1)$$

$$H_2 + \frac{1}{2}O_2 \rightarrow H_2O \quad (2)$$

$$Na_2S + 2O_2 \rightarrow Na_2SO_4 \quad (3)$$

$$H_2S + 1\frac{1}{2}O_2 \rightarrow SO_2 + H_2O \quad (4)$$

Drying and pyrolysis of black liquor occur in the drying zone of the furnace. Water content of black liquor is evaporated, and volatile organic gases are released. Sodium hydroxide is reacted with carbon dioxide in order to form sodium carbonate and water vapor. (Biermann, 1996; Hupa & Hyöty, 2002)

$$\text{Organics} \rightarrow C + CO + H_2 \quad (5)$$

$$2NaOH + CO_2 \rightarrow Na_2CO_3 + H_2O \quad (6)$$

4.2 Char bed reactions – reduction and combustion

Char is mainly composed of organic carbon, sodium carbonate (Na_2CO_3), sodium sulfate (Na_2SO_4), and sodium sulfide (Na_2S). Additionally, char may contain small fractions of hydrogen, potassium and chloride, which are presented in the form of NaCl and KCl -salts. Small quantities of sulfite (SO_3^{2-}), thiosulfate ($S_2O_3^{2-}$), and polysulfide anions may also be presented in the char. (Grace, 2004; Vakkilainen, 2008b)

Char bed is composed of several physical layers. The upper layer is active, where combustion and reduction occur. Below the active layer is inactive core, which is consisted of colder solidified smelt and carbon. (Grace & Frederick, 1997; Tran, et al., 2015) Char has lighter density than smelt and it forms a sponge-like structure, which floats on the surface of smelt (Tran, et al., 2015). The porosity of char bed decreases, when moving towards the bottom of the furnace (Grace, 2004).

In the active bed layer temperature varies between the range of 1000 ºC and 1200 ºC. As the distance from the surface of the bed increases, temperature decreases until smelt solidifies approximately at 760 ºC. (Grace & Frederick, 1997) Typically, temperature of molten smelt flowing out of the furnace varies between the range of 800 ºC and 850 ºC (Taranenko, et al., 2014). Practical experience of the recovery boiler in operation, however, has shown that temperature of molten smelt may increase over 1000 ºC depending on smelt composition and boiler operation conditions (Vihavainen, 2016; Pakarinen, 2016). High smelt temperatures have been especially observed when smelt has flown poorly and there have been increased amount of unburned char mixed with smelt (Pakarinen, 2016).

Operation temperature of the lower furnace has a significant role in the formation of sodium thiosulfate ($Na_2S_2O_3$) and other salt fumes. According to Warnqvist (1992), Grace and Frederick (1997), low bed temperature, namely below 500 ºC, and high oxygen level may induce the formation of thiosulfate. At normal operation temperature thiosulfate is chemically unstable, and will be decomposed (Grace & Frederick, 1997). Hupa and Hyöty (2002) state, however, that the

increasing of bed temperature will induce the formation of sodium gases, but reduce sulfur gas release.

During boiler operation bed temperature may be affected by changing the composition and distribution of combustion air, increasing dry solids content of combustion liquors, and operating the boiler at overcapacity (Klarin, 1993). The control of black liquor droplet size sprayed into the boiler and combustion air distribution are the most central parameters in the adjustment of bed temperature (Pakarinen, 2016). During operation the increasing of local bed temperatures may change the porous structure of char and lead to formation of smelt pools, which may enhance the corrosion of boiler wall or floor tubes (Vihavainen, 2016).

Circumstances for the reduction are created optima by maintaining the amount of oxygen low in the lower part of the furnace. The active char layer prevents oxygen to react with smelt compounds, and hence enhances the reduction, since highly reduced char has a high tendency to react with oxygen spontaneously (Grace, 2004; Grace & Frederick, 1997). Organic carbon of char tends to react with sodium sulfate, Na_2SO_4, in order to form sodium sulfide, Na_2S. Increasing of oxygen level induces the formation of carbon oxides, which will be released as fuel gases from the surface of char bed. (Biermann, 1996; Vakkilainen, 2005; Vakkilainen, 2008b; Warnqvist, 1992)

Biermann (1996) states following reduction reactions occurring in the char bed:

$$\text{Organics} \rightarrow C + CO + H_2 \quad (7)$$

$$2C + O_2 \rightarrow CO \quad (8)$$

$$Na_2SO + 4C \rightarrow Na_2S + 4CO \quad (9)$$

$$C + H_2O \rightarrow CO + H_2 \quad (10)$$

Grace and Frederick (1997), however, determine the char burning process as a redox reaction, where oxygen is transported to char bed surface and reacts with sulfide to form sulfate, while sulfate is reduced by carbon to form CO, CO_2, and sulfide. Redox cycle is illustrated in Figure 6.

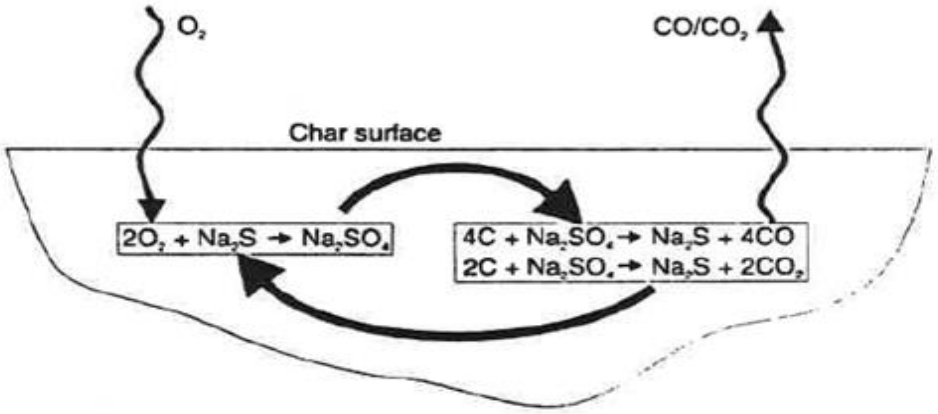

Figure 6. The sulfate-sulfide cycle occurring on the surface of kraft recovery boiler char bed. (Grace & Frederick, 1997)

As a conclusion, conversion of sodium salts (Equation 6) and reduction of make-up chemicals, namely sodium sulfate (Equation 9), can be stated to be the overall reactions of recovery boiler. (Biermann, 1996)

4.3 Thermal properties of char bed

The physical properties of char bed vary depending on the char bed layer and material. Typical values of char bed thermal properties are summarized in Table IV. Naturally, smelt occurring below the char layer has the highest density and heat capacity. Char, floating on the surface of smelt is lighter and works as an insulator. (Adams & Frederick, 1988)

Table IV The thermal properties of char bed, adapted from the table of (Adams & Frederick, 1988)

Material	Density, ρ [kg/m^3]	Heat Capacity, c_p [J/kg °C]	Thermal conductivity, k [W/m °C]	Thermal Diffusivity, α [m^2/s]
Inactive char	480–1330	1254	0.078	$0.5–0.75 \cdot 10^{-7}$
Active char	290–460	1254	0.28–0.38	$0.5–1.0 \cdot 10^{-6}$
Smelt, liquid	1923	1338	0.45	$1.81 \cdot 10^{-7}$
Smelt, solid	2163	1421	0.882	$2.84 \cdot 10^{-7}$

4.4 Reduction rate and reduction efficiency

Traditionally, reduction reaction can be estimated by reduction rate (Equation 11) and reduction efficiency (Equations 12 and 13). Reduction rate is dependent on char bed temperature and carbon content. (Vakkilainen, 2008b) The reduction rate increases linearly along the growth of char carbon content, and is doubled, if temperature is increased with 60 °C (Adams & Frederick, 1988; Hupa & Hyöty, 2002).

$$\frac{\partial[SO_4]}{\partial t} = K_{red}\frac{[SO_4]}{B+[SO_4]}[C]e^{-\frac{E_a}{RT}} \quad (11)$$

where B an empirical constant, 0.022 ± 0.008 kmol/m^3

[C] carbon concentration of smelt, kmol/m^3

E_a activation energy, 122 kJ/kmol

K_{red} pre-exponential factor for sulfate reduction, 1.31 ± 0.41 ·10^3 1/s

R ideal gas constant, 8.314 kJ/kmolK

[SO] sulfate concentration of smelt, kmol/m^3

T temperature, K

(Vakkilainen, 2008b)

$$\eta_{reduction} = 100\left(\frac{[S_{tot}]-[SO_4]}{[S_{tot}]}\right) \quad (12)$$

where $\eta_{reduction}$ fractional sulfur reduction efficiency

$[S_{tot}]$ total concentration of sulfur in smelt

$[SO_4]$ concentration of sulfate in smelt

(Adams & Frederick, 1988)

Smelt reduction may also be expressed as a molar ratio of sodium sulfide and sodium carbonate. Typically, Equation 13 is used for the determination of reduction degree from green liquor. It should be noticed, however, that reduction degrees determined from green liquor analysis are usually few units of percentage

lower than the reduction degrees measured from smelt. (Engdahl, et al., 2008; Vakkilainen, 2005; Vakkilainen, 2008b)

$$\text{Reduction} = \frac{Na_2S}{(Na_2S+Na_2SO_4)} \quad (13)$$

where Na_2S the amount of sodium sulfide, mol

Na_2SO_4 the amount of sodium sulfate, mol

The reduction efficiency is dependent on the amount of char and smelt residence time in the char bed. Warnqvist (1992) investigated char bed and smelt properties at Swedish pulp mills. He states that the amount of char varies from 5 to 20 w-% of insoluble residue in different parts of the bed.

According to Warnqvist (1992) the sufficient amount of char in output smelt required to reduce all sulfur is expected to be above 7 w-%. Carbon is the active compound of char participating in sulfur reduction reaction. Aho and Saviharju (2007) investigated the effect of carbon in smelt on smelt reduction based on the experimental studies performed at 15 different recovery boilers (Figure 7). It was discovered that sufficient reduction is achieved more likely, when the amount of smelt carbon is higher (Aho & Saviharju, 2007). Even though high reduction is a desirable feature in boiler operation, great amount of carbon in smelt will be transferred to green liquor, which increases the amount of green liquor dregs, and hence solid waste output of the mill. Great amount of carbon or dregs may also cause problems in the recausticising plant.

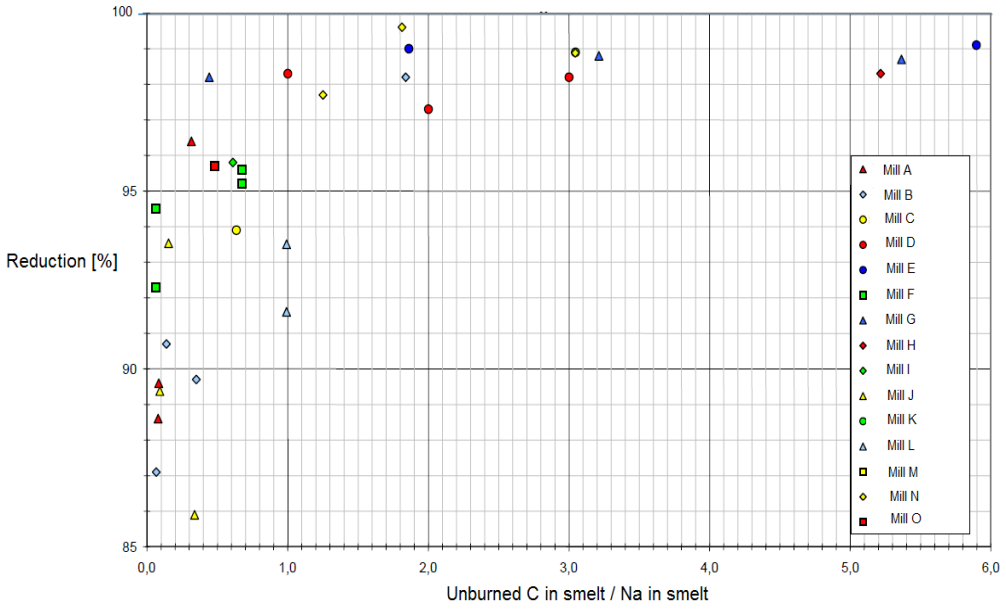

Figure 7. The effect of carbon in smelt on smelt reduction. (Aho & Saviharju, 2007)

Additionally, the amount of smelt carbon is one of the indicators describing the boiler efficiency. Increasing of carbon content will decrease the boiler efficiency in terms of heat recovered, even though the reduction efficiency is increased. (Grace & Frederick, 1997; Warnqvist, 1992) Boiler efficiency is reduced, when excess carbon passes the boiler without burning, and won't release its enthalpy into flue gas. Thus the amount of flue gas enthalpy is reduced, leading to less amount of available energy for steam and electricity generation. (Pakarinen, 2016) Typically, the reduction efficiency ranges between 95–98 mol-% in modern well operating kraft recovery boilers (Vakkilainen, 2005). The rate of reduction decreases as the efficiency increases over 95 mol-% (Biermann, 1996; Vakkilainen, 2005; Vakkilainen, 2008b).

In practice smelt reduction efficiency is recommended to estimate regularly from every spout for controlling purposes. Smelt samples tend to oxidize easily, and hence sampling procedure has to be performed carefully. (Oy Keskuslaboratorio - Centrallaboratorium Ab , 1993) Alternatively, smelt reduction is possible to estimate visually. During boiler operation, smelt sample for reduction analysis is taken with a special rod tool, which is fed into a smelt spout. After sampling, the reduction degree can be estimated from the colour of the sample (Figure 8). The

higher the reduction efficiency, the lighter or more grey is the color of the sample. Red or reddish brown colour of the sample indicates to oxidized smelt, and hence poor reduction. Black residue on the surface of samples is unburned carbon. (Pakarinen, 2016; Vihavainen, 2016)

Figure 8. Smelt reduction samples of a certain recovery boiler, with boiler load of 1100 tDS/d and with different distribution of combustion air. The amount of total air and steam were maintained constant during every sampling. Grey or lighter red colour of the sample indicates the reduction efficiency degree, which is increasing from left side sample A to C. Right side sample A has a good reduction, since it contains unburned carbon, occurring as black residue on the surface of the sample. The amount of primary air fed to boiler is the lowest in case A sample, and the highest in case B. The amount of tertiary air was increased as a relation to primary and secondary air in every case. The highest tertiary air condition was in case A, and the lowest in case B. (Andritz Oy , 2015)

5 GREEN LIQUOR BALANCE OF KRAFT RECOVERY BOILER

Green liquor balance of recovery boiler can be limited to the area of dissolving tank. However, in order to understand dissolving tank operation more deeply, one has to widen perspective further in the boiler performance. For instance, black liquor properties and combustion, including amount of air and auxiliary fuels fed to boiler, will affect smelt formation and composition. Thus they have major effect on dissolving tank balance. Similarly, weak white liquor fed to the tank from recausticising plant will affect the vent gas formation and dissolving tank temperature.

The boundaries of the kraft recovery boiler green liquor system can be stated to begin from the lower part of the boiler, where from smelt runs off to dissolving tank via smelt spouts, and end to vent gas scrubber above the tank and green liquor lines surrounding the tank. Smelt flow in the smelt spouts is cooled down by cooling water circulation and shattered with steam jets in order to prevent explosions in the dissolving tank. In the dissolving tank smelt is mixed and dissolved in weak white liquor (WWL) in order to produce green liquor, which is fed back to recausticization. (Tran, et al., 2015) Vents produced during the dissolution are sucked to vent stack, where from they are fed to vent gas scrubber for purification and drying. The schematic configuration of boiler furnace bottom area, dissolving tank and vent stack leading to the vent gas scrubber are illustrated in Figure 9.

In this chapter smelt and its properties have been discussed based on literature available. Dissolving tank balance has been discussed more detailed in the experimental part of this work.

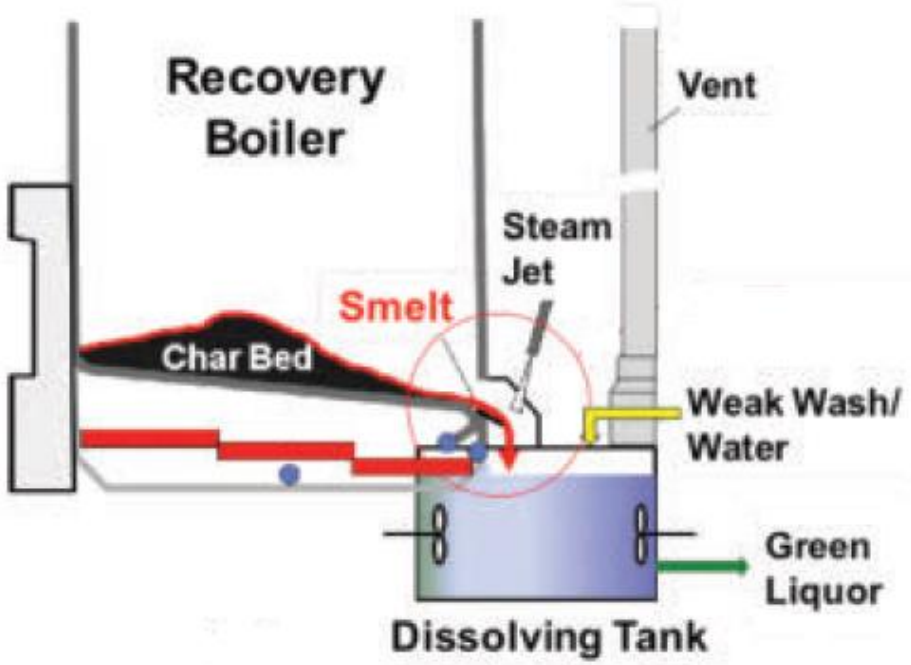

Figure 9. The schematic configuration of kraft recovery boiler lower furnace, dissolving tank, and vent stack leading to the vent gas scrubber (Tran, et al., 2015)

6 THEORY OF KRAFT RECOVERY BOILER SMELT

Smelt is produced via two different routes during char bed processing. First, smelt is bound to solid char, containing carbon. During char combustion the most of carbon is burned to carbon monoxide and carbon dioxide, leading to the release of liquid smelt from the char net. The amount of released smelt is increased as more carbon is burned. Eventually, molten smelt starts flowing off the surface of char and is concentrated near the bottom of the furnace, where from it flows towards smelt spouts due to gravity. (Grace, 2004)

Secondly, smelt is formed during melting of frozen smelt. Generally, frozen smelt can exist in the wall of upper furnace or formed due to low temperature conditions of the furnace. The melting of frozen smelt will occur rapidly, when the temperature of bed is increased over the minimum melting point of smelt. (Grace, 2004; Grace & Frederick, 1997)

6.1 Smelt composition

Smelt flowing out of boiler furnace is mainly composed of sodium carbonate and sulfide, since the most of organics are combusted in the char bed (Jin, et al., 2013; Vakkilainen, 2009). The detailed composition of smelt is dependent on wood species used, black liquor sulfidity, temperature conditions of char bed and the addition of auxiliary fuel (Tran, et al., 2015).

Typical composition of smelt from soft- and hardwood are presented in Table V. Other compounds of smelt are unburned carbon, sodium and potassium chlorides. In addition small traces of other potassium salts and sodium borates may occur. (Vakkilainen, 2009) The concentration of sodium thiosulfate is low due to its poor chemical stability under normal smelt running out temperatures (800–850 °C) (Grace & Frederick, 1997), as discussed in chapter 4.2.

Table V Typical composition of smelt, adapted from the table of (Vakkilainen, 2009)

Compound	Softwood [w-%]	Hardwood [w-%]
Na_2S	25–28	19–21
Na_2CO_3	66–68	72–75
Na_2SO_4	0.4–1.0	0.6–1.4
$Na_2S_2O_3$	0.3–0.4	0.2–0.4
Others	5.0–6.0	3.0–5.0

6.1.1 Sulfidity and melting properties of smelt

The most important parameter expressing the composition of smelt is sulfidity, which can be determined as either the molar ratio of sodium sulfide to the total alkali content (Equation 14) from black liquor or the ratio of Na_2S to active alkali (Na_2S + NaOH) in molar equivalents from white liquor (Equation 15) (Engdahl, et al., 2008; Tran, et al., 2015; Vakkilainen, 2005). Even though both equations represent the sulfidity of smelt, their meaning differs from each other. Generally at mills, while discussing about sulfidity, it is typically referred to Equation 15 (Pakarinen, 2016).

$$\text{Sulfidity} = \frac{S_{tot}}{Na_2+K_2} \cdot 100\ \% \quad (14)$$

where S_{tot} the total amount of sulfur, determined as sodium sulfide, in molar equivalents, mol

Na_2 the amount of sodium, in molar equivalents, mol

K_2 the amount of potassium, in molar equivalents, mol

$$\text{Sulfidity} = \frac{Na_2S}{Na_2S+NaOH} \cdot 100\ \% \quad (15)$$

where Na_2S the amount of sodium sulfide, in molar equivalents, mol

NaOH the amount of sodium hydroxide, in molar equivalents, mol

Sulfidity, depicted in Equation 14, is dependent on black liquor circulation at mill. According to Tran et al. (2009) typical sulphide content of smelt, expressed as S/Na_2+K_2, is approximately 30 mol-%, and may vary between the range of 20 and 45 mol-%.

Ideally, smelt running out from the furnace is composed of Na_2S and Na_2CO_3. In reality smelt has multicomponent system, which behavior with different mole fractions and temperatures is difficult to predict. Thus for simplification, smelt phase diagrams are usually presented either as binary or ternary systems. (Karidio, et al., 2004; Lindberg, et al., 2007)

The phase diagram of Na_2CO_3–Na_2S system is presented in Figure 10. The eutectic point, where the liquidus and solidus temperatures of the system are the same, is reached at 762 °C. Solidus temperature of smelt is defined as the freezing point of smelt. (Karidio, et al., 2004; Tegman & Warnqvist, 1972) The solidus temperature of binary Na_2CO_3–Na_2S system is presented as a horizontal line. Liquidus temperatures represent the melting temperatures of the smelt, and are presented with a scatter and a trend line in Figure 10. (Karidio, et al., 2004) According to Karidio et al. (2004) the eutectic nature of smelt systems is commonly observed among researched molten smelts.

The determination of accurate smelt solidus temperatures is challenging due to difficult sampling, and uncertainty of measuring results (Lindberg, et al., 2007; Tran, et al., 2004). Additionally, the solidus temperature is strongly dependent on smelt composition (Karidio, et al., 2004). Karidio et al. (2004) states the range of the solidus temperatures to be between 712 °C and 762 °C. Tran et al. (2004), however, estimate the range of solidus temperature a slightly higher − between 740 °C and 780 °C − for smelt, containing 60–70 w-% of Na_2CO_3, 20–30 w-% of Na_2S, and small fractions of Na_2SO_4, NaCl, potassium salts, and char.

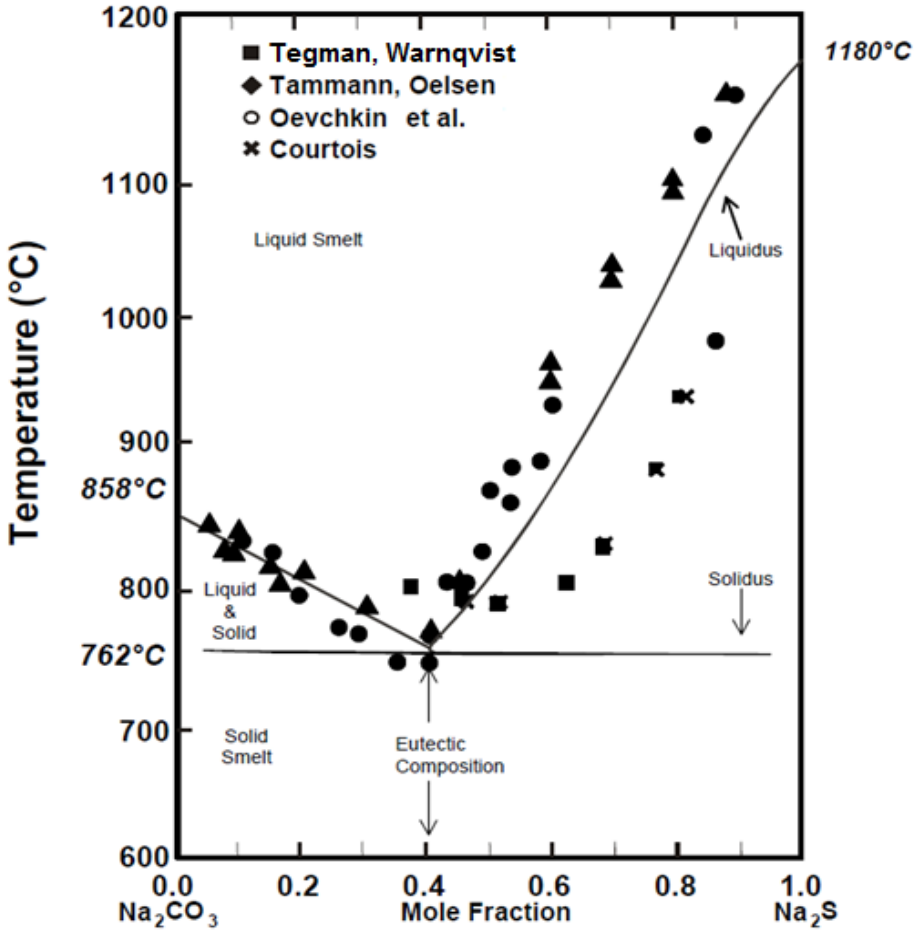

Figure 10. Phase diagram of Na_2CO_3–Na_2S system. Data points from laboratory studies of Tegman & Warnqvist (1972), Tammann & Oelsen (1930), Oveshkin et al. (1971), and Courtois (1939) and predicted melting points (liquidus temperatures) are expressed with symbols. The horizontal line represents the solidus temperature or freezing temperature of the system. The eutectic point (762 °C) of binary system is reached with sulfidity of 40 %. Adapted from the figure of (Karidio, et al., 2004)

Sulfidity of the salt blend in the eutectic point is 40 %. Liquidus temperature of smelt is decreasing, while sulfidity converges to the eutectic point. As mole fraction of Na_2S exceeds 40 %, liquidus temperature increases rapidly. Thus in modern kraft mills the sulfidity of smelt is recommended to maintain under 40 % during operation, since the tendency of smelt freezing is then lower. (Karidio, et al., 2004; Kubiak, 1973; Lindberg, et al., 2007; Tran, et al., 2015)

Sulfidity has the greatest effect on smelt melting temperature. Calculated phase diagrams for the ternary or three component system of smelt are presented in Figure 11. The boundary temperatures of ternary system are shown in the axis of phase diagram in Figure 11A. The melting temperatures of eutectic blends are plotted as vertical lines drawn along the curved line. The melting points of the ternary system are presented in Figure 11B. To maintain smelt in a liquid stage the operation temperature of smelt should be higher than the liquidus temperature of the system. (Karidio, et al., 2004)

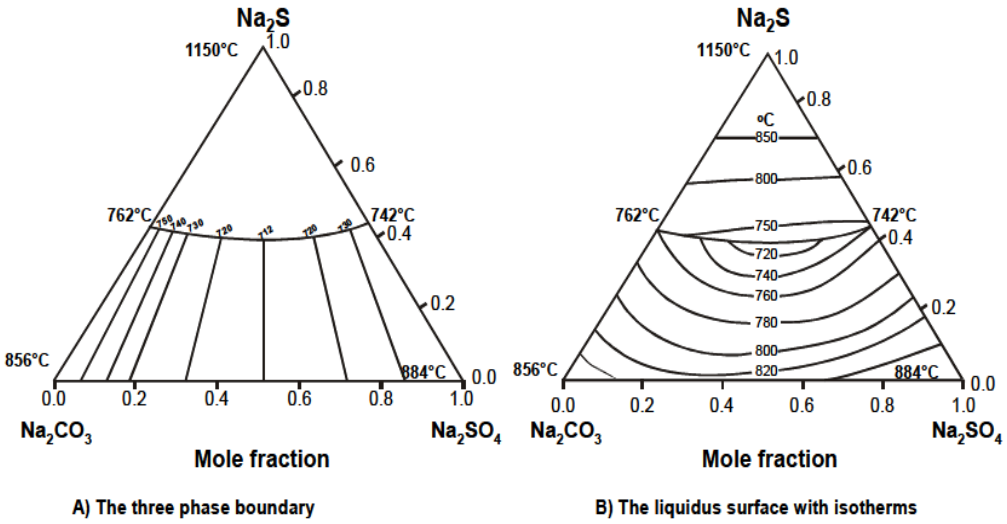

Figure 11. The phase diagram of the ternary system Na_2CO_3 – Na_2SO_4 – Na_2S, where the boundary temperatures (a) and liquidus temperatures (b) are presented. (Karidio, et al., 2004)

In addition to the melting point and smelt flowing properties, sulfidity is closely related to other variables in boiler operation. According to Karidio et al. (2004) sulfidity may be increased temporarily due to the high flows of recycled electrostatic precipitator (ESP) ash. Slight increase in sulfidity may also be observed due to the use of start-up oil burners and boiler upsets. High bed

temperatures increase the reduction efficiencies, and hence increase the sulfidity of smelt. Conversely, the increasing of boiler reduced sulphur gas emissions decrease the sulfidity. (Karidio, et al., 2004)

6.2 Chemical thermodynamics of smelt

Typical values of smelt compound melting enthalpies and specific heat capacities are presented in Table VI. Specific heat capacity of 0.94 kJ/kg °C may be used for compounds, which are not listed below. Similarly, the melting enthalpy of 200 kJ/kg and the specific enthalpy of 1350 kJ/kg may be used. (Vakkilainen, 2009)

Table VI Typical melting enthalpies, specific heat capacities, and enthalpies of smelt components, adapted from the table of (Vakkilainen, 2009)

Component	**The melting enthalpy of smelt component at 25 °C, h_m [kJ/mol]**	**The specific heat capacity of smelt component, c_p [kJ/mol °C]**	**The specific enthalpy of smelt component at 850 °C, h_c [kJ/mol]**
Na_2CO_3	29.7	0.157	163.4
Na_2S	19.2	0.096	100.7
Na_2SO_4	23.8	0.188	183.4
NaCl	28.3	0.063	81.6
$Na_2S_2O_3$	29.7	0.133	142.9
K_2CO_3	27.9	0.159	163.3
K_2S	16.2	0.098	99.2
K_2SO_4	34.4	0.187	193.5
KCl	14.9	0.075	97.2
$NaBO_2$	15.7	0.088	90.3
Na_3BO_3	20.1	0.141	139.5

6.3 Smelt rheology

From the dissolving tank operation point of view, a steady flow of smelt ensures the uniform composition of green liquor and prevents hazardous smelt-water interactions. The main variable affecting to smelt flowing properties is viscosity. Low-viscous smelt is usually desirable due to its good fluidity and shattering properties. (Tran, et al., 2015) Highly viscous molten smelt or also called "jelly-roll" smelt has a viscoelastic nature, which is thickened due to the shear stress. Due to its high viscosity, jelly-roll smelt may plug smelt spouts, and hence increase the risk of smelt-water explosions. (Tran, et al., 2004)

Smelt viscosity depends on bed temperature, sulfidity and smelt composition. Tran et al. (2004) investigated the viscosity and flowing properties of smelt in order to examine jelly-roll phenomena and discover solutions to prevent that. They discovered that viscosity of smelt increases rapidly, when smelt temperature reaches the solidus temperature range of smelt (Figure 12).

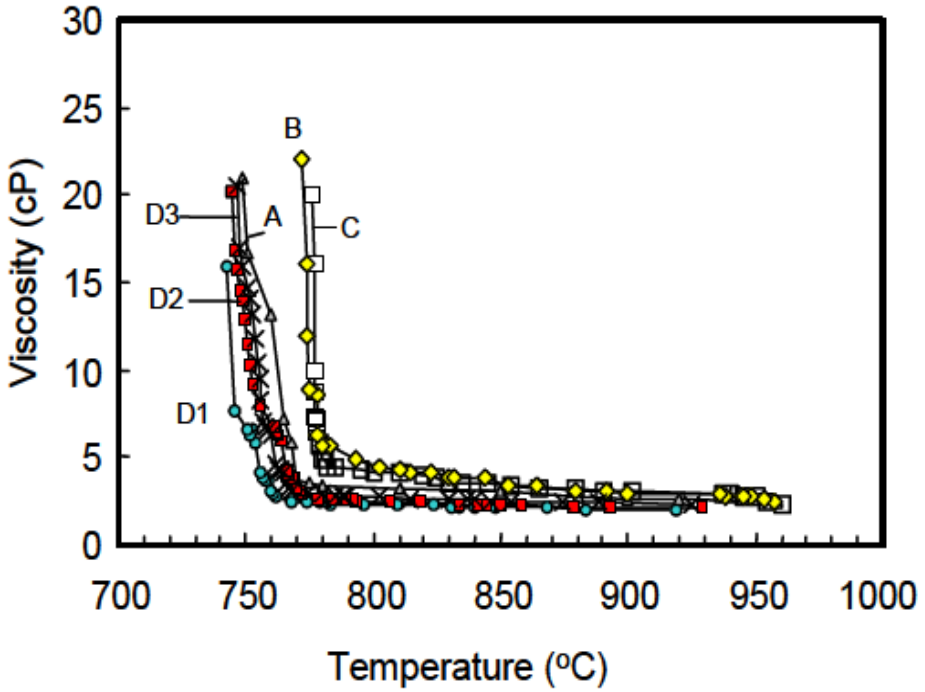

Figure 12. The effect of smelt temperature on viscosity. Viscosity of smelt decreases rapidly, as the breakpoint temperature range (765–780 °C) is reached. (Tran, et al., 2004)

The melting point of smelt has also an effect on smelt viscosity. According to Karidio et al. (2004) smelts that have higher liquidus temperatures, have typically higher viscosities.

Conversely, the reliance between sulfidity and viscosity is not equally clear. Klarin (1993) gathered data from Scandinavian pulp mills between years of 1987 and 1992 in order to examine the floor tube corrosion at boilers. She discovered that the viscosity of smelt decreases approximately 50 %, as sulfidity increases from 30 mol-% to 40 mol-%. Additionally, the increasing of potassium content in smelt was discovered to decrease smelt viscosity (Figure 13). (Klarin, 1993)

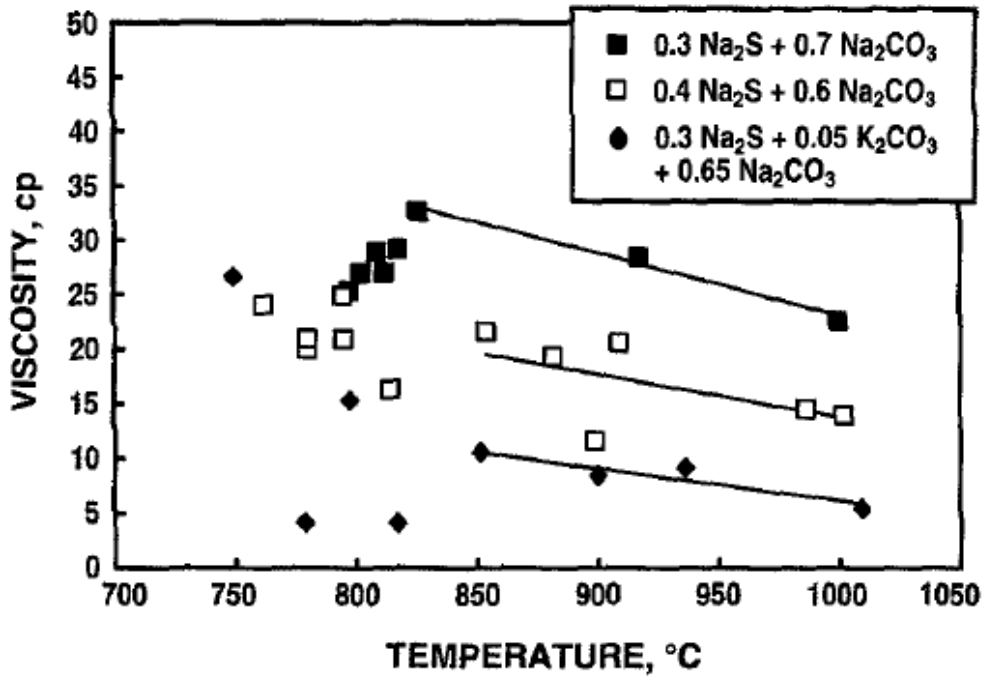

Figure 13. The viscosity of smelt binary system Na_2S – Na_2CO_3 at sulfidity levels of 30 % and 40 % at different temperatures. As a reference smelt composition with 5 mol-% of potassium substitution is presented. (Klarin, 1993)

6.4 Smelt flowing properties

During normal operation the amount of smelt flow varies depending on the char bed height and black liquor spraying (Vihavainen, 2016). The average smelt flow rate is stated to be approximately 45 % of virgin black liquor solids firing rate. The smelt flow rate depends on the number of spouts and may range between 0.7 and 1.3 l/s, but the average flow rate of 1 l/s is normally estimated (Jin, et al.,

2013; Tran, et al., 2015). However, smelt flow rates per spout greater than 1.5 l/s have been determined for the modern boilers operated with higher loads (Pakarinen, 2016). During boiler operation smelt flows out independently without direct flow control, which hinders the control of dissolving tank operation (Tran, et al., 2015).

Thus prevention of excess smelt flows – *heavy run offs* is a critical issue in boiler operation. Main reasons for heavy run offs are the plugging of smelt spouts and the increasing of char bed height. Other explanations for heavy run offs are a sudden collapse of the char bed, the misuse of auxiliary fuels, the variations of liquor sulfidity levels, and misuse of combustion air. Additionally, the shape of furnace floor may increase the tendency of heavy run off (Figure 14). (Frederick, et al., 2011; Taimisto, 1975; Tran, et al., 2015)

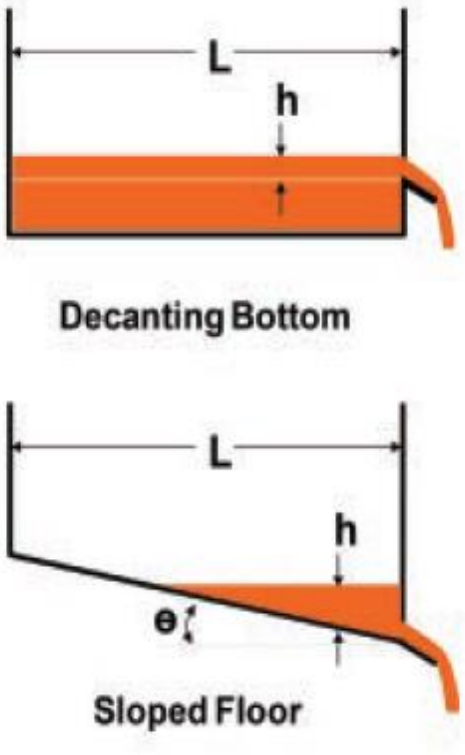

Figure 14. The shapes of boiler furnace hearth: decanting and sloped floor bottoms. The height of smelt pool is depending on the inclination angle of the floor. The higher the angle, the higher the local height of smelt pool and hence higher risk for smelt run off. (Tran, et al., 2015)

The cause for smelt run off is typically the accumulation of smelt in the bottom of the furnace or the drop of smelt slag from the furnace walls into the bed. Tran et

al. (2015) presented in their research the number of smelt-water explosions as a function of the furnace hearth shape. Typical hearth shapes were: sloped, decanting and partial or V-shaped floors. Sloped floors were stated to be more vulnerable to smelt run offs, and hence dissolving tank incidents than other floor shapes. The vulnerability can be explained by the acceleration of smelt flow as the slope of the floor is increased. The tolerance against run offs may be increased by increasing the number of spouts, which also ensures the boiler operation with higher firing capacities. (Tran, et al., 2015)

Typical responses against excess smelt flows are: the reducing of black liquor firing rates, which in turn reduces the formation of smelt, the addition of auxiliary fuel near spouts, and the adjustment of smelt shattering jets. Additionally, bed shape and size may be controlled by adjustment of combustion air distribution, liquor spraying, and air dampers. (Tran, et al., 2015; Pakarinen, 2016)

7 DISSOLVING TANK

Dissolving tank has a significant role in boiler operation and safety. Despite of its importance the lack of proper knowledge about the operation such as smelt flowing properties, mass and energy balance, and solubility of smelt components in green liquor and their thermodynamics, is obvious. Additionally, the number of studies made related to the topic has been few. (Grace & Tran, 2010)

The principle of dissolving tank operation is rather simple. Smelt enters the dissolving tank via smelt spouts. Before reaching the tank smelt flow is shattered with medium pressure steam in order to prevent smelt-water interactions and lessen noise. Smelt spouts are also cooled with warm water due to risk of NaOH - corrosion. In the dissolving tank dispersed smelt is dissolved into weak white liquor (WWL) pumped from the recausticising plant in order to form green liquor. Produced green liquor is pumped then back to recausticization for further processing. The level of dissolving tank and green liquor density are monitored carefully during the process. While green liquor is pumped out of the tank, weak white liquor is fed to the dissolving tank for replacement. (Vakkilainen, 2005)

Figure 15 illustrates a schematic material and energy balance of dissolving tank. Traditionally dissolving tank contains two green liquor lines, which are used in turns in order to prevent the precipitation of pirssonite being the main cause of pipeline scaling. As one green liquor line is on operation, weak white liquor is fed to the tank in reverse direction via other line. (Grace & Tran, 2010; Vakkilainen, 2005)

During smelt dissolution water is evaporated, leading to vent gas formation. Vent gases are drawn to vent gas scrubber via dissolving tank vent stack. Before entering the scrubber, gas flow is pre-washed with water in order to reduce part of gas moisture and carbonate residue. The quality of water added to dissolving tank varies from mechanically purified water to chemically purified, so called demineralized water. The main purpose of inlet water streams are to work as back-up fire water used for controlling green liquor density in case of close-up of WWL line. Condensates from the scrubber and pre-wash of the vent stack are also normally reversed into the tank. Air leaks in the tank due to smelt spout openings. The most of leaked air is removed from the tank with aid of vent gas fan locating after the scrubber. (Andritz Oy, 2016b)

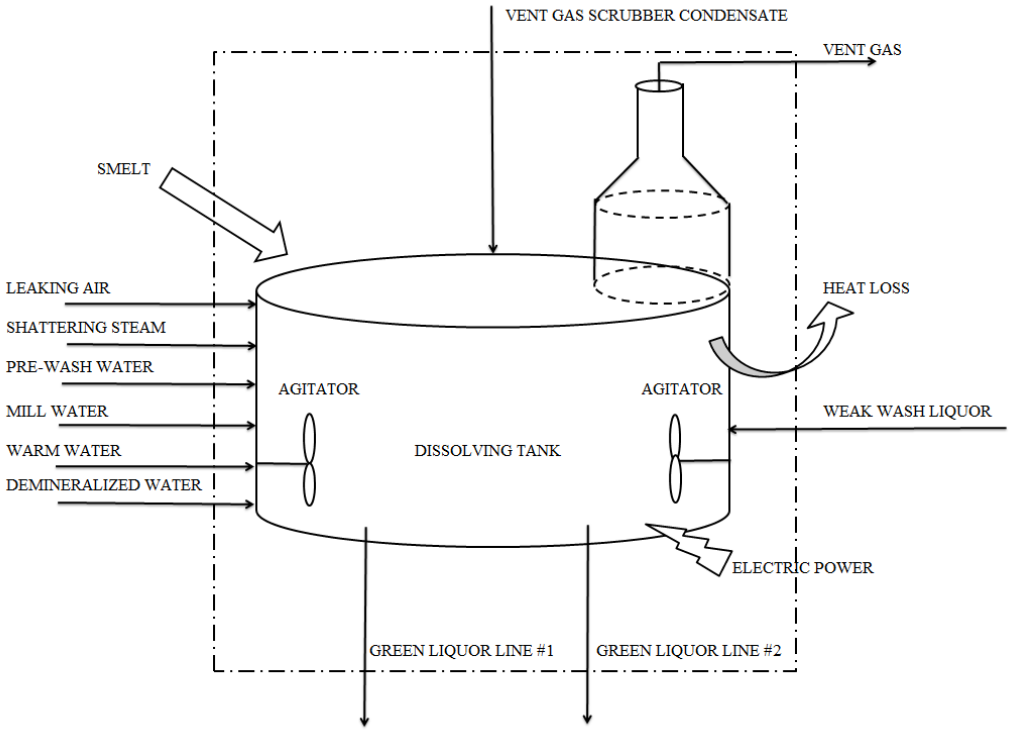

Figure 15. Mass and energy balance of kraft recovery boiler dissolving tank.

In modern kraft recovery boilers oval-shaped or octagon-shaped dissolving tanks have been used. In addition to oval-shaped tanks, rectangular with rounding-off corners have been used. However, their popularity has been decreased due to poorer mixing properties than in oval-shaped dissolving tanks. (Ljungvist & Theliander, 1996; Sebbas, et al., 1983)

Dissolving tanks are insulated with concrete sealing due to violent conditions and possible hazardous reactions occurring during the smelt dissolution. Generally tanks are made of either acid-proof stainless steel or carbon steel, and consist typically equal or more than two impellers. The number and positioning of impellers used are dependent on the boiler size and design. (Heinola, 2016) Agitators are used for ensuring faster cooling of smelt and a proper dispersion of shattered smelt into weak wash/green liquor solution. In addition to dispersing of smelt, agitators are used for preventing deposit formation, such as pirssonite formation, in the tank. (Frederick, et al., 2011; Salmenoja & Kosonen, 1996)

From the dissolving tank operation point of view, adequate process control system is required for ensuring the safety of operation and monitoring of vents. Main parameters to be monitored are dissolving tank temperature, green liquor density, and tank liquid level. The temperature of dissolving tank is dependent on the temperature and amount of weak white liquor and smelt. In practice, however, the control of mentioned variables is challenging due to unsteady smelt flow. Thus quick-response measurement controls are required. (Frederick, et al., 2011)

The density of green liquor is typically controlled continuously by adjusting the amount of weak white liquor flow. Green liquor and weak white liquor flows are also continuously adjusted in order to prevent high liquid level in the tank. (Frederick, et al., 2011)

7.1 Green liquor

Green liquor produced in the dissolving tank contains mainly sodium sulfide and sodium carbonate in aqueous solution. The detailed composition of green liquor is presented in Table VII. (Frederick, et al., 1996)

Table VII Typical green liquor compositions, adapted from the tables of (Engdahl, et al., 2008; Frederick, et al., 1996)

Reference	**Green liquor composition acc. Frederick et al. (1996)**		**Green liquor composition acc. Engdahl et al. (2008)**	
Green liquor analysis	**g Na_2O/L**	**g NaOH /L**	**g Na_2O/L**	**g NaOH /L**
Suspended solids	–	–	0.47–0.54	0.6–0.7
NaHS	31.2	40.3	–	–
Na_2S	–	–	39–50	50–65
NaOH	14.6	18.8	4–19	5–25
Na_2CO_3	74.2	95.7	78–101	100–130
Na_2SO_4	3.3	4.3	3–6	4–8
$Na_2S_2O_3$	3.3	4.3	–	–
NaCl	4.8	6.2	–	–
Other compounds	–	–	5–10	6–13

Green liquor physical properties vary depending on the composition and temperature of liquor. Typically the temperature range of green liquor is from 80 °C to 103 °C (Engdahl, et al., 2008; Pakarinen, 2016). Density varies between the range of 1.12 and 1.20 kg/L. Density of green liquor may also be determined as total titratable alkali (TTA), which is expressed in terms of NaOH or Na_2O molar equivalents. (Engdahl, et al., 2008) TTA-content of green liquor ranges from 105 to 140 g Na_2O/L (DeMartini, 2009).

$$\mathrm{TTA} = [\mathrm{NaOH}] + [\mathrm{Na_2CO_3}] + [\mathrm{Na_2S}] \quad (16)$$

where [NaOH] sodium hydroxide concentration, g NaOH/L or g Na_2O/L

[Na_2CO_3] sodium carbonate concentration, g NaOH/L or g Na_2O/L

[Na_2S] sodium sulfide concentration, g NaOH/L or g Na_2O/L

(DeMartini, 2009)

Even though TTA (total titratable alkali) and green liquor density are directly proportional to each other, green liquor dregs won't affect green liquor TTA value. As the amount of dregs increases, the density of green liquor increases, while TTA remains the same. (Salmenoja & Kosonen, 1996)

Viscosity and heat capacity are determined as 0.9 cP at 90 °C and 3.3–3.8 kJ/kgK, respectively. (Engdahl, et al., 2008) Green liquor boils approximately between the range of 102 °C and 104 °C. When dissolving tank temperature exceeds the boiling point of green liquor, the vaporization of liquor fastens, and hence greater amount of vent gas is produced. (Pakarinen, 2016)

7.2 Weak white liquor

Main compounds of weak white liquor pumped from the recausticising plant are sodium hydroxide and sodium carbonate in aqueous solution (Frederick, et al., 1996). The rest components of weak white liquor are presented in Table VIII.

Table VIII Typical composition of weak white liquor (Frederick, et al., 1996)

Weak white liquor analysis	g Na_2O/L	g NaOH /L
NaHS	6.2	8.0
NaOH	14.6	18.8
Na_2CO_3	74.2	95.7
Na_2SO_4	0.7	0.9
$Na_2S_2O_3$	0.7	0.9
NaCl	1	1.3

From dissolving tank operation point of view the most significant physical property of weak white liquor is temperature. It has an effect on green liquor temperature, and hence on the temperature of dissolving tank and the amount of vents produced. (Pakarinen, 2016; Vihavainen, 2016) In literature the temperature of weak white wash has been determined between the range of 50 and 60 °C (Engdahl, et al., 2008), but in practice temperature range may be wider, from 50 to 70 °C (Andritz Oy, 2016a). The density of weak white liquor is near the density of water (Pakarinen, 2016), ranging approximately from 1.01 to 1.04 kg/L.

7.3 Dissolving tank emissions

Dissolving tank venting is rarely studied or discussed in literature. Thus the understanding of causes for vent gas formation, the control of dissolving tank operation during unsteady smelt flow, and their impacts on the capacity of vent gas scrubbing system have become an important topic. Dissolving tank emissions can be roughly divided either in gas emissions or solid residues, such as dust in gas flow or dregs precipitated in the solution. At modern boilers gas emissions are not considered as a problem, since they are usually combusted with air in the

furnace after scrubbing. Dregs, however, are still considered as a challenge due to their tendency of accumulation in the recausticization.

Dissolving tank vent gas contains mainly air and steam. The source of air in vent gas are the smelt spout openings, where from air leaks to dissolving tank due to the under pressure occurring in the vent stack and the vent gas scrubber inlet. Evaporated vapor of vent gas is mainly produced, when smelt with high enthalpy is dissolved into cooler weak white liquor. Vapor is also produced due to the shatter jet steam used for atomization of smelt in the spouts. (da Silva Medeiros, et al., 2002)

In addition to air and steam, vent gas produced contains also relatively high amount of total reduced sulfur compounds (TRS gases) and solid particulates. (da Silva Medeiros, et al., 2002) da Silva Medeiros et al. (2002) compared the dissolving tank vent stack emissions to boiler main stack emissions. The compositions of both vents are presented in Table IX. Operational values were given for a kraft recovery boiler with capacity of 2000 tDS/d. TRS content of dissolving tank vent gas ranged typically from 5 to 50 ppm, and dust content of vent gas was 8 kg/h or approximately 160 mg/m^3n.

Table IX Typical composition of vent gas determined from kraft recovery boiler main stack and dissolving tank vent stack. The capacity of the boiler is 2000 tdS/d. Adapted from the table of (da Silva Medeiros, et al., 2002)

Vent gas analysis	Unit	Boiler main stack	Dissolving tank vent stack
Gas flow	m^3n/s	100	14
TRS content	ppm	<1	5–50
	kg/h	0.4	1.3
Particulate content	kg/h	8	8

Solid particulates of vent gases are mainly composed of the same compounds presented in smelt and green liquor, which are solidified due to the cooling of vent gas temperature (Rantanen, 1986). The amount of solid particulates presented by da Silva Medeiros et al. (2002) is low when compared to the results of Rantanen (1986), who studied vents of three Finnish recovery boilers. According to

Rantanen (1986) solid particulate content of untreated vent gas may vary between the range of 550 and 5700 mg/m^3n.

The amount of vent gas dust is dependent on smelt flow into the dissolving tank and its operation. Naturally, the amount of dust in vent gas flow is increasing during the smelt run off. Additionally, dust content may vary extensively depending on whether the vents of mixing tank are fed to the dissolving tank vent stack or not. This, for instance, could be one reason for the relatively wide range of dust content stated by Rantanen (1986). Other researched data available concerning dust in vent gas flow is very limited. Thus the estimation of dust load in vent gas may be challenging.

Other emissions of dissolving tank are ammonia, green liquor dregs and deposits precipitated in the tank during the operation. They are discussed more detailed in following chapters.

7.3.1 Theory of vent gas formation

The factors affecting the amount of vent gas produced and its vapor content are not completely known. Practical experiences have shown that vent gas flow out of the tank is not constant at a certain time period. Additionally, the enthalpy of vent gas varies with the composition of gas. Several theories, however, have been presented in recent few decades.

Generally it is expected that increased boiler load will increase smelt flow, which in turn will increase the temperature of dissolving tank, and hence the amount of evaporated water vapor. Conversely, as dissolving tank temperature decreases, water vapor pressure decreases, leading to less production of vapor. (Ahlstrom Machinery Corporation, 1997)

On the other hand the moisture content of vent gas is stated to depend on the size of the dissolving tank draft, since the higher the draft, the higher the absolute moisture flow due to decreasing steam pressure over liquid surface. However, the size of under pressure in the vent stack is small when compared to atmospheric pressure. Thus the effect of vent stack under pressure on the vent gas formation is rather unlikely. (Ahlstrom Machinery Corporation, 1997; Vihavainen, 2016)

The degree of vaporization may also be indirectly dependent on green liquor density. As the density of green liquor increases, tank temperature will decrease and vice versa. (Ahlstrom Machinery Corporation, 1997)

The amount and quality of vent gas produced have a significant effect not only on dissolving tank design, but also on vent gas scrubbing system and emission control of recovery boiler (Frederick, et al., 2011)**.** Unsteady smelt flow, operational hazards, the lack of dissolving tank feedback and smelt analysis data are the few reasons for the challenges in the modelling of dissolving tank balance.

Currently, it has been observed based on practical experiences that high bed temperatures are correlating with the amount of unburned carbon in the char bed and outflowing smelt. As the enthalpy of smelt and/or the amount of smelt flow are increased, the formation of vent gas is increased due to the induced evaporation of green liquor in the dissolving tank. The amount of leaking air from the smelt spouts is estimated to correlate with under pressure and open area of spouts. However, during normal operation the amount of leaking air can be considered as constant. Thus the total flow of vent gas increases, since more vapor is produced and bound in the constant amount of leaking air. (Pakarinen, 2016; Vihavainen, 2016)

Increased enthalpy and the amount of total vent gas flow will therefore affect the dimensioning of the scrubber and its auxiliary equipment. In practice, the size of the scrubber and other auxiliary equipment, such as circulation water heat exchanger, are enlarged. Additionally, more circulation water is required to transfer excess heat in the scrubber packing layer. (Pakarinen, 2016; Vihavainen, 2016)

7.3.2 TRS

Main gas emissions formed during the smelt dissolution are TRS gases. (Frederick, et al., 1996; Iisa, 1997) Even though TRS content of dissolving tank vent gas is relatively higher than in vents of the main boiler stack, as discussed in chapter 7.3, the amount of reduced sulfur gases released are presented in rather small quantities.

TRS gases are composed mainly of hydrogen sulfide (H_2S), methyl mercaptan (CH_3SH), dimethyl sulfide ($(CH_3)_2S$), and dimethyl disulfide ($(CH_3)_2S_2$), from which hydrogen sulfide is considered as the main emission gas in dissolving tank area. (Frederick, et al., 1996; Iisa, 1997)

Typical properties of TRS gases are pungent unpleasant odor even at low concentrations and high volatility. Additionally, TRS gases, especially H_2S, are hazardous to health at higher concentrations. Due to previous reasons, TRS gases are removed among vents from the dissolving tank in order to prevent them spreading into tank surrounding or boiler house. (Iisa, 1997)

H_2S is formed, when air reacts with green liquor, weak white liquor or smelt. Green liquor and weak white liquor contain sodium hydrosulfide (NaHS), which in water forms equilibrium with Na_2S and H_2S. In Equations 17–19 are concluded the main equilibrium reactions of H_2S in green liquor or weak white liquor. In reality other parallel reactions will occur, which involve derivatives of carbonate ion, carbon dioxide and ions of water dissociation: CO_2, H_2CO_3, HCO_3^-, CO_3^{2-}, H^+ and OH^-. (Frederick, et al., 1996)

$$H_2S(g) \leftrightarrow H_2S(aq) \tag{17}$$

$$H_2S(aq) \leftrightarrow HS^- + H^+ \tag{18}$$

$$HS^- \leftrightarrow S^{2-} + H^+ \tag{19}$$

When Na_2S dissolves into water, a hydrogen sulfide anion and a proton are produced. Hydrogen sulfide anion then tends to combine with proton to produce hydrogen sulfide, which can be released into gas phase as TRS emissions. The high sulfidity of smelt, and hence green liquor, induces H_2S emissions. Respectively, high concentration of NaOH in liquor reduces the emission of H_2S. (Frederick, et al., 1996)

Fredrick et al. (1996) investigated H_2S emissions of dissolving tank. According to them the most significant source of TRS emissions in dissolving tank are the shatter jets of smelt spouts. Na_2S reacts with steam and carbon dioxide to produce H_2S, as depicted in following equations:

$$Na_2S(l) + 2H_2O \leftrightarrow H_2S(g) + 2NaOH \quad (20)$$

$$Na_2S(l) + H_2O + CO_2 \leftrightarrow H_2S(g) + Na_2CO_3 \quad (21)$$

Fredrick et al. (1996) discovered that the maximum concentrations of H_2S sourced from green and weak white liquor are 20–30 ppm. The concentrations of H_2S in the smelt spout openings and at shatter jets can rise up to several hundreds of ppm. Thus it is stated that H_2S gas is emitted from shatter jets, if the concentration exceeds 50 ppm at the scrubber inlet. (Frederick, et al., 1996; Iisa, 1997; Vihavainen, 2016)

Other organosulfur gases, methyl mercaptan, dimethyl sulfide and dimethyl disulfide, are mainly sourced from foul condensates fed to the tank among make-up water. H_2S and methyl mercaptan have acidic nature and are only very slightly soluble in water. Dimethyl sulfide and dimethyl disulfide are neutral compounds and nearly insoluble into water. (Frederick, et al., 1996) Due to poor solubility in water, TRS emissions are typically treated with alkaline solutions (pH up to 13) in the vent gas scrubbers (Andritz Oy, 2016a).

7.3.3 Nitrogen compounds

Wood chips processed in the digesting and washing stage are the main source of nitrogen in recovery cycle. Nitrogen occurs mainly in forms of ammonia (NH_3), organic nitrogen (N_2) and nitrogen oxides (NO_x). Kymäläinen et al. (2001) investigated the fate of nitrogen in recovery cycle at Finnish pulp mills. They discovered that approximately a third (30–34 %) of black liquor nitrogen was removed from the boiler furnace with smelt to dissolution, as one may observe in Figure 16. In the smelt dissolution region main part of nitrogen is removed with green liquor to further processes. In the recausticising plant 60 % of smelt nitrogen is fed to cooking process with white liquor. Part of nitrogen is returned back to the beginning of the cycle, when white liquor from recausticization is fed to the digester. Despite of a closed loop formed, nitrogen does not accumulate in the process. (Kymäläinen, et al., 2001)

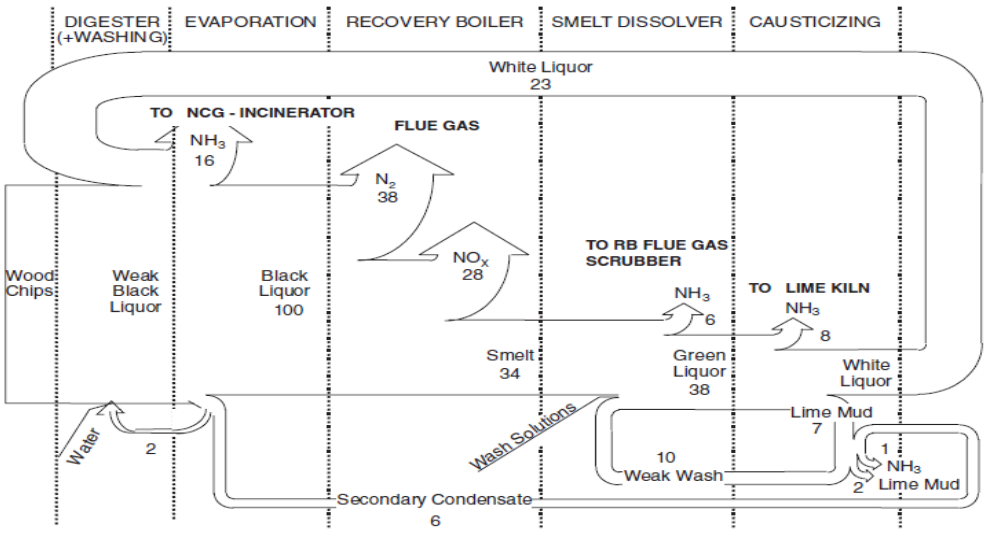

Figure 16. The pathway of nitrogen in the recovery cycle of Finnish pulp mill. Nitrogen entered with the wood chips is removed from the cycle in forms of NH_3, N_2 and NO_x gases. The amount of nitrogen in each stage is given in mass percentage values as a relation to nitrogen of black liquor fed into the boiler. (Kymäläinen, et al., 2001)

The amount of nitrogen in smelt is also dependent on wood species used. According to Kymäläinen et al. (2001) the amount of smelt nitrogen was 20.8 w-% of softwood black liquor and 24.2 w-% of hardwood black liquor. As mentioned earlier, approximately 30–34 w-% of black liquor nitrogen enters to dissolving tank. (Kymäläinen, et al., 2001) Kymäläinen et al. proved in 2002 that smelt nitrogen is in form of cyanate, which is then converted to ammonia in green liquor.

Cyanate is formed during char conversion in the boiler furnace, and it is easily decomposed under high temperatures (Kymäläinen, et al., 2002). According to Vähä-Savo (2014) atmosphere consisted of oxygen induces the decomposition of smelt cyanate. Conversely, CO_2 and inert gas atmospheres enhance the stability of cyanate ion. Depending on the gas conditions, the maximum temperature, in which cyanate does not decompose, is increased. The maximum critical temperature for cyanate is, for instance, stated to be 900 °C in CO_2 atmosphere. (Vähä-Savo, 2014)

During the decomposition of sodium cyanate (NaOCN), sodium cyanide (NaCN), sodium carbonate, nitrogen, carbon monoxide or carbon dioxide are produced. Alkali metals are required for the catalysis of the cyanate conversion. In Equations 22 and 23 the temperature ranges are 500–700 °C and over 700 °C, respectively. (Kymäläinen, et al., 2002)

$$5NaOCN \rightarrow 3NaCN + Na_2CO_3 + N_2 + CO_2 \quad (22)$$

$$4NaOCN \rightarrow 2NaCN + Na_2CO_3 + N_2 + CO \quad (23)$$

Despite of poor temperature resistance and tendency of decomposition, sodium cyanate can be transferred to the dissolving tank in smelt due to inadequate residence time of smelt in the boiler. The schematic pathway of char nitrogen is presented in Figure 17. (Kymäläinen, et al., 2002)

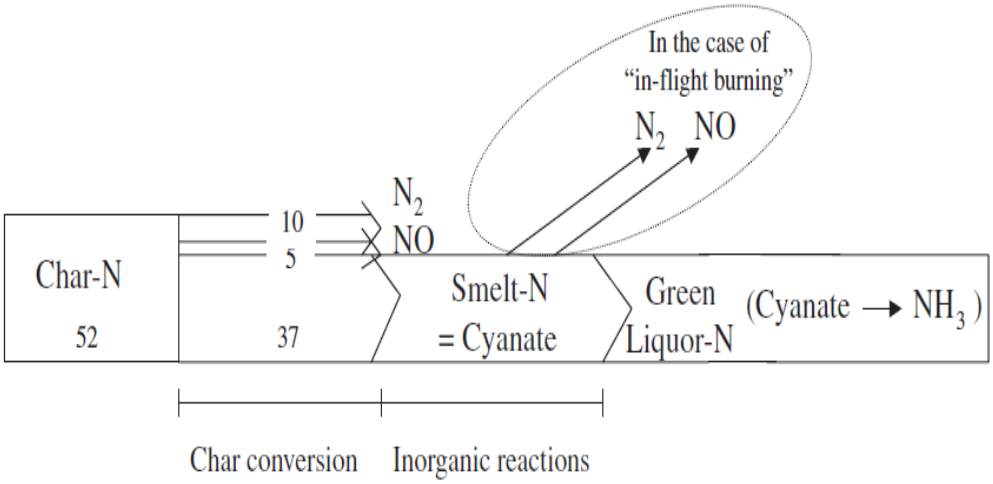

Figure 17. The pathway of char nitrogen during char conversion in smelt bed of kraft recovery boiler. (Kymäläinen, et al., 2002)

Cyanate is converted to ammonia in the dissolving tank and further in green liquor handling processes. Reactions are dependent on temperature and pH conditions of the aqueous solution, as presented in Figure 18. In alkaline conditions of the dissolving tank the reaction rate of ammonia formation is slow. (DeMartini & Hupa, 2006)

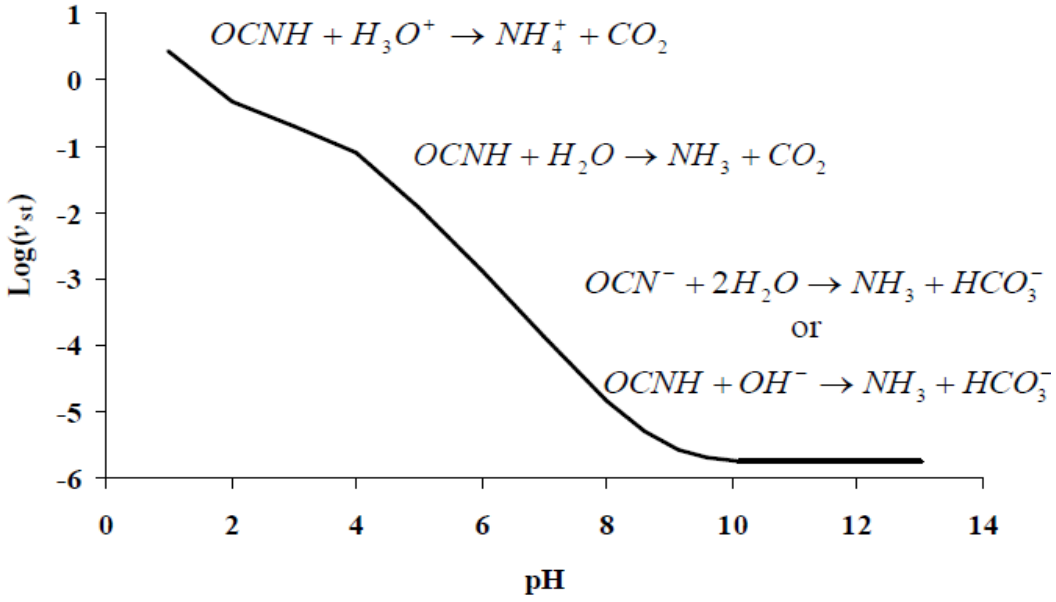

Figure 18. The cyanate reactions in aqueous solution presented at 30 °C. The standardized reaction rate decreases as pH of the solution increases. In alkaline conditions (pH > 10), such as in green liquor and weak wash, cyanate is presented whether in anionic cyanate or isocyanic acid form. (DeMartini & Hupa, 2006)

Weak white liquor contains mainly ammonia. In green liquor the presence of ammonia is minor, considering only 20 % of nitrogen. The rest of nitrogen is presented in form of cyanate. (Kymäläinen, et al., 2001; DeMartini & Hupa, 2006)

Ammonia has been shown to occur in dissolving tank vent gases (Tarpey, 1995; Tarpey, et al., 1996). Tarpey (1995) investigated TRS and particulate emissions of dissolving tank vent stack at the Peace River pulp mill in Canada. He discovered that the part of particulates recovered from the dissolving tank vent stack were ammonium chloride (NH_4Cl). Tarpey et al. (1996) performed subsequent emission tests at the same mill. According to them particulates were consisted mainly of ammonium ions, ammonium sulfate, $(NH_4)_2SO_4$, and organic ammonium, NH_3.

According to Tarpey et al. (1996) the formation of ammonium salts are resulted most likely from direct reactions between NH_3 -gas, water vapor, sulphur oxides (SO_3 and SO_2), and oxygen. The presence of ammonium chloride precipitation, detected during the first test, was explained by the reaction between HCl and NH_3

gases. The source of sulfur oxides and HCl were expected to be through smelt spout openings. (Tarpey, 1995; Tarpey, et al., 1996)

Tarpey et al. (1996) state three possible scenarios for the presence of NH_3 in dissolving tank vent gas. First, NH_3 may be released as a result of local green liquor boiling or natural emission with water vapor. The solubility of ammonia decreases as the temperature of green liquor is increased. Secondly, NH_3 may be sourced from green liquor droplets formed during smelt shattering or due to smelt-green liquor interactions in the tank. According to the third scenario, ammonia is assumed to be formed in the lower furnace and entered the dissolving tank through smelt spout openings. (Tarpey, et al., 1996)

7.3.4 Dead load chemicals

The recovery cycle of pulp mill can be considered to be very efficient. Typically the recovery efficiency of process chemicals is over 97 %. However, 20 % of inorganic chemicals circulating in the recovery cycle do not participate in recovery processes, and hence are classified as dead load chemicals. (Grace & Tran, 2009) Grace and Tran (2009) define dead load chemicals as: "– – inorganic chemicals in white liquor that do not participate in pulping reactions in the digester and are capable or circulating through the pulping and recovery cycle."

Typical dead load chemicals are alkali carbonate, thiosulfate, sulfate and chloride, which are presented as in forms of sodium or potassium salts. Typical sources of dead load chemicals may be: the incomplete conversion during recausticization (Na_2CO_3), the incomplete reduction in the recovery boiler furnace (Na_2SO_4), oxidation with air ($Na_2S_2O_3$ in white liquor) or variation in chemical input streams (Cl input). (Grace & Tran, 2009)

Dead load chemicals have an influence on equipment operation and can reduce their capacities. According to Grace and Tran (2009) smelt flow increases from the boiler furnace to the dissolving tank as the amount of available sodium associating with dead load chemicals is increased. The increase in flowing could be even 15 % compared to the normal operation with low dead load. Other possible harmful effects of increased dead load are:

- decreasing of shatter jet and agitator capacities, which in turn can increase the risk of dissolving tank malfunction and smelt-water interactions
- increasing of weak wash and green liquor flow out of the tank
- decreasing of dissolution residence time
- increasing of heat input and vent gas production
- increasing of vent gas formation and emissions

(Grace & Tran, 2009)

7.3.5 Non-process elements and green liquor dregs

With term of non-process elements (NPEs) is referred to all elements, excluding Na, S, C, H or O, circulating in the recovery cycle. Thus the difference between concepts ‘non-process elements’ and ‘dead load chemicals’ are very narrow. The effect of NPEs on recovery boiler processes are typically element-specific and material involved in the reactions is in small quantities. (Grace & Tran, 2009)

Böök et al. (2006) investigated the fate of noble EU 12 -metals at six Finnish recovery boilers. Main metals accumulating in the green liquor dregs are: Cd, Co, Cr, Cu, Mg, Ni, Pb, Tl, and V. The summary of results is presented in the following Table X. According to the results, especially cadmium, manganese, and lead tend to accumulate in green liquor dregs. Respectively, cadmium, lead, and thallium enrich in the recovery boiler ash cycle. (Böök, et al., 2006)

Table X The distribution of EU 12 -metals in Kraft Recovery Boiler chemical cycle: the amount of EU 12 -metals in black liquor, in flue gas, in green liquor dregs. Abbreviations ++, +, – refer to which element accumulates the mostly in green liquor dregs, which element accumulates partly in green liquor dregs and partly remains in the liquor cycle, and which element remains in the liquor cycle, respectively. (Böök, et al., 2006)

Element	**in Black liquor**	**in Flue gas**	**in Ash cycle**	**in Green liquor dregs**
Unit	**mg/kg DS**	**µg/m^{3}n**	**% of virgin BL**	
Arsenic, As	0.05–0.1	0.02–0.1	32	–
Cadmium, Cd	0.03–0.13	0.02–0.2	400–1000	++
Cobalt, Co	0.2–0.78	0.01–6.3	1–30	+
Chromium, Cr	0.06–0.5	0.3–1.3	2–4	+
Copper, Cu	0.95–1.4	0.03–0.2	1–18	+
Mercury, Hg	0.004–0.01	0.05–1.1	–	
Manganese, Mn	54–100	0.3–9.1	5–8	++
Nickel, Ni	0.6–2	0.1–0.2	3–19	+
Lead, Pb	0.1–0.2	0.1–0.4	62–160	++
Antimony, Sb	0.05–0.45	0.01–0.1	6–15	–
Thallium, Tl	0.01–0.2	0.001–0.07	250–480	+
Vanadium, V	2.5–30	0.03–1.4	3–8	+

The inorganic residues or non-process elements of green liquor are determined as green liquor dregs. Their removal from green liquor is vital in order to prevent accumulation in the causticising processes. Saviharju et al. (2006) determined the composition of green liquor dregs at Finnish and foreign recovery boilers. They discovered that the composition of green liquor dregs varies form one mill to another. Dregs content is strongly affected by the composition of weak white liquor, the addition of magnesium in fiber line, the amount of carbon in green liquor, and the formation of pirssonite in green liquor (Saviharju, et al., 2006). Pirssonite may be also formed during smelt dissolution (Salmenoja & Kosonen, 1996).

According to Engdahl et al. (2008) the amount and composition of dregs are dependent on the degree of mill closure cycle, delignification process, and raw materials of pulping. Additionally, the amount of carbon in green liquor dregs may be increased due to incomplete bed reactions of recovery boiler. Mud carryover of weak white liquor used in smelt dissolution can be due to improper lime mud washing in the recausticising plant. (Engdahl, et al., 2008)

One example of green liquor dregs composition is presented in **Figure 19**. The main components of dregs are magnesium salts and calcium carbonate. However, the amount of carbon in green liquor dregs may vary from few milligrams per liter to 650 mg/l, as presented in Figure 20. Total amount of green liquor dregs may range from 600 to 2000 mg/L (Engdahl, et al., 2008; Saviharju, et al., 2006). The high content of calcium in green liquor is speculated to relate in high dry solids content of black liquor and small boiler bed size. It is possible that in optimal conditions calcium (Ca) exits from the furnace in the form of CaO instead of CaS. CaO is expected to convert to pirssonite more likely than calcium carbonate in green liquor. (Saviharju, et al., 2006)

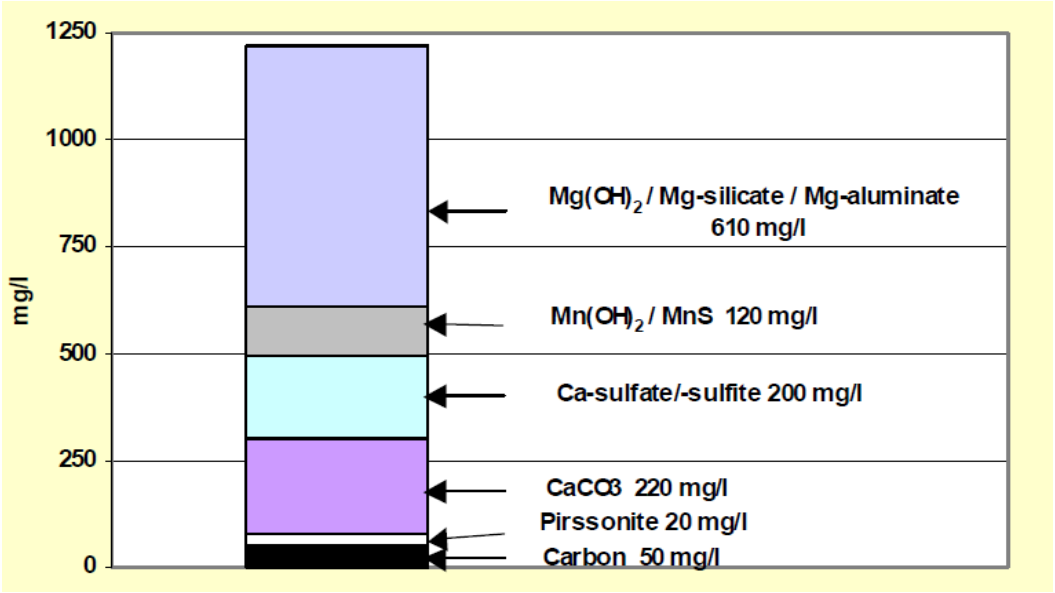

Figure 19. The composition of green liquor dregs based on analysis of Saviharju et al. (2006). The amount of carbon in sample is low. Magnesium salts form the main part of green liquor dregs. (Saviharju, et al., 2006)

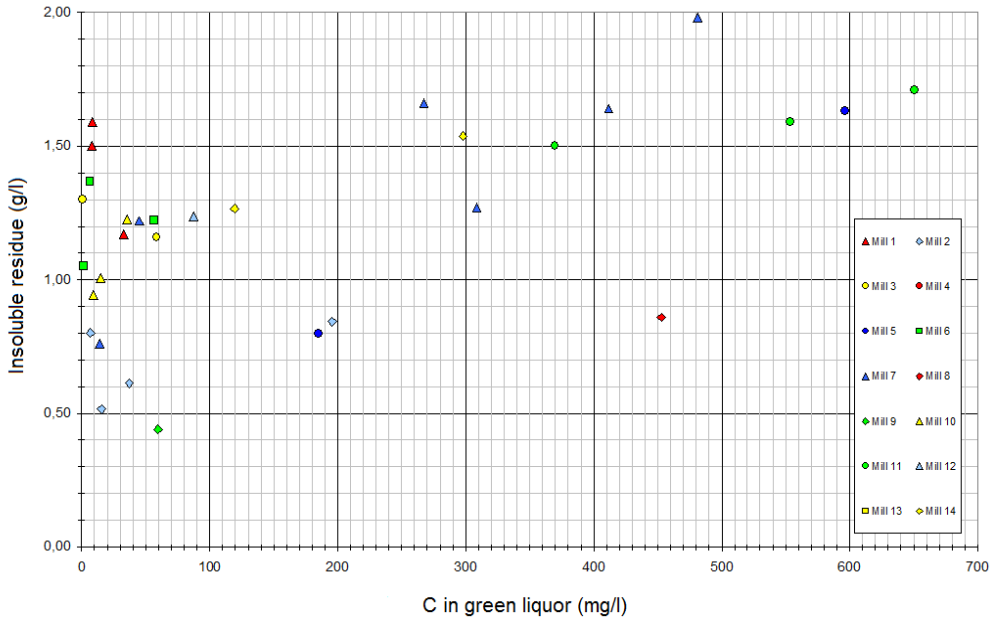

Figure 20. The ratio of green liquor carbon to total amount of green liquor dregs. (Saviharju, et al., 2006)

7.3.6 Pirssonite

Precipitation of solid residue in the dissolving tank, in its equipment, and in green liquor pipelines is the main reason for scaling and problems in the process operation. Pirssonite ($Na_2CO_3 \cdot CaCO_3 \cdot 2H_2O$) is a multi-compound salt composed of sodium carbonate, calcium carbonate and crystal water. It is typically formed during smelt dissolution in green liquor or on the surface of lime mud particles carried with weak white liquor into the dissolving tank. (Frederick, et al., 1990)

The solubility of pirssonite is strongly dependent on green liquor temperature and TTA content of liquor. The main inducers of pirssonite formation are Na^+, Ca^+, and CO_3^{2-} -ions from smelt and weak wash. The sources of Na^+ and Ca^+ -ions may be for instance Na_2CO_3, NaOH or $CaCO_3$. As the concentration of sodium or calcium ions increase, the solubility of pirssonite in green liquor decreases. Respectively, the increasing of green liquor temperature increases the solubility of pirssonite. (Salmenoja & Kosonen, 1996)

Generally, pirssonite is expected to precipitate above solubility limit as far as there is sufficient amount of calcium in green liquor (DeMartini, 2009). According to DeMartini (2009) the lack of available calcium in liquor, high

sulfidity level and low reduction efficiency favor more the formation of other sodium multi-compound salts, such as sodium carbonate monohydrate ($Na_2CO_3 \cdot H_2O$) and burkeite ($Na_6(SO_4)_2(CO_3)$), than pirssonite. The precipitation of burkeite and $Na_2CO_3 \cdot H_2O$ are dependent on the molar ratio of CO_3 and SO_4 in green liquor. (DeMartini, 2009)

Salmenoja and Kosonen (1996) investigated the scaling of dissolving tank in recover boiler RB6 at Enso-Gutzeit Oy Imatra Kaukopää Mills. They determined the formation curves of pirssonite deposit at different temperatures as presented in Figure 21. One may observe that with constant TTA content of green liquor the tolerance against pirssonite formation increases as temperature is increased. The tendency of pirssonite precipitation increases as the temperature isotherm line is intercepted. (Salmenoja & Kosonen, 1996)

In practice the formation of pirssonite is prevented by maintaining the dissolving tank temperature approximately between the range of 95 and 100 °C, while the homogeneity of the solution is ensured with proper mixing. (Frederick, et al., 1990) To ensure proper mixing and avoid high local concentrations in the solution, weak white liquor should be fed into the tank below the surface level of green liquor solution, typically into the root of the impeller (Heinola, 2016). Additionally, TTA-content of green liquor is also recommended to adjust at 90 % of TTA saturation level in order to avoid pirssonite precipitation (Salmenoja & Kosonen, 1996).

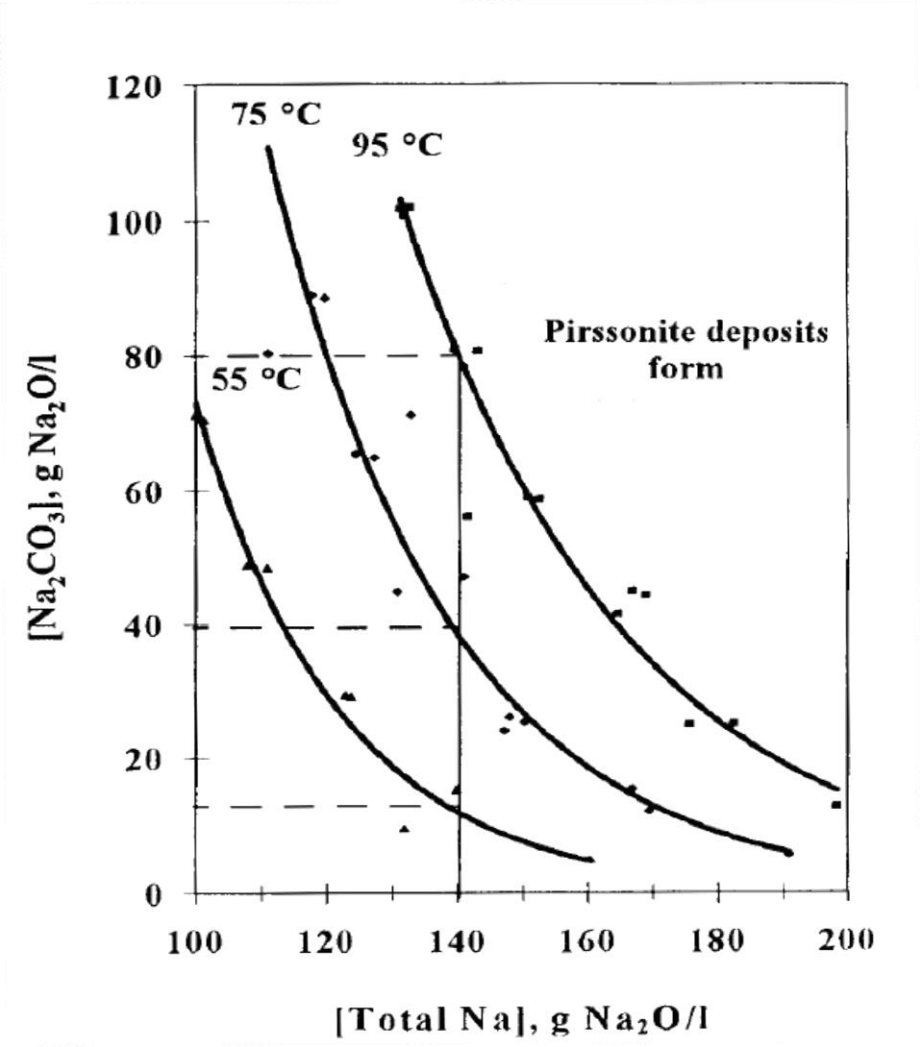

Figure 21. Solubility of pirssonite at different temperature zones. The formation of pirssonite may occur as the total amount of sodium and the concentration of sodium carbonate increase above the curves. (Salmenoja & Kosonen, 1996)

8 GAS-LIQUID COOLING COLUMNS

Vent gas produced in the dissolving tank is dried and purified in wet scrubbers placed in the vent stack system. (da Silva Medeiros, et al., 2002) According to da Silva Medeiros et al. (2002) dissolving tank vents account for 3 to 6 % of the total recovery boiler combustion air requirement. Due to its relatively small amount, scrubbed vent gases can be fed back to boiler with air for combustion.

The main components to be removed are gas emissions and excess moisture of gas. Different types of wet scrubbers can be used depending on the process requirements, such as compositions of scrubber inlet streams, the green liquor system, boiler construction, and emission regulations.

In this work the main focus is in the dissolving tank operation, and hence vent gas scrubbers are introduced briefly in the following chapters. Few studies concerning scrubbing technologies have been for instance made by Kaksonen (2009) and Keikko (1998).

8.1 Spray tower and venturi scrubber

At old mills, typical wet scrubber technologies utilized are spray tower scrubbers, their applications, and venturi scrubbers (Figures 22–23). The principle of conventional spray tower is simple: gas enters the scrubber from the bottom and exits from the top of the scrubber. Scrubbing liquid flows counter-currently against gas flow. The scrubbing liquid is sprayed through wash nozzles with sufficient pressure and volume flow. (Lammentausta & Kiiskilä, 1996)

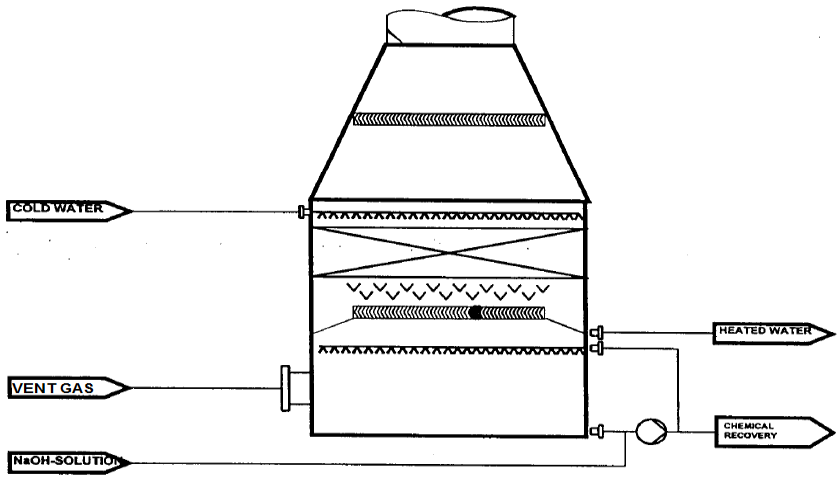

Figure 22. The schematic configuration of packed bed scrubber with spray stage, designed by A. Ahlstrom Corporation, adapted from the figure of (Lammentausta & Kiiskilä, 1996)

Venturi scrubber, however, contains a separate venturi tube, where gas flow is washed with high pressure co-current sprays. Washing stage diminishes the pressure drop in the scrubber and ejects gas flow further to the scrubber. Turbulence generated, while gas flows downstream the venturi, enhances the mass transfer between phases. As a result water droplets are separated from gas stream. (Lammentausta & Kiiskilä, 1996)

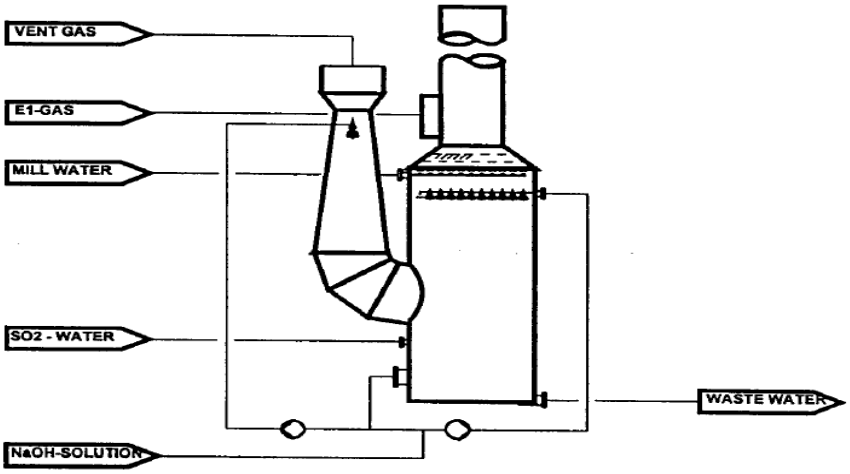

Figure 23. The principle of Venturi Scrubber, designed by A. Ahlstrom Corporation, adapted from the figure of (Lammentausta & Kiiskilä, 1996)

8.2 Packed bed scrubber

Commonly used wet scrubber models at modern mills are packed bed scrubbers and their modifications. The schematic flowsheet of vent gas scrubbing system, including packed bed scrubber with closed scrubbing liquid circulation and circulation cooler, installed during the retrofit of Aracruz recovery boiler, is presented in Figure 24. (da Silva Medeiros, et al., 2002)

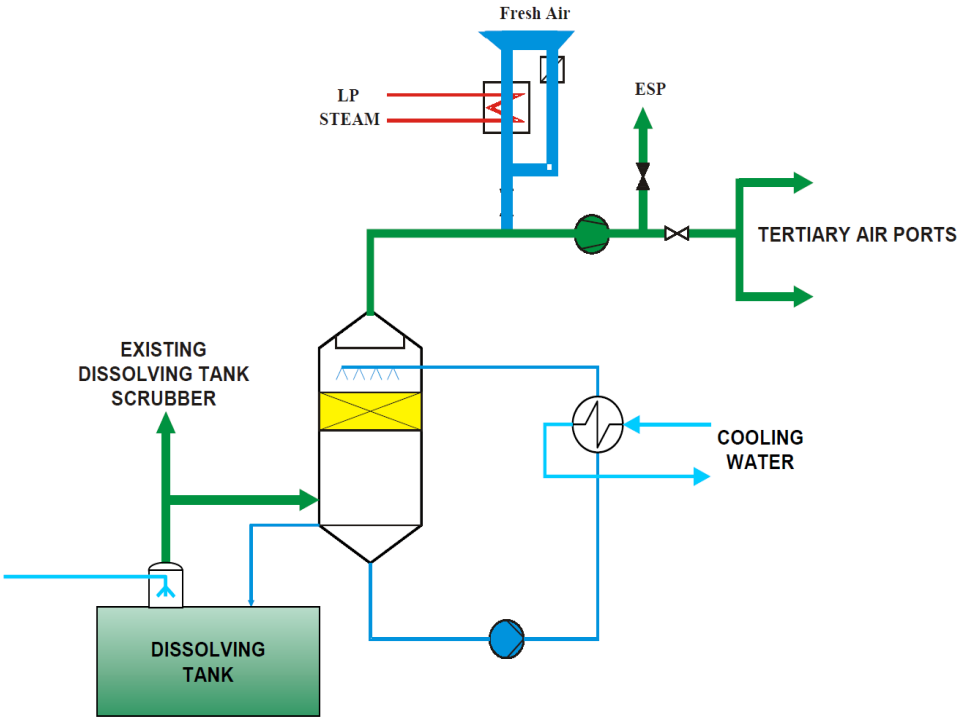

Figure 24. The schematic flowsheet of dissolving tank vent gas handling system, including packed bed scrubber with closed circulation of scrubbing liquid and heat exchanger, during the retrofit of Aracruz recovery boiler. (da Silva Medeiros, et al., 2002)

In the packed bed scrubber gas flows upwards through the packing layer, where in the enthalpy of gas is recovered into scrubbing liquid. In order to enhance mass and energy transfer between gas and liquid phases, scrubbing liquid is sprayed on the surface of packing layer. Gas and liquid flows of the dissolving tank scrubbers are usually relatively high. Thus the packing layer is typically composed of thin wall and hollow shaped packing material, such as steel Pall rings or Intalox saddles, in order to ensure sufficient void structure and contact area. (Andritz Oy, 2016a; Lammentausta & Kiiskilä, 1996; McGabe, et al., 2005)

Weak wash, mill water with NaOH -addition or other alkaline liquid have been traditionally used as scrubbing medium in the scrubbers due to the inadequate scrubbing efficiency of pure water towards TRS gases. (da Silva Medeiros, et al., 2002; Frederick, et al., 1996; Lammentausta & Kiiskilä, 1996) pH of circulation water is monitored during the operation (Lammentausta & Kiiskilä, 1996). However, practical experiences have suggested that the utilization of weak wash or water with high hardness might have enhanced the scaling of the scrubber and its auxiliary equipment. The scaling has been detected to be due to the

accumulation of calcium carbonate ($CaCO_3$) in the scrubber. (da Silva Medeiros, et al., 2002; Andritz Oy, 2016a)

The purpose of the circulation cooler is to remove excess heat from circulation liquid before entering to the scrubber. The cooling medium of the heat exchanger is dependent on the use of purpose, but mill water is commonly utilized. (Andritz Oy, 2016a) Heated cooling water may be used in mill processes (Lammentausta & Kiiskilä, 1996).

8.3 Principle and practice of packed bed vent gas scrubber

Dimensioning of vent gas scrubber can be based on the laws of gas absorption and mass- and energy balance, which are more detailed presented by Keikko (1998), Kaksonen (2009), and McGabe et al. (2005). During the scrubber operation gas is contacted with thin liquid film formed on the surface of packing material. During the contact mass and energy are transferred from gas phase to liquid phase and vice versa. Due to its dual function several variables are affecting the scrubber design. Scrubber diameter is determined based on the pressure drop of the scrubber and flooding gas velocity. The height of the scrubber, however, is dependent on mass and energy balances. (McGabe, et al., 2005)

The outlet temperature of gas after the scrubber determines the amount of heat transferred, water condensed and circulation water required. Other variables affecting the scrubber design are the velocity of gas flow, saturation temperature of vent gas at scrubber inlet, and moisture content of vent gas at scrubber inlet and outlet. Since vent gas is mainly composed of air and water vapor, the amount of enthalpy flow transferred and water vapor condensed may be considered as the most significant factors affecting dissolving tank vent gas scrubber design.

From the scrubber operation point of view important parameters are gas and liquid velocities, which are adjusted in order to prevent *flooding* or *channeling* of the scrubber. Scrubber is flooding, when the velocity of gas is increasing too high causing the increasing of pressure drop and liquid holdup in the scrubber. Eventually, as the gas velocity rises, liquid accumulates in the scrubber and becomes continuous phase. Thus the point, where liquid holdup is presented, is

determined as the *loading point* of the scrubber. In practice the loading point can be considered as the maximum capacity of the scrubber. In addition to gas velocity, tendency of flooding is dependent on the packing material size and type. (McGabe, et al., 2005)

Practical experiences have shown that the flooding of dissolving tank scrubber is rather rare in reality. Instead of flooding, in some cases the "boiling" of scrubbing liquid has been met during the malfunction of dissolving tank scrubbers. This might be explained by decreased temperature difference between scrubber circulation water and vent gas in the scrubber, which in turn leads to the increased temperature inside the scrubber. (Vihavainen, 2016)

Channeling, however, is due to the low velocity of liquid. In reality liquid is distributed over the surface of the packing material unevenly, leading to the formation of dry spots on the some part of the packing layer or small liquid flows – rivulets on the other. Channeling can be prevented by the optimization of scrubber diameter and packing diameter ratio. (McGabe, et al., 2005)

From dissolving tank balance point of view, the estimation of heat transferred in the packing layer can be used as the base of initial estimation of total vent gas enthalpy, and hence vapor content of gas. As the enthalpy and mass flow of vent gas are known, the amount of heat removed from the tank with green liquor can be estimated.

EXPERIMENTAL PART

The experimental part of this work considers the determination of dissolving tank mass and energy balance. In order to estimate the amount of scrubber condensate reversed into the tank, mass and energy balance of the vent gas scrubber was also determined.

9 MEASUREMENTS AND CALCULATIONS

The calculation procedure of mass and energy balance presented in this work is based on the basic laws of thermodynamics and earlier studies made related to the topic. The main purpose of balance calculation was to estimate the total amount of vent gas and its vapor content evaporated during smelt dissolution. The total enthalpy flow of vent gas was estimated based on moisture content of gas and the enthalpy flow of air. Since the specific enthalpy of water vapor is greater than in air, the main part of vent gas enthalpy flow is sourced from evaporated vapor.

System boundaries drawn around the dissolving tank and vent gas scrubber are presented in Figure 25. System was assumed to be adiabatic, and reference conditions were set at 0 °C and 1.013 bar(a).

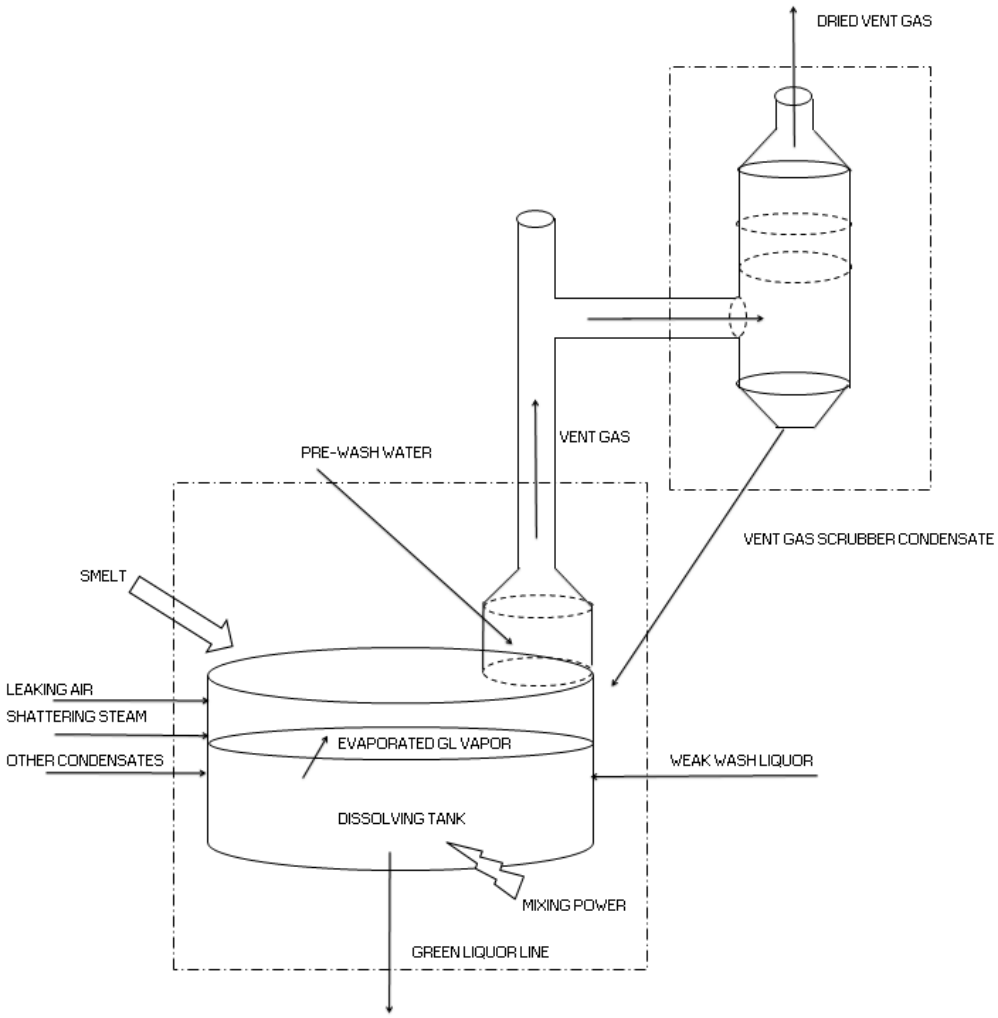

Figure 25. Mass and energy balance of dissolving tank.

Even though the main focus of balance calculations were in dissolving tank, the mass and energy balance of vent gas scrubber were calculated in order to determine the process values of condensed water reversed to the tank from the scrubber. The flow of *other condensates* indicates to all other water streams fed to the tank. As a simplification pre-wash flow fed to vent stack was set inside the system boundaries of dissolving tank, and the velocity of vent gas in the stack was assumed to be as slow as that all sprayed water drops ended up to the tank rather than to be caught by vent gas flow.

The mass and energy balance equations of dissolving tank were derived from the first law of thermodynamics (Equation 24), where internal energy $\frac{dU}{dt}$ is the sum of input and output heat and enthalpy flows, including power fed and removed from the system.

$$\frac{dU}{dt} = \sum \dot{Q} + \sum \dot{H} - P \quad (24)$$

where $\frac{dU}{dt}$ internal energy, kJ/s

$\dot{Q}$ heat flow, kW

$\dot{H}$ enthalpy flow, kW

P power, kW

Since dissolving tank is assumed to be open adiabatic system, internal energy $\frac{dU}{dt}$ and heat flow $\dot{Q}$ are equal zero. Thus Equation 24 may be simplified into a following form:

$$\sum \dot{H}_{in} + P_{mix} - \sum \dot{H}_{out} = 0 \quad (25)$$

Similarly, the mass balance of the tank can be derived as follows:

$$\sum_i^n \dot{m}_{i,in} - \sum_i^n \dot{m}_{i,out} = 0 \quad (26)$$

9.1 Smelt

The mass flow of smelt was calculated based on smelt composition determined from the mass and energy balance of recovery boiler. Generally, the input values of dissolving tank balance, such as estimated composition of smelt and its temperature were got from ANITA – Andritz recovery boiler dimensioning tool.

Actual flow of smelt into the tank was calculated as follow:

$$\dot{m}_{smelt} = \sum_{i=1}^{n} x_i \, \dot{m}_{BL\ WO\ ASH} \quad (27)$$

where $\dot{m}_{smelt}$ mass flow of smelt, kg/s

x_i mass fraction of smelt component per virgin black liquor, kg/kgDS

$\dot{m}_{BL\ WO\ ASH}$ mass flow of black liquor without ash, kgDS/s

The mass flow of black liquor without ash was determined from the boiler load:

$$\dot{m}_{BL\ WO\ ASH} = \frac{\dot{m}_{load}}{1000\frac{kg}{t}} \cdot 3600\frac{s}{h} \cdot 24\frac{h}{d} \quad (28)$$

where $\dot{m}_{load}$ boiler operation load without ash, tDS/d

The total enthalpy of molten smelt was calculated as a sum of single component enthalpies (Equation 29). When calculating the enthalpy of a smelt component, the melting enthalpy and specific enthalpies of components should be considered (Equation 30). (Vakkilainen, 2009) The effect of dissolution enthalpies on the total smelt enthalpy was assumed to be minor, and hence they were ignored from the calculations. Typical values for melting enthalpies and specific heat capacities of smelt components have been presented in Table VI in chapter 6.2.

$$\dot{H}_{smelt} = \dot{m}_{BL\ WO\ ASH} \sum_{i=1}^{n} h_{c,i} \quad (29)$$

where $\dot{H}_{smelt}$ enthalpy flow of smelt, kW

$h_{c,i}$ specific enthalpy of the component i, kJ/kgDS

$$h_{c,i} = b_i\left[h_m + c_{p,i}\left(T_{smelt} - T_{ref}\right)\right] \quad (30)$$

where b_i molality of smelt component per virgin black liquor, mol/kgDS

h_m melting enthalpy of component, kJ/mol

$c_{p,i}$ specific heat capacity of component, kJ/molK

T_{smelt} smelt temperature, K

T_{ref} reference temperature, K

9.2 Green liquor

Since sodium sulfide and carbonate are the main components of smelt and weak wash, excluding sodium hydroxide of WWL, they may be considered as the main components of green liquor as well. Thus the volume flow of green liquor may be converted from mass flow of green liquor by dividing it with TTA-value (Equation 31).

$$\dot{V}_{GL} = \frac{\dot{m}_{GL\ as\ NaOH}}{TTA_{NaOH}} \tag{31}$$

where $\dot{V}_{GL}$ volume flow of green liquor, l/s

$\dot{m}_{GL\ as\ NaOH}$ mass flow of green liquor expressed in terms of NaOH mass equivalents, g NaOH/s

TTA_{NaOH} total titratable alkali in terms of NaOH molar equivalents, g NaOH/l

$$\dot{m}_{GL\ as\ NaOH} = \dot{m}_{\text{BL WO ASH}}\left[\left(b_{Na_2S} + b_{Na_2CO_3}\right)2M_{NaOH}\right] \tag{32}$$

where $b_{Na_2CO_3}$ molality of Na_2CO_3 in smelt, mol/kg

b_{Na_2S} molality of Na_2S in smelt, mol/kg

M_{NaOH} molar mass of NaOH, kg/mol

The volume flow of green liquor can be converted to mass flow by multiplying it with green liquor density.

$$\dot{m}_{GL} = \dot{V}_{GL} * \rho_{GL} \tag{33}$$

where ρ_{GL} density of green liquor, kg/l

In the dissolving tank balance system heat exits mainly from the tank in vent gas or green liquor. Specific enthalpy of green liquor is dependent on dissolved salts, which are originally from smelt and weak wash liquor. The amount of dissolved salts will determine the boiling point rise of green liquor, and hence the amount of energy required to heat green liquor up to boiling point. Due to the great amount of dissolved salts and complicated chemistry involved, the determination of green liquor boiling point elevation is challenging. In literature boiling point elevations of different black liquors have been more commonly studied, even though the number of research made are still few. However, based on the results of research and theory presented for single salt component solutions in literature, it can be assumed that the boiling point of green liquor will rise along the dry solids content of green liquor.

The boiling point elevation of green liquor may be approximated from the following equation of boiling point elevation of single component solution (Partanen & Partanen, 2010). In case of green liquor the molality of salts and number of ions formed, which are expressed with van't Hoff constant, should be considered in calculations (Equation 34).

$$\Delta T_b = T_b - T_b^* = \frac{R M_{H_2O} \left(T_b^*\right)^2}{\Delta H_{vap}\left(T_b^*\right)} b_i = K_b b_i i \tag{34}$$

where

T_b	the boiling point of solution, K
T_b^*	the boiling point of pure water, K
R	gas constant, 8.314 J/molK
M_{H_2O}	molar mass of pure water, g/mol
$\Delta H_{vap}(T_b^*)$	enthalpy of vaporization of pure water, J/mol
b_i	molality of the component, mol/kg
K_b	ebullioscopic constant, kgK/mol
i	van't Hoff constant, –

Enthalpy of green liquor is dependent on the tank process conditions. Green liquor is assumed to boil between the range of 102–104 °C dependent on the liquor composition and density. Heat is required for warming green liquor until it reaches the boiling point. The specific sensible enthalpy of liquid phase green liquor increases during the heating process. However, at the boiling point the specific sensible enthalpy of liquid phase reaches its maximum, and excess heat is transferred to gas phase during evaporation of green liquor. Thus enthalpy of green liquor may be determined with two equations.

If temperature of green liquor T_{GL}, is less than the temperature of boiling point $T_{b,GL}$, then enthalpy flow of liquid phase $\dot{H}_{GL}$ may be calculated from the energy balance of dissolving tank as depicted in Equation 35.

If $T_{GL} < T_{b,GL}$, then

$$\dot{H}_{GL} = \dot{H}_{smelt} + \dot{H}_{air} + \dot{H}_{steam} + \dot{H}_{oc} + \dot{H}_{pre-wash} + \dot{H}_{sc} + \dot{H}_{WWL} + P_{mix} - \dot{H}_{VG\ DRIED,vapor} \quad (35)$$

where

$\dot{H}_{air}$	enthalpy flow of leaking air, kW
$\dot{H}_{steam}$	enthalpy flow of shattering steam, kW
$\dot{H}_{oc}$	enthalpy flow of other condensates, kW
$\dot{H}_{pre-wash}$	enthalpy flow of pre-wash spray, kW
$\dot{H}_{sc}$	enthalpy flow of scrubber condensate, kW
$\dot{H}_{WWL}$	enthalpy flow of weak white liquor, kW
P_{mix}	power of mixing, kW

In case of green liquor temperature being equal to the temperature of boiling point, enthalpy flow is calculated based on the specific heat capacity and mass flow of green liquor at existing temperature (Equation 36).

If $T_{GL} = T_{b,GL}$, then

$$\dot{H}_{GL} = \dot{m}_{GL} c_{p,GL} \left(T_{GL} - T_{ref}\right) \quad (36)$$

The specific heat capacity of green liquor is determined based on the specific heat capacities of single green liquor compounds and their mass fractions.

$$c_{p,GL} = \sum_{i=1}^{n} x_i c_{p,i} \tag{37}$$

where $c_{p,GL}$ specific heat capacity of green liquor, kJ/kgK

$c_{p,i}$ specific heat capacity of a compound, kJ/kgK

x_i mass fraction of a green liquor compound, –

9.3 Green liquor evaporation

During dissolution the evaporation of green liquor will occur at the boundary of phases. In reality evaporated vapor contains TRS gases, ammonia, and particulates. However, in this work vapor evaporated from green liquor is assumed to be completely composed of water vapor.

The evaporation of green liquor may be described with Newton's law of convection. The equation of mass transfer is analogous to the heat equation and hence the amount of evaporated green liquor can be determined as depicted in Equation 38. (Incropera, et al., 2007)

$$N_{GL,evap} = \bar{h}_m A_s \left(C_{GL,s} - C_{GL,\infty}\right) \tag{38}$$

where $N_{GL,evap}$ molar flux of vapor evaporated from GL, kmol/s

$\bar{h}_m$ convection mass transfer coefficient, m/s

A_s area of the surface, m^2

$C_{GL,s}$ vapor concentration at the surface of GL, $kmol/m^3$

$C_{GL,\infty}$ vapor concentration at the interface, $kmol/m^3$

On the other hand, vapor pressure at the surface of green liquor may be assumed to be saturated, and hence concentration of vapor may be expressed in terms of ideal gas law:

$$C_{GL,S} = \frac{p_{sat}(T_s)}{RT_s} \tag{39}$$

where $p_{sat}(T_s)$ saturated vapor pressure at the surface of GL, Pa

R universal gas constant, 8.314 J/molK

T_s temperature at green liquor surface, K

In order to determine the concentration of green liquor at the surface, the temperature of vapor at the interface $T_{GL,int.}$ is stated to be equal to the surface temperature T_s. (Incropera, et al., 2007) Thus Equation 38 is simplified as follows:

$$\dot{m}_{GL,evap} = N_{GL,evap} M_{H_2O} = \frac{\bar{h}_m A_s M_{H_2O}}{RT_s}\left(p_{sat}(T_s) - p_{GL,int.}(T_s)\right) = C_m(p_{sat}(T_s) - p_{GL,int.}(T_s)) \tag{40}$$

where M_{H_2O} molar mass of water vapor; kg/mol

C_m mass transfer constant, ms

p_{sat} pressure of saturated vapor, Pa

$if\ T_{GL} > T_{b,GL,}\ then\ p_{sat} = 1.013\ bar\ otherwise\ p_{sat} = p_{sat}(T_s)$

$p_{GL,int.}(T_s)$ partial pressure of vapor at interface, Pa

Sensible enthalpy of evaporated green liquor vapor is assumed to be saturated vapor above the phase boundary, and may be calculated as follows:

$$\dot{H}_{GL,evap} = \dot{m}_{GL,evap}\left(h''(T_{GL}) - h\left(p_{ref}; T_{ref}\right)\right) \tag{41}$$

where $\dot{m}_{GL,evap}$ mass flow of evaporated vapor, kg/s

$h''(T_{GL})$ enthalpy of saturated vapor at GL temperature, kJ/kg

9.4 Weak white liquor

Weak wash liquor (WWL) is fed to the tank in order to control the density of green liquor. Thus the mass flow of WWL can be determined through the mass balance of the dissolving tank.

$$\dot{m}_{WWL} = \dot{m}_{GL} + \dot{m}_{VG,DRIED,vapor} - \dot{m}_{smelt} - \dot{m}_{oc} - \dot{m}_{steam} - \dot{m}_{sc} - \dot{m}_{pre-wash} \quad (42)$$

where

$\dot{m}_{GL}$	mass flow of green liquor, kg/s
$\dot{m}_{oc}$	total mass flow of other condensates, kg/s
$\dot{m}_{pre-wash}$	mass flow of pre-wash water, kg/s
$\dot{m}_{sc}$	mass flow of scrubber condensate, kg/s
$\dot{m}_{smelt}$	mass flow of smelt, kg/s
$\dot{m}_{steam}$	mass flow of shattering steam, kg/s
$\dot{m}_{VG,DRIED,vapor}$	mass flow of vapor in dried vent gas, kg/s

Sensible enthalpy of WWL is calculated based on the specific heat capacity and temperature.

$$\dot{H}_{WWL} = m_{WWL} c_{p,WWL} (T_{WWL} - T_{ref}) \quad (43)$$

Since weak white liquor is mainly composed of water and the amount of solids in weak white liquor are small, the specific heat capacity of WWL $c_{p,WWL}$ can be assumed to be equal to the specific heat capacity of water $c_{p,H2O}$.

$$c_{p,WWL} \approx c_{p,H2O} \quad (44)$$

where

$c_{p,H2O}$	specific heat capacity of water, 4.19 kJ/kgK

9.5 Leaking air

The source of leaking air to dissolving tank is via hoods of smelt spouts. During normal operation hood doors are maintained open due to the monitoring and safety. The amount of leaking air is dependent on the area of hood, number of spouts, and under pressure maintained in the tank.

$$\dot{V}_{air} = A_{Hoods}\sqrt{\frac{2*\Delta p_{tank}}{\rho_{air}*f_D}} \quad (45)$$

where $\dot{V}_{air}$ volume flow of air, m^3/s

A_{Hoods} The total area of hoods, m^2

Δp_{tank} under pressure in the dissolving tank, Pa

f_D the pressure loss factor, –

ρ_{air} density of air, kg/m^3

The mass flow of air is then calculated:

$$\dot{m}_{air} = \dot{V}_{air} * \rho_{air} \quad (46)$$

where $\dot{m}_{air}$ mass flow of leaking air, kg/s

The enthalpy flow of air is calculated as depicted in Equation 47. When flowing through the tank, air is heated to the temperature of exiting vent gas. Thus inlet and outlet enthalpy flows of air should be taken in consideration in the balance calculations.

$$\dot{H}_{air} = \dot{m}_{air} c_{p,air}(T_{air} - T_{ref}) \quad (47)$$

where $\dot{H}_{air}$ enthalpy flow of leaking air, kW

$c_{p,air}$ the specific heat capacity of air, kJ/kgK

T_{air} temperature of air, K

9.6 Shattering steam

Medium pressure steam is fed through a nozzle for smelt shattering in every spout. The amount of steam can be estimated based on the equation of superheated steam at critical flow through an orifice (European Committee for Standardization, 2004).

$$\dot{m}_{steam,i} = \frac{\sqrt{R}}{10} C_{is} A_{nozzle} K_{dr} \sqrt{\frac{p_0}{v}} = 0.2883\ C_{is} A K_{dr} \sqrt{\frac{p_0}{v}} \tag{48}$$

where $\dot{m}_{steam,i}$ mass flow of shattering steam per spout, kg/h

C_{is} coefficient based on isentropic exponent, –

A_{nozzle} area of the nozzle, mm^2

K_{dr} the coefficient of discharge,–

p_0 pressure of steam before the nozzle, Pa

v specific volume of steam, m^3/kg

The isentropic coefficient C_{is} is calculated as:

$$C_{is} = 3.948 \sqrt{k \left(\frac{2}{k+1}\right)^{(k+1)(k-1)}} \tag{49}$$

where k isentropic exponent, –

Total mass flow of shattering steam is then calculated from the sum of steam flows fed to each spout.

$$\dot{m}_{steam} = \sum_{i=1}^{n} \dot{m}_{steam,i} \tag{50}$$

The sensible enthalpy of shattering steam is then calculated as:

$$\dot{H}_{steam} = \dot{m}_{steam} \left(h(p_{steam}; T_{steam}) - h\left(p_{ref}; T_{ref}\right) \right) \tag{51}$$

where $\dot{H}_{steam}$ enthalpy flow of shattering steam, kW

$h(p_{steam}; T_{steam})$ enthalpy of steam at prevailing conditions, kJ/kg

$h\left(p_{ref}; T_{ref}\right)$ reference enthalpy, kJ/kg

9.7 Pre-wash water

The amount of pre-wash water is estimated based on the experience. Enthalpy flow of water spray is calculated similarly as other water flows presented in next chapter 9.8.

9.8 Other condensates

Other water flows, excluding scrubber condensate and pre-was water, fed into the tank consider normally only minor part of dissolving tank inlet liquid flows. The mass flows of other condensates are given as an input value. The enthalpy flow of a single water flow may be calculated as depicted in Equation 52.

$$\dot{H}_{H_2O,i} = \dot{m}_{H_2O,i} c_{p,H_2O} (T_{H_2O,i} - T_{ref}) \quad (52)$$

where $\dot{H}_{H_2O,i}$ enthalpy flow of water stream i, kW

$\dot{m}_{H_2O,i}$ mass flow of water stream, kg/s

$T_{H_2O,i}$ temperature of water stream, °C

9.9 Mixing power

Mixing power of the tank is dependent on the number of impellers. Electrical power required is provisionally estimated based on the dissolving tank design and confirmed by the sub-suppliers.

9.10 Mass and energy balance of vent gas scrubber

As a simplification leaking air can be stated to flow through the tank and entering to the vent stack and finally to the scrubber. Along the way through the dissolving tank air combines moisture produced during evaporation of green liquor. In this work vent gas is assumed to be composed only of water and air. In reality besides of water vapor and air vent gas contains varying amount of particulates, TRS emissions, and ammonia from the tank. Currently, in case of packed bed scrubbers vent gas is cooled and dried in the scrubber, and as a result condensed water is

reversed back to the dissolving tank, while dried vent gases are fed to the combustion.

In the vent gas scrubber fan the mass flow of air is assumed to be equal to the mass flow of leaking air. The amount of vapor in vent gas can be determined based on the equation of humidity in air *Y* (Zeller & Busweiler, 2010).

$$Y = \frac{R_{air}}{R_{H_2O,vapor}} * \frac{p_D}{p - p_D} = 0.622 \frac{\varphi p_D}{p - \varphi p_{DS}} \quad (53)$$

where

p	atmospheric pressure, Pa
p_D	partial pressure of water vapor in moist air, Pa
p_{DS}	partial saturation pressure of water vapor at stated temperature, Pa
R_{air}	gas constant of air, 287 J/kgK
$R_{H_2O,vapor}$	gas constant of water vapor, 461 J/kgK
φ	relative humidity, -

According to Zeller and Busweiler (2010) relative humidity is defined as:

$$\varphi = \frac{p_D}{p_{DS}};\ 0 \leq \varphi \leq 1 \quad (54)$$

Mass flow of water vapor in the vent gas scrubber fan is calculated by multiplying mass flow of air with humidity of vent gas flow.

$$\dot{m}_{VG,DRIED,vapor} = Y * \dot{m}_{air} \quad (55)$$

Total flow of dried vent gas is received from the sum of air and vapor flows.

$$\dot{m}_{VG,DRIED} = \dot{m}_{VG\ DRIED,vapor} + \dot{m}_{air} \quad (56)$$

Enthalpy of dried vent gas is determined with aid of specific enthalpy per dry gas and mass flow of air.

$$\dot{H}_{VG\ DRIED} = h_{VG\ DRIED} * \dot{m}_{air} \quad (57)$$

where

$\dot{H}_{VG\ DRIED}$	enthalpy of dried vent gas, kW

$h_{VG\ DRIED}$ specific enthalpy of dried vent gas, kJ/kg$_{\text{dry gas}}$

In order to determine the enthalpy of dried vent gas, the specific enthalpy of gas is calculated. Zeller and Busweiler state an equation for specific enthalpy at reference temperature of 0 °C as follows:

$$h_{VG\ DRIED} = c_{p,air}\vartheta + Y(\Delta h_{V\circ} + c_{p,H_2O}\vartheta) \quad (58)$$

where $c_{p,air}$ specific heat capacity of air, 1.0 kJ/kgK

c_{p,H_2O} specific heat capacity of vapor, 1.86 kJ/kgK

$\Delta h_{V\circ}$ latent heat of water, 2500 kJ/kg

ϑ temperature of saturated gas, K

The mass flow of vent gas entering the scrubber is the sum of leaking air and evaporated green liquor vapor mass flows.

$$\dot{m}_{VG,WET} = \dot{m}_{GL,evap} + \dot{m}_{air} \quad (59)$$

Equation 57 may be used for determining the specific enthalpy of wet vent gas, and hence enthalpy flow of wet vent gas:

$$\dot{H}_{VG\ WET} = h_{VG\ WET} * \dot{m}_{air} \quad (60)$$

where $\dot{H}_{VG\ WET}$ enthalpy flow of wet vent gas, kW

$h_{VG\ WET}$ specific enthalpy of wet vent gas, kJ/kg$_{\text{dry gas}}$

The amount of scrubber condensate is determined from the subtraction of vent gas inlet and outlet streams. The temperature of condensate is estimated based on saturated temperature of wet vent gas.

$$\dot{m}_{sc} = \dot{m}_{VG,WET} - \dot{m}_{VG,DRIED} \quad (61)$$

Enthalpy flow of scrubber condensate reversed to the tank:

$$\dot{H}_{sc} = \dot{m}_{sc}c_{p,H_2O}(T_{sc} - T_{ref}) \quad (62)$$

10 EVALUATION OF PROCESS FEEDBACK DATA AND THE MODEL

Process feedback data concerning dissolving tank and vent gas system were collected from pulp mill data system of four different mills, and Andritz remote data collection system (ACD) under different operation conditions. Additionally, field data measurements were performed in order to measure some physical properties, such as smelt and vent gas temperatures. New dissolving tank balance model was created and tuned based on feedback data collected.

10.1 Boiling point of green liquor

Due to small amount of data available concerning green liquor boiling point in literature, the boiling point was determined during boiler visit at Mill A. The results obtained are presented in Table XI. In literature the boiling point of green liquor is estimated to vary from 100 to 104 °C. The results obtained are higher than expressed in literature. This might be due to different pressure conditions compared to literature values and uncertainty of the measurements.

Table XI The boiling point of green liquor with different liquor composition. Green liquor samples were taken from dissolving tank during normal boiler operation at Mill A.

Date	Sample	Density of GL [kg/l]	TTA [g Na_2O/l]	Boiling point of GL, $T_{B,GL}$ [°C]
25.10.2016	1	1.202	138.9	105
25.10.2016	2	1.202	142	107

10.2 Smelt temperature

Smelt temperatures during normal boiler operation were measured with a thermocouple from smelt spouts at Mills A and B. The average temperatures of spouts with different boiler loads are presented in Table XII**.** According to the results smelt temperature is independent on the boiler load. However, high smelt temperature may indicate to the variation in smelt composition and boiler firing conditions, such as air distribution and oxygen level in the lower bed.

Table XII Smelt temperatures measured from the smelt spout during normal kraft recovery boiler operation of Mills A and B.

Mill	A	B	B	B	B
Date	25.10.2016	10.5.2016	11.5.2016	11.5.2016	12.5.2016
Time	8:20 - 8:33	13:36 - 15:45	10:29 - 11:45	15:34 - 16:55	10:44 - 11:00
Load [tDS/d]	X	X	X	X	X
Smelt T [°C]	825.7	803.1	836.6	814.7	803.2

10.3 Mass balance of dissolving tank

Collected feedback data was used for the determination of dissolving tank mass balance during normal operation. The results were then compared to the results obtained from the created dissolving tank model. Due to the lack of some measuring points in feedback data, some of the streams were estimated based on the equations presented in chapter 9.

Depending on the boiler case, the amount of dried vent gas flow was determined from the vent gas scrubber fan curve based on pressure difference over the fan and fan speed. The amount of leaking air was then estimated based on the amount of dried vent gas flow. Additionally, the amount of smelt spout hoods cooling water and pre-wash spray were assumed to be constant in the model calculations. In feedback data balance some additional water was added to the system in order to adjust the difference of outlet and inlet streams to zero.

The tuning of dissolving tank model to fit for process data of every boiler was observed to be challenging during the work. As explained in chapter 9 the mass transfer coefficient of evaporated vapor between green liquor liquid and gas phase has an effect together with pressure gradient on the amount of evaporated vapor. Constant parameter C_m, presented in Equation 40, was observed to vary depending on the boiler and its conditions. This can be observed from Figures 26–29, where dissolving tank mass balances of Mills A, B, C and D with different boiler operation loads calculated based on feedback data and the model are presented.

According to simulation test runs performed with different parameter C_m, it was observed that the surface area, where mass transfer occurs, does not necessarily equal to the surface area of dissolving tank. This might be due to the location of smelt spouts in comparison to the location of vent stack. In modern boilers spouts are often located on the long sidewall of the elliptical dissolving tank, while the vent stack is located on the one head of the tank. During the dissolution vent gas is drawn to vents stack due to the under pressure of the stack. It could be possible that air does not spread out evenly in the tank, but flows mainly in the front of the spouts and considers only some specific effective surface area of the tank. Thus an assumed effective surface area of dissolving tank was used in the model calculations.

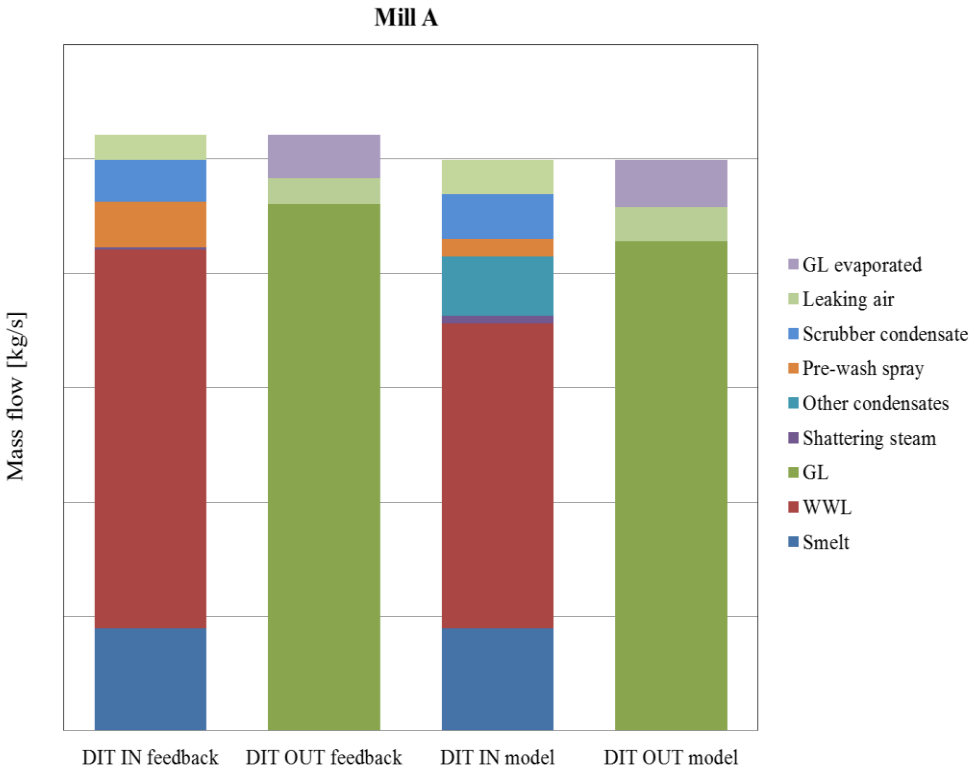

Figure 26. The dissolving tank mass balance of Mill A estimated based on feedback data and dissolving tank balance model.

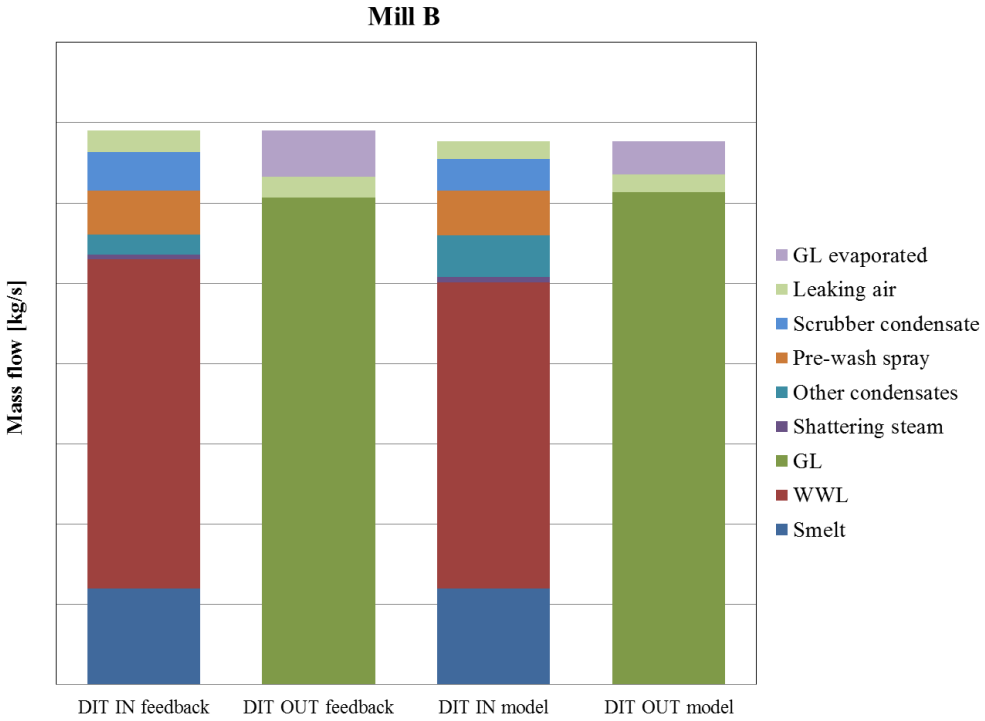

Figure 27. The dissolving tank mass balance of Mill B estimated based on feedback data and dissolving tank balance model.

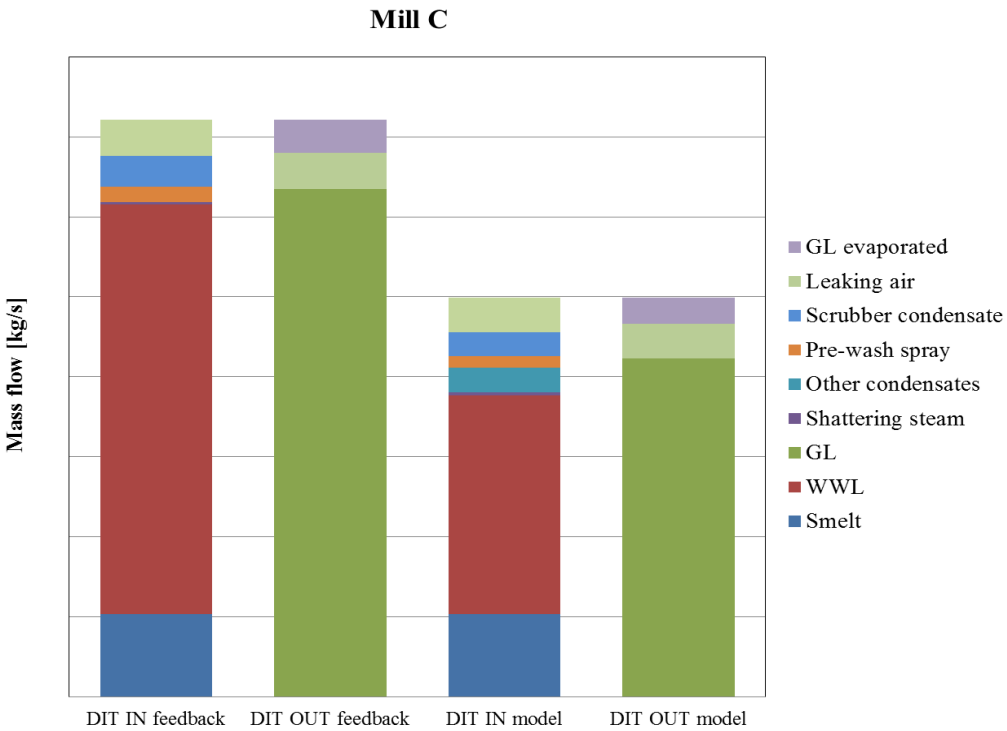

Figure 28. The dissolving tank mass balance of Mill C estimated based on feedback data and dissolving tank balance model.

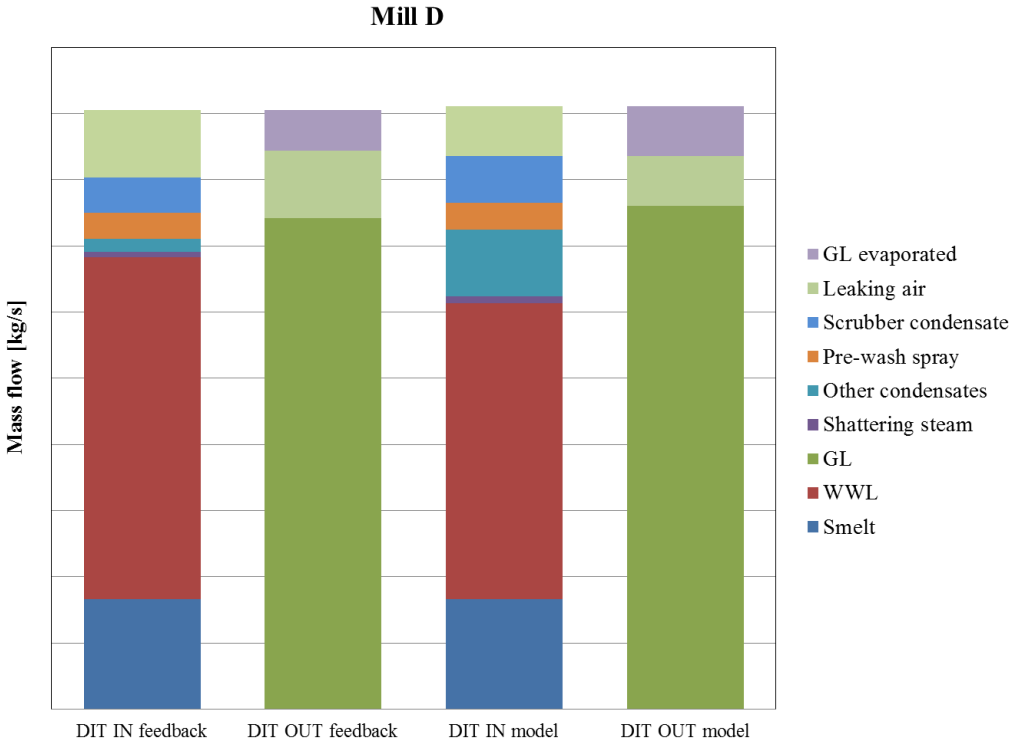

Figure 29. The dissolving tank mass balance of Mill D estimated based on feedback data and dissolving tank balance model.

According to the model the amount of evaporated vapor is approximately in the same range as vapor evaporated during the actual process in the case of all four mills. However, the total mass flows into the tank are greater according to feedback data than the model. Especially, the total outlet and inlet mass flows of Mill C simulation are 30 % smaller compared to the results of feedback calculations.

One reason for the difference may be due to unknown accurate composition and density of green liquor, causing deviation in the calculation of green liquor mass flows. In the model calculations smelt composition was given as an input value, and thus it is not necessarily valid for all boiler loads. Additionally, the amount of pre-wash and other condensates fed to the tank are changing constantly in reality, while they were assumed to be constant during the simulations. According to both model and process feedback data green liquor flow out of the dissolving tank varies approximately between 80–90 w-% of outlet stream. Depending on the boiler load, the amount of weak white liquor flow varies from 60 to 70 w-% of input streams.

10.4 Energy balance of dissolving tank

As a result of the energy balance calculation heat input and output streams, including the heat output of total vent gas, were calculated. By terms heat input and output are referred to inlet and outlet enthalpy flows, mechanical powers and heat flows of the system introduced in chapter 9. The results obtained were calculated in chosen reference conditions of 0 °C and 1.013 bar(a). Thus the percentage values presented may vary with different reference conditions.

In process data balance heat output of total vent gas flow was estimated based on the heat transferred to circulation water in the scrubber. In the case of model the heat output of vent gas was calculated based on the mass flow of evaporated green liquor vapor.

According to both process feedback data balance and the model evaporated vapor covers approximately 40 % of total heat outputs (Figure 30). The rest of the heat is removed with green liquor. The heat output of air is only a fraction compared to heat of vapor and green liquor due to the lower specific enthalpy. As expected smelt heat input covers the half of total heat input flows into the dissolving tank. The heat input of weak white liquor is approximately 30 to 40 %. The difference between the results of model and feedback data is due to the different amount of water flows fed into the tank.

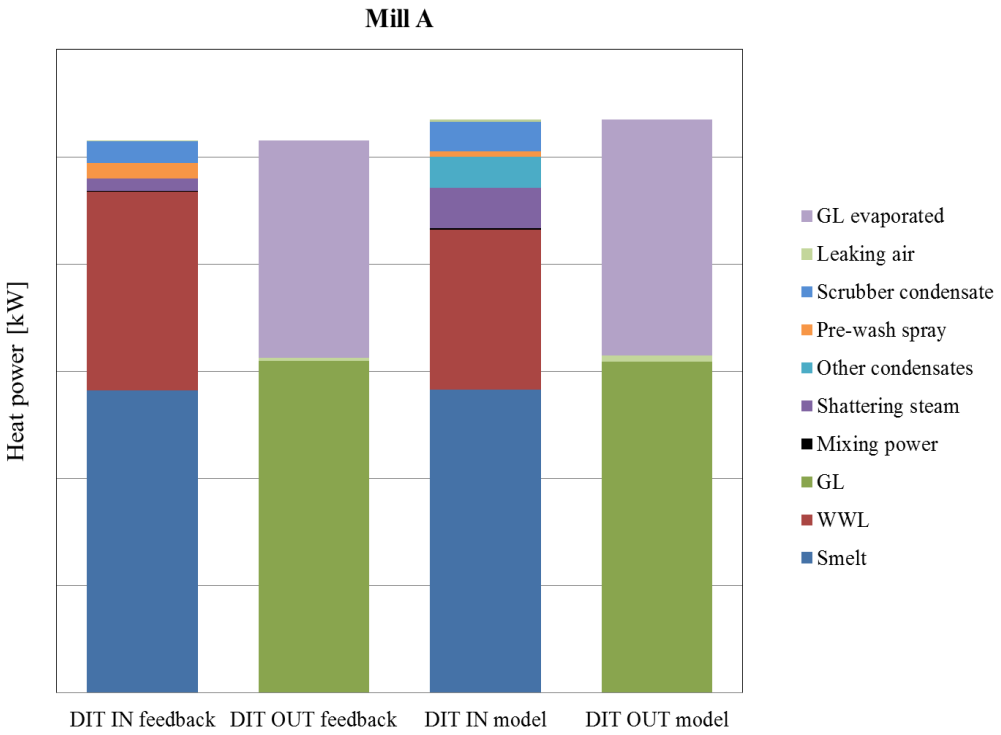

Figure 30. Heat input and output streams obtained from the energy balance of feedback data and dissolving tank model at Mill A.

10.4.1 Properties affecting vent gas formation – Boiler load

The heat output of dissolving tank vents increases as the boiler is operated with higher loads, as one may observe from Figure 31. In the case of Mill A and D the heat output of total vent gas flow is estimated to be greater according to the model than feedback data. Contrary to previous cases, in the case of Mill C and B heat outputs of total vent gas flow estimated by the model are less than obtained from the feedback calculations.

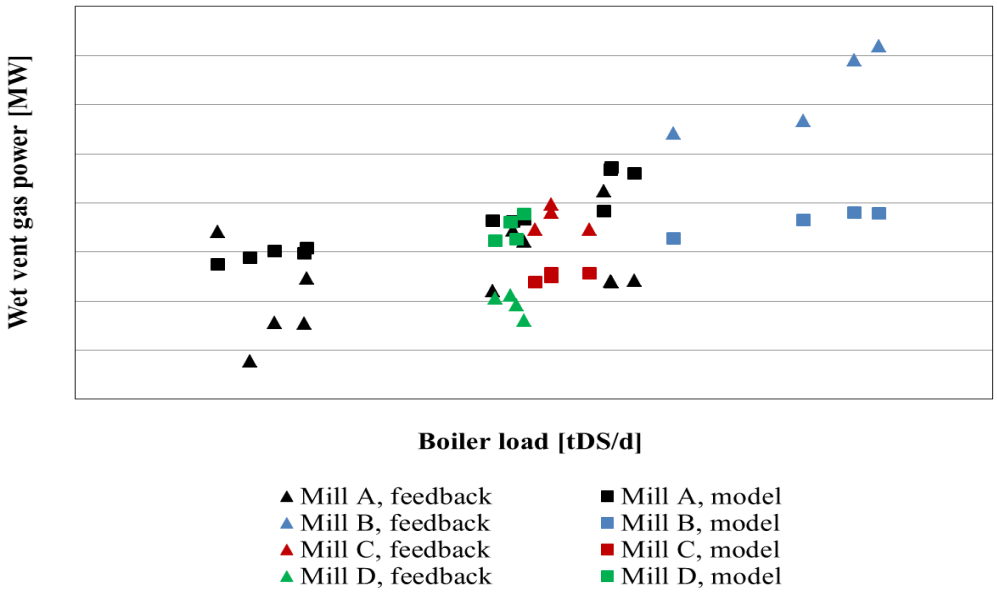

Figure 31. The heat output of total vent gas flow with different boiler loads of Mills A, B, C, and D.

The reason for the difference between model and feedback data may be due to the different smelt composition, uncertainty in the amount of actual smelt flow, and variation of smelt temperature. One indicator of smelt properties is the heat transferred to cooling water of smelt spouts. The average heat transferred to cooling water of smelt spouts per 1000 tDS/d at boilers A, B, C and D are presented in Figure 32. It was discovered that more heat was transferred to cooling water in average in case of boiler C than in case of other test boilers. This is supported by the observations made during the test period of Mill C. During field measurements smelt temperature was stated to be significantly increased and the appearance of smelt was observed to be viscous and resemble jelly. Additionally, smelt reductions were stated to be high. These observations may explain the higher heat outputs of total vent gas flows compared to the model at Mill C.

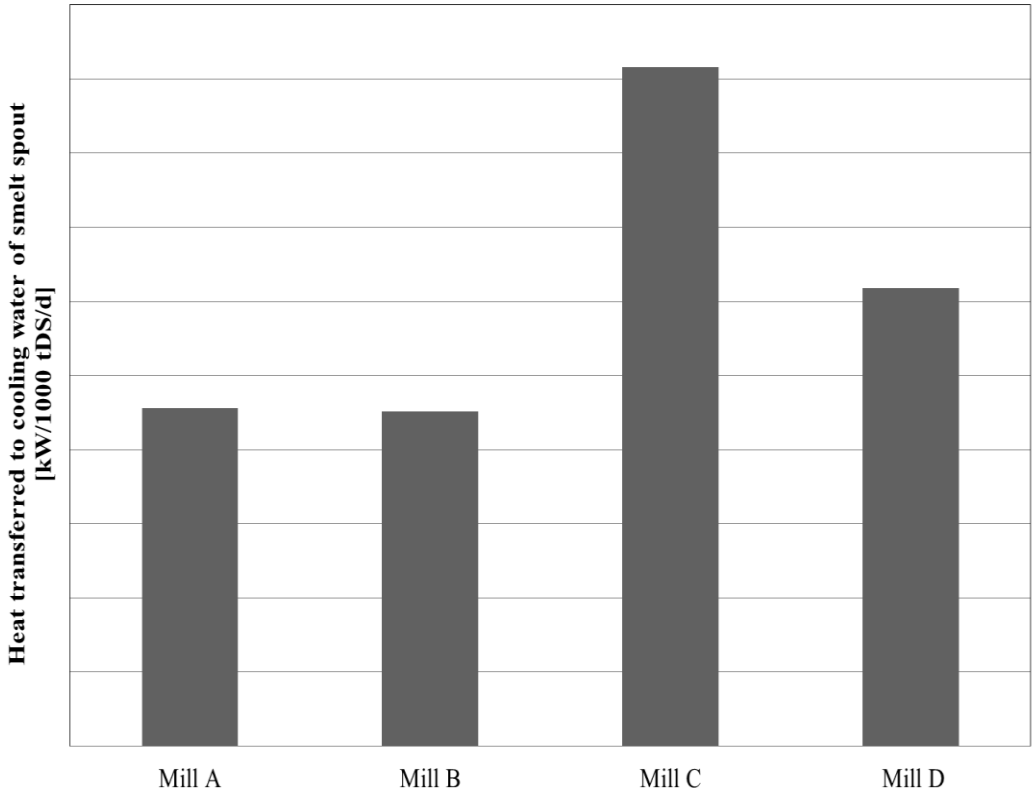

Figure 32. The average heat transferred to cooling water of smelt spouts per 1000 tDS/d at Mills A, B, C, and D.

However, the results of Mill D are opposite to the results of Mill C. Even though the average heat transferred to cooling water is greater than in case of Mill A and B, heat output of vent gas flow remains low (Figure 32). This might be due to uncertain amount of scrubber condensate, which creates an error both in mass balance and in heat output of total vent gas flow.

10.4.2 Properties affecting vent gas formation – WWL T and GL density

The relation between weak white liquor (WWL) temperature and heat output of total vent gas flow was not as clear as expected (Figure 33). The initial estimation was that the higher the temperature of weak white liquor fed into the tank, the higher the amount of vent gas produced. According to feedback data a slight increasing of vent gas heat output was observed inside the individual boiler cases, but in general view changes were minor. The effect of WWL temperature on the amount of heat output was observed to be clearer than in feedback cases. Thus more data would be required in order to determine the effect of weak white liquor temperature on vent gas formation with higher level of confidence.

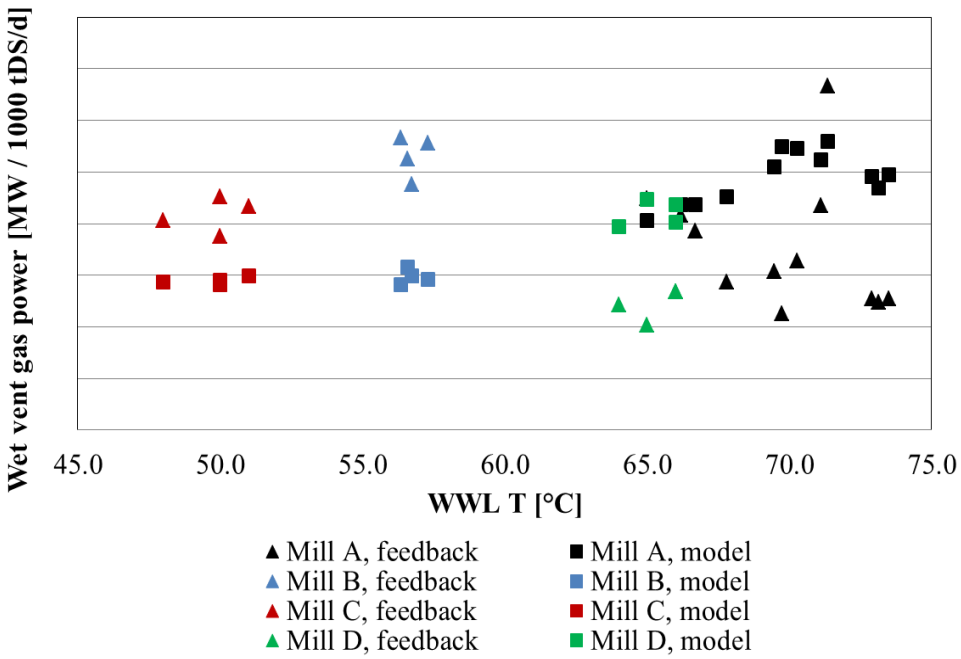

Figure 33. The effect of WWL temperature on the heat output of total vent gas flow per 1000 tDS/d at Mills A, B, C, and D.

The effect of green liquor density on the heat output of total vent gas flow is presented in Figure 34. According to the feedback data heat output of vent gas seems to increase as the density of green liquor increases in case of individual boilers. Generally, the comparison of boiler cases in each other is difficult due to the different operation conditions of boilers. According to the model, heat output of vent gases increased as density of green liquor was increased and other parameters, such as WWL temperature and boiler load were remained constant. In order to gain higher confidence of the results, more feedback data and analysis are required.

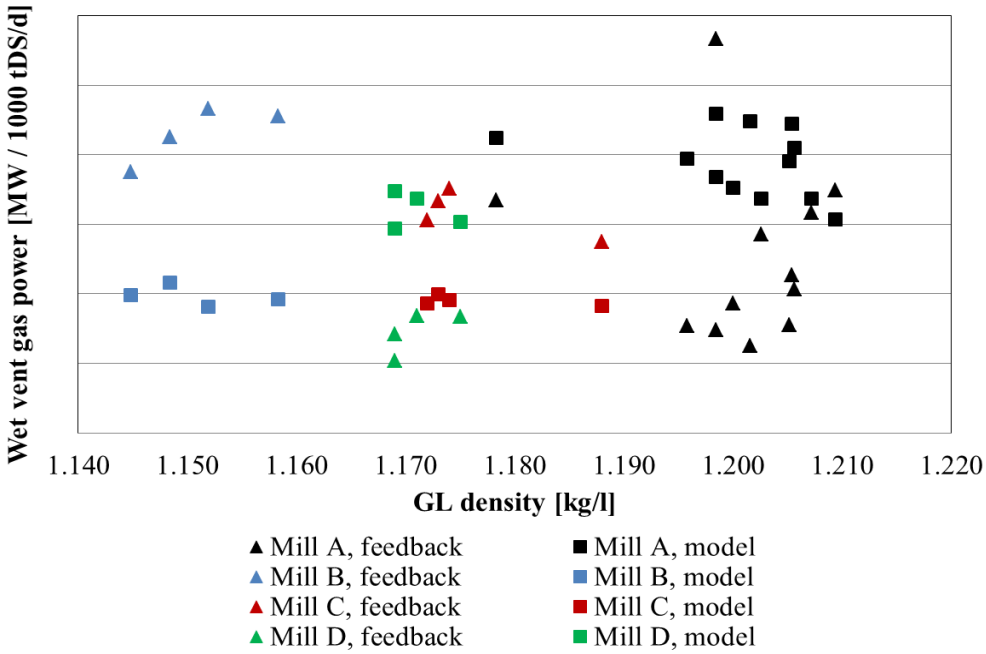

Figure 34. The effect of green liquor density on the heat output of total vent gas flow per 1000 tDS/d at Mills A, B, C, and D.

Initially it was assumed that heat is removed from the balance system mainly in vent gas or green liquor. The heat outputs of green liquor gas and liquor phase with different boiler loads at Mill A are presented in Figure 35. The heat curves of gas and liquid phases seem to reflect each other, which may indicate to the state of heat distribution. As the evaporation of green liquor decreases more heat is removed with green liquor and vice versa.

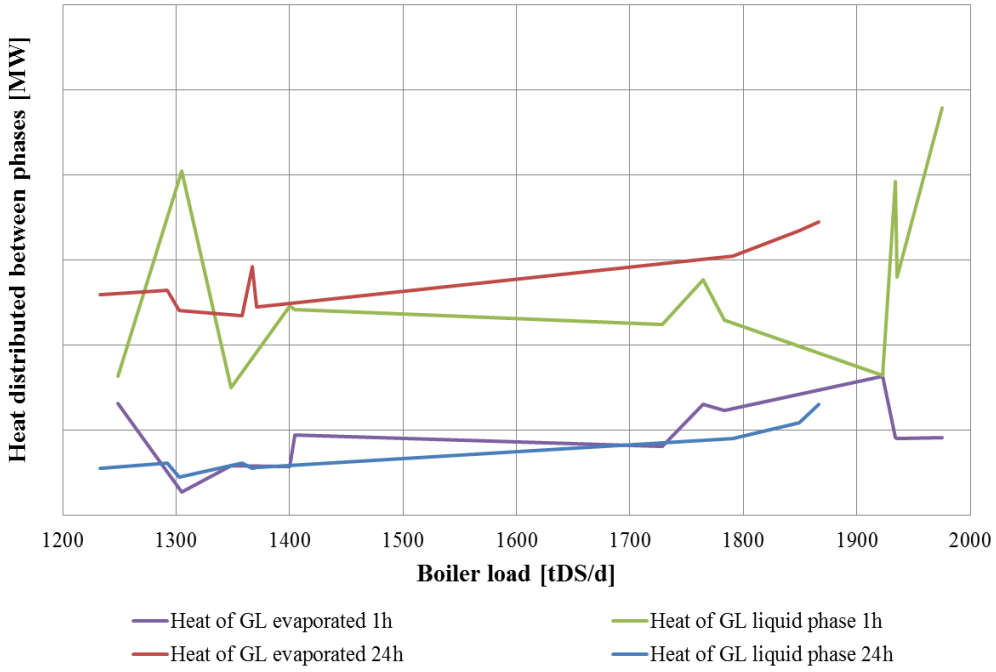

Figure 35. The heat outputs of green liquor liquid and gas phase during smelt dissolution with different boiler loads of Mill A. Curves are based on 1-hour- and 24-hour-average values.

10.4.3 Properties affecting vent gas formation – GL temperature

The relation between green liquor temperature and total heat output of vent gases is presented in Figure 36. In general view the effect of green liquor temperature was not clear as in case of individual boilers. According to feedback data heat output of vent gas was increased as the temperature of green liquor increased inside the individual boiler cases. When compared the results of the feedback data to the model, it was observed that temperature range of green liquor was wider in the model than in field measurements.

Simulated heat output of vent gas was slightly increased in case of Mills C and D or remained stable as in case of Mill B. However, heat output of vent gases at Mill A seemed to be decreased as green liquor temperature was increased. This may be due to different operation conditions of test boilers. During the simulations it was observed that as green liquor temperature was increased the heat output of vent gases increased as well, while WWL temperature and green liquor density were remained constant.

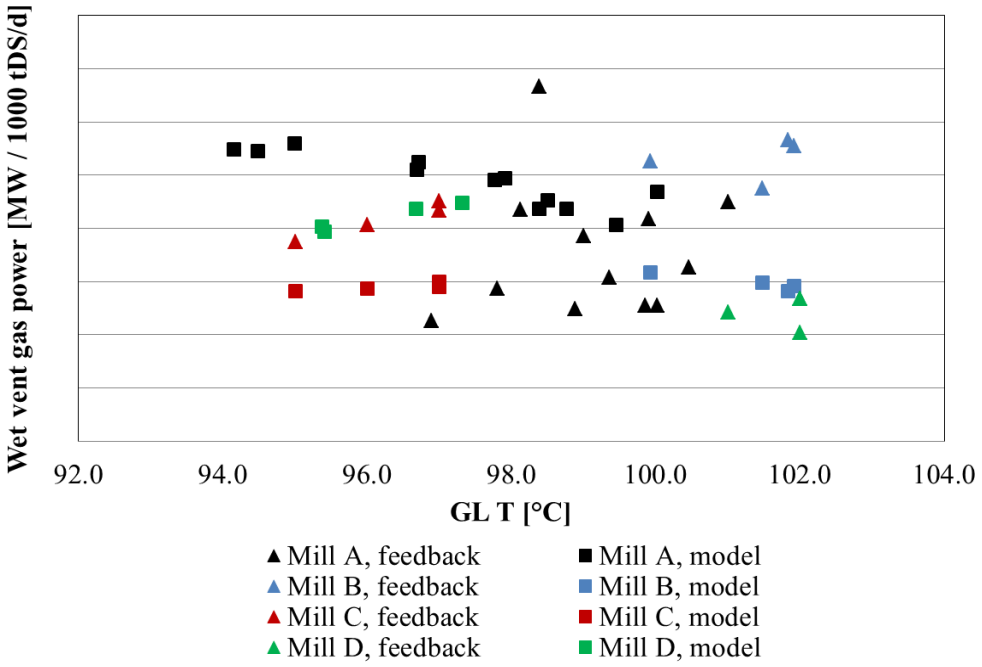

Figure 36. Heat output of total vent gas flow based on different green liquor temperatures with 1000 tDS/d of boiler load at Mills A, B, C, and D.

11 CONCLUSION

Main objectives of this master's thesis were to study the operation of kraft recovery boiler dissolving tank, understand its processes, especially the phenomena behind the formation of vent gases, and create a workable numerical balance model to describe the operation of the tank.

Theory of black liquor combustion, char bed and smelt properties were discussed together with smelt dissolution and its properties in literature part of this thesis. Additionally, dissolving tank venting and vent gas handling system were introduced briefly.

In experimental part of the work process feedback data of dissolving tank and vent gas scrubber operation was collected from the mill data systems of four different recovery boilers. Collected feedback data was used for the tuning of a created dissolving tank mass and energy balance model. Finally, calculated feedback data balances were compared to the results of simulations. The main target of the study was to determine the amount and heat output of evaporated vapor and vent gas produced during dissolution. Additionally, the effect of green liquor density, weak white liquor temperature, green liquor temperature and boiler operation load on dissolving tank vent gas formation were determined.

11.1 Summary of the results

The initial hypothesis were that total heat output of the dissolving tank is distributed between vent gas, including leaking air and evaporated green liquor vapor, and green liquor liquid phase. Additionally, it was assumed that increasing of green liquor temperature in the tank increases the evaporation of green liquor.

The tuning of the model in order to fit generally for all test boilers was discovered to be challenging. Estimated mass and enthalpy flows of the model deviated from their reference streams of feedback data. This may be due to uncertainty in the determination of leaking air mass flow, smelt composition and accurate green liquor density. In case of the model initial composition of smelt and green liquor density were assumed to be constant compared to real processes, where density and composition were constantly changing.

Simulated vapor and green liquor flows were in the same range with feedback data, excluding the case of Mill C. In the case of Mill C, one possible reason for the variation in the amount of produced vapor may be the higher specific enthalpy of smelt and higher actual smelt temperature than estimated in the model.

The heat output of total vent gas flow increased as the boiler load was increased. The trend between previous parameters was observed to be linear. Contrary to initial expectations temperature of weak white liquor had minor effect on vent gas heat output. It was observed that increasing of weak white liquor temperature increased the heat output of vent gases in case of individual boilers. In general view the trend was not equally unambiguous. Thus more feedback data is required to enhance the reliability and to form further conclusions. According to feedback data green liquor density had an increasing effect on the heat output of vent gas flow. The increasing of green liquor temperature was observed to increase the evaporation of green liquor in case of individual boilers. In general view the trend between green liquor temperature and heat output of total vent gas flow was not stated to be equally clear.

11.2 Error evaluation

The results obtained from the model matched the feedback data satisfactorily. Main reason for the deviation of the results is the limited amount of feedback data with limited range of boiler loads and uncertain properties of input streams, such as smelt flow, smelt temperature, green liquor composition and actual amount of leaking air.

Additionally, the created model represents very simplified conditions in the dissolving tank. In reality, for instance, flowing conditions and mixing will influence on the dissolving tank balance output.

However, despite of its uncertainties, the results of the model can be considered as a good reference to the measured values and giving the basic knowledge of dissolution inside individual boiler cases at given loads. In order to predict results with higher boiler loads and capacities, more feedback data is required.

11.3 Recommendations for further studies

From mass and energy balance point of view, dissolving tank operation can be considered as a complicated process, since chemical reactions are involved in addition to heat and mass transfer. Thus some simplifications and generalizations were done in this work in order to create a workable numerical balance model. For instance, dissolution enthalpies of smelt compounds were ignored in the balance calculations due to limited available empirical data and their assumed minor effect on total enthalpy flow of smelt. Smelt temperatures were also assumed to be constant, which may cause uncertainty in balance calculations.

In order to enhance energy balance of the tank green liquor composition and boiling point elevation are significant properties to analyze. Additionally, the lack of feedback data set some limitations on the work. For instance, the amount of leaking air was an open issue in feedback data calculations. During the balance calculations it was assumed that the amount of leaking air will affect dissolving tank venting. One solution for the estimation of leaking air mass flow and its effect on dissolving tank venting is to perform leak-air-test, where smelt spout hoods will be closed for preventing air flow into the tank. During the test dissolving tank venting can be determined by monitoring the temperature of scrubber circulation water and exit temperature of dried vent gas out of the scrubber, which indicate the amount of heat transferred in the scrubber. The amount of the leak air can be estimated then from the fan operation.

One possible way to control dissolving tank venting is to adjust green liquor temperature by decreasing the temperature of incoming weak white liquor in a cooler. In this work the effect of WWL temperature on vent gas heat output was discovered to be minor and not so unambiguous than initially expected. In future it is recommended to collect more data from the effect of WWL temperature on dissolving tank venting, and hence on scrubber operation.

In future it is also recommended to study how much the total heat output of vent gas decreases, when the temperature of WWL is decreased, for instance, from 70 ºC to 50 ºC in the cooler. The cost effects and benefits of cooler utilization in the reduction of dissolving tank venting compared to heat recovery from scrubber

circulation water should also be considered. Another question to be considered is the effect of WWL cooler on the formation of pirssonite scaling.

Another way to control green liquor temperature is to recover heat from green liquor by flashing or with other suitable heat recovering system. Current balance model does not consider heat collection from green liquor. Thus a flash tank can be included to the model in order to control dissolving tank venting in future.

In this work it was discovered that the amount of heat transferred to smelt spout cooling water was not depending on boiler load or capacity (Figure 32). Thus smelt enthalpy and temperature would be significant parameters to determine in future research. One way to estimate smelt enthalpy flow, and hence temperature could be, for instance, the determination of the heat conducted with aid of heat transferred to cooling water of smelt spout. Additionally, one possibility to estimate accurate temperature of the smelt during normal operation is to determine it as a function of boiler floor surface area. This could be implemented, for instance, based on heat radiation from the bed.

Finally, the modelling of dissolving tank fluid dynamics could provide essential knowledge about the effective area of green liquor evaporation, flowing conditions and mixing. Laboratory scale model study could also provide significant information about the amount of leaking air, vent gas formation and other variables affecting dissolving tank operation.

12 REFERENCES

Adams, T., 1997. General Characteristics of Kraft Black Liquor Recovery Boilers. In: T. N. Adams, ed. *Kraft Recovery Boilers.* New York: TAPPI PRESS, pp. 3-38.

Adams, T. N. & Frederick, J., 1988. *Kraft Recovery Boiler Physical and Chemical Processes.* 9-251 ed. New York: The Recovery Boiler Research and Development Sub-committee - American Paper Institute.

Ahlstrom Machinery Corporation, 1997. *Smelt Dissolving Tank Emissions - A Compilation report,* Helsinki: Ahlstrom Machinery Corporation.

Aho, K. & Saviharju, K., 2007. *Reduction Efficiency - the Parameters Influencing in Modern Boilers,* Varkaus: Andritz Oy [Internal material].

Andritz Oy , 2015. *RB upgrade - Start-up and Comissioning and Carry-Over Evaluation,* Varkaus: Andritz Oy [Internal material].

Andritz Oy, 2008. *Lipeänpoltto ja kemikaalitase.* Kotka, Recovery Division, Andritz Oy [Internal material].

Andritz Oy, 2016a. *Recovery Boiler audit 2016 - Dissolving tank build-up problems,* Varkaus: Andritz Oy [Internal material].

Andritz Oy, 2016b. *Process description and design by systems - Green liquor, smelt and vent stack systems,* Kotka: Andritz Oy [Internal material].

Biermann, C. J., 1996. Kraft Spent Liquor Recovery. In: *Handbook of Pulping and Papermaking.* 2nd ed. London: Academic Press, pp. 101-122.

Böök, F., Konttinen, J. & Hupa, M., 2006. *Soodakattiloiden raskasmetallitaseet,* Turku: Åbo akademi - Process Chemistry Centre Combustion and Materials Chemistry.

Cardoso, M., de Oliveira, É. D. & Passos, M. L., 2009. Chemical composition and physical properties of black liquors and their effects on liquor recovery operation in Brazilian pulp mills. *Fuel,* Volume 88, pp. 756-763.

Costa, A. O. S., Biscaia, E. C. J. & Lima, E. L., 2005. Chemical Composition Determination at the Bottom Region of a Recovery Boiler Furnace by Direct Minimization of Gibbs Free Energy. *The Canadian Journal of Chemical Engineering,* Volume 83, pp. 477-484.

Courtois, G., 1939. *Comptes Rendus,* Volume 208, p. 277.

da Silva Medeiros, A., Kaila, J. & Simonen, L., 2002. *Recovery boiler dissolving tank - eliminating the final emission source.* San Diego, TAPPI.

DeMartini, N., 2009. *Calculations of green liquor density vs TTA as a function of composition,* New York: American Forest & Paper Association Recovery Boiler Program.

DeMartini, N. & Hupa, M., 2006. *Cyanate and Ammonia in the Kraft recovery Process.* Chigaco, Tappi.

Engdahl, H. et al., 2008. White liquor preparation. In: P. Tikka, ed. *Chemical Pulping Part 2, Recovery of Chemicals and Energy, Papermaking Science and Technology.* 2nd ed. Jyväskylä: Paper Engineers' Association/Paper ja Puu Oy, pp. 122-193.

European Committee for Standardization, 2004. *Safety devices for protection against excessive pressure - Part 1: Safety valves (ISO 4126-1:2004).* Brussels: CEN - European Committee for Standardization.

Frederick, J., Porter, J. & Tran, H., 2011. *Mitigating the risk of smelt-water explosions in dissolving tanks.* Portland, Tappi, pp. 1-9.

Frederick, J. W. & Söderhjelm, L., 1997. Black Liquor Properties. In: T. N. Adams, ed. *Kraft Recovery Boilers.* New York: TAPPI PRESS, pp. 61-99.

Frederick, W. J., Danko, J. P. & Ayers, R. J., 1996. Controlling TRS emissions from dissolving tank vent stacks. *Tappi Journal,* 79(6), pp. 144-148.

Frederick, W. J. & Hupa, M., 1991. *The Effect of Swelling on Droplet Trajectories, Carbon Burn-out, and Entrainment in Black Liquor Combustion.* s.l., Tappi, pp. 79-89.

Frederick, W. J., Hupa, M., Clay, D. & Verrill, C., 1997. Black Liquor Droplet Burning Processes. In: T. N. Adams, et al. eds. *Kraft Recovery Boilers.* New York: TAPPI PRESS, pp. 131-160.

Frederick, W. J. J., Krishnan, R. & Ayers, R. J., 1990. Pirssonite deposits in green liquor processing. *Tappi Journal,* 73(2), pp. 135-140.

Grace, T. & Frederick, W. J., 1997. Char Bed Processes. In: T. N. Adams, ed. *Kraft Recovery Boilers.* Atlanta: TAPPI PRESS, pp. 161-180.

Grace, T. M., 2004. *A review of char bed processes.* Porvoo, Suomen Soodakattilayhdistys - Finnish Recovery Boiler Committee, pp. 21-29.

Grace, T. M. & Tran, H., 2009. The effect of dead load chemicals in the kraft pulping and recovery system. *Tappi Journal,* July.pp. 18-24.

Grace, T. & Tran, H., 2010. *Critical issues in smelt dissolving tank operation.* Williamsburg, TAPPI, pp. 1-6.

Heinola, A., 2016. *Discussion about kraft recovery boiler dissolving tank design* [Interview] (16 August 2016).

Hupa, M., 2004. *Research highlights in recovery boiler chemistry.* Porvoo, Suomen soodakattilayhdistys - Finnish recovery boiler committee, pp. 125-132.

Hupa, M. & Hyöty, P., 2002. Mustalipeän poltto ja soodakattila. In: T. a. -. D. t. a. r.y., ed. *Poltto ja palaminen.* Helsinki: International Flame Research Foundation - Suomen kansallinen osasto, pp. 522-556.

Hupa, M., Solin, P. & Hyöty, R., 1987. Combustion Behavior of Black liquor Droplets. *Journal of Pulp and Paper Science,* 13(2), pp. J67-J72.

Iisa, K., 1997. Recovery Boiler Air Emissions. In: T. N. Adams, ed. *Kraft Recovery Boilers.* New York: TAPPI PRESS, pp. 217-244.

Incropera, F. P., Dewitt, D. P., Bergman, T. L. & Lavine, A. S., 2007. *Fundamentals of Heat and Mass Transfer.* 6th ed. Hoboken: John Wiley & Sons.

Jin, X., Bussmann, M. & Tran, H., 2013. *An experimental study of smelt-water interaction in the recovery boiler dissolving tank.* Green Bay, TAPPI, pp. 1-13.

Jones, A. K. & Nagel, A., 1998. *The Real Benefits of High Solids Firing.* s.l., TAPPI, pp. 313-322.

Järvinen, M., Zevenhoven, R., Vakkilainen, E. & Forssén, M., 2003. Black liquor devolatilization and swelling - a detailed droplet model and experimental validation. *Biomass and Bioenergy,* Volume 24, pp. 495-509.

Kaksonen, K., 2009. *Liuottajasäiliön hönkien käsittely täytekappalepesurilla,* Lappeenranta: Lappeenrannan teknillinen yliopisto.

Karidio, I., Uloth, V. & Porter, J., 2004. *A Review Of The Conditions in Chemical Recovery Boilers That Result In Poor-Flowing Smelt.* Charleston, TAPPI, pp. 1-8.

Keikko, K., 1998. *Modelling of Mass and Heat Transfer in Packed Column.,* Tampere: Tampereen teknillinen korkeakoulu.

Klarin, A., 1993. Floor tube corrosion in recovery boilers. *Tappi Journal,* December, 76(12), pp. 183-188.

Kubiak, J., 1973. Melting Point Curve of Smelt vs. Composition. *Tappi Journal,* April, 56(4), p. 172.

Kymäläinen, M., Forssén, M., Jansson, M. & Hupa, M., 2002. The Fate of Nitrogen in the Chemical Recovery Process in a Kraft Pulp Mill. Part IV: Smelt Nitrogen and its Fromation in Black Liquor Combustion. *Journal of Pulp and Paper Science,* May, 28(5), pp. 151-158.

Kymäläinen, M., Holmström, M., Forssén, M. & Hupa, M., 2001. The Fate of Nitrogen in the Chemical Recovery Process in a Kraft Pulp Mill. Part III: The Effect of Some Process Variables. *Journal of Pulp and Paper Science,* September, 27(9), pp. 317-324.

Lammentausta, S. & Kiiskilä, E., 1996. *Wet Scrubbing Applications in the Pulp and Paper Industry.* Orlando, Tappi, pp. 813-816.

Lindberg, D., Backman, R. & Chartrand, P., 2007. Thermodynamics evaluation and optimization of the (Na2CO3 + Na2SO4 + Na2S + K2CO3+K2SO4+K2S) system. *Journal of Chemical Thermodynamics,* Issue 39, pp. 942-960.

Ljungvist, M. & Theliander, H., 1996. Mixing conditions in the smelt dissolver. *PULP AND PAPER CANADA,* 97(6), pp. 53-58.

Llamas, P. et al., 2007. A novel viscosity reducer for kraft process black liquors with a high solids content. *Chemical Engineering and Processing,* Volume 46, pp. 193-197.

McGabe, W. L., Smith, J. C. & Harriott, P., 2005. *Unit Operations of Chemical Engineering.* 7th ed. Singapore: McGraw-Hill.

Oveshkin, E. K., Shevtsova, L. N., Voitsechovsky, A. E. & Kuznetsova, L. V., 1971. *Zhur. Neorg. Khim.,* Volume 16, p. 3156.

Oy Keskuslaboratorio - Centrallaboratorium Ab , 1993. *Suositus sulan ja viherlipeän reduktioasteen määrittämiseksi,* Espoo: ETY-Soodakattilavaliokunta.

Pakarinen, L., 2016. *Process Design Manager, Andritz Oy* [Interview] (10th June 2016).

Partanen, J. I. & Partanen, L. J., 2010. *Luentomoniste opintojaksoon BJ80A1000 Kemiallinen termodynamiikka - Kemiallisen termodynamiikan sovellutukset - Osa 2.* Lappeenranta: Lappeenrannan teknillinen yliopisto.

Rantanen, A., 1986. *Soodakattilan liuotinhöngän koostumuksen ja käsittelymenetelmien tutkiminen,* Lappeenranta: Lappeenrannan teknillinen korkeakoulu.

Salmenoja, K., 2015. *KRP Days - June 2-3, 2015 - Recovery Boiler Technology Review.* Varkaus, Andritz Oy.

Salmenoja, K. & Kosonen, J., 1996. *Solving deposit problems in the smelt dissolving tank.* Atlanta, TAPPI, pp. 793-797.

Saviharju, K., Aho, K. & Pynnönen, P., 2006. *Viherlipeäsakka.* Kotka, Suomen Soodakattilayhdistys ry, pp. 46-53.

Sebbas, E., Ahonen, A. & Haasiosalo, T., 1983. Jäteliemien poltto, kemikaalien talteenotto ja keittoliuosten valmistus. In: N. Virkola, ed. *Puumassan valmistus II.* 2nd ed. Turku: Suomen paperi-insinöörien yhdistys, pp. 1236-1237.

Taimisto, M., 1975. *Kemikaalisulan ominaisuudet ja liuotus,* Helsinki: Teknillinen korkeakoulu.

Tammann, G. & Oelsen, W., 1930. Die Reaktionen beim Zusammenschmelzen con Glassätzen. *Z. Anorg. Allg. Chem.,* Volume 193, pp. 245-269.

Taranenko, A., Bussmann, M. & Tran, H., 2014. A laboratory study of recovery boiler smelt shattering. *Tappi Journal,* August, 13(8), pp. 19-26.

Tarpey, T., 1995. *Adressing ammonia and particulate emissions from a kraft smelt tank.* Atlanta, Tappi, pp. 917-924.

Tarpey, T., Tran, H. & Mao, X., 1996. Emissions of Gaseous Ammonia and Particulate Containing Ammonium Compounds from a Smelt Dissolving tank. *Journal of Pulp and Paper Science,* April, 22(4), pp. J145-J150.

Tegman, R. & Warnqvist, B., 1972. On the Phase Diagram Na2CO3 - Na2S. *Acta Chem. Scand.,* 26(1), pp. 413-414.

Theliander, H., 2009. Recovery of Cooking Chemicals: the Treatment and Burning of Black Liquor. In: M. Ek, G. Gellerstedt & G. Henriksson, eds. *Pulp*

and Paper Chemistry and Technology - Pulping Chemistry and Technology. s.l.:Walter de Gruyter GmbH, pp. 297-334.

Tran, H., Jones, A. K. & Grace, T. M., 2015. Understanding recovery boiler smelt runoff phenomena. *Tappi Journal,* January, 14(1), pp. 41-50.

Tran, H., Mao, X. & Chartrand, P., 2009. *Effects of sulphide on melting temperatures of smelt and carryover in kraft recovery boilers.* Tennesee, TAPPI Engineering, pp. 1-9.

Tran, H., Sunil, A. & Jones, A. K., 2004. *The Fluidity of Recovery Boiler Smelt.* Charleston, TAPPI, pp. 1-10.

Vakkilainen, E., 2008a. Chemical recovery. In: *Chemical Pulping Part 2, Recovery of Chemicals and Energy, Papermaking Science and Technology.* 2nd ed. Jyväskylä: Paper Engineers' Association/Paperi ja Puu Oy, pp. 10-34.

Vakkilainen, E., 2008b. Recovery boiler. In: P. Tikka, ed. *Chemical pulping Part 2, Recovery of Chemicals and Energy, Papermaking Science and Technology.* Jyväskylä: Paper Engineers' association/Paperi ja Puu Oy, pp. 86-121.

Vakkilainen, E., 2009. *Soodakattilan keon lämmönsiirto-ominaisuudet - Kirjallisuuskatsaus,* Lappeenranta: Suomen soodakattilayhdistys ry - Finnish Recovery Boiler Committee.

Vakkilainen, E. K., 2005. *Kraft Recovery Boilers - Priciples and practice.* Helsinki: Suomen Soodakattilayhdistys r.y..

Warnqvist, B., 1992. *Char Bed and Smelt Properties - Mill Studies.* s.l., Tappi Proceedings, pp. 551-556.

Vihavainen, E., 2016. *Product Manager, Andritz Oy* [Interview] (12th July 2016).

Vähä-Savo, N., 2014. *Behavior of Black Liquor Nitrogen in Combustion - Formation of Cyanate,* Turku: Åbo akademi - Process Chemistry Centre.

Zeller, M. & Busweiler, U., 2010. Humidifying and Drying of Air. In: P. Stephan, et al. eds. *VDI Heat Atlas.* 2nd ed. Berlin: Springer, p. 1343.